THE SURFACE CHEMISTRY AND FLOCCULATION OF COAL

A thesis submitted for the degree of
Doctor of Philosophy of the University of London

By

MEHMET LEKILI

Department of Mineral Resources Engineering
Royal School of Mines
Imperial College of Science and Technology
University of London

November 1982

ABSTRACT

The physical and chemical properties and flocculation of coal have been reviewed. The surface chemistry of coal and the methods available to determine surface groups have been discussed.

The electrokinetic properties of coal samples of various ranks and lithotypes were established by electrophoresis. The effect of pH on the electrophoretic mobilities was studied, and the IEP values were determined. The effects of indifferent electrolytes and polyvalent metal ions were also evaluated.

Adsorption of OH^- ions by the coal surface was studied by a potentiometric technique and the PZC values were determined.

The results showed that the coal surfaces were negatively charged in water, and that polyvalent metal ions were specifically adsorbed by the coal. Combination of electrophoretic mobility measurements and titration results emphasized the potential determining role of H^+ and OH^- ions.

Attempts to determine the different acidic groups on the surfaces by direct titrations failed because of difficulties in defining clear end points.

Ionizable hydrogen associated with acidic oxides on the surface was removed by methylation with diazomethane. Methylation of the samples did not significantly affect the electrophoretic mobilities obtained. However, the OH^- ion abstraction decreased.

The hydrophobic character of the samples was decreased by controlled oxidation. Oxidation was found to increase the negative value of the electrophoretic mobilities and decrease the IEP values.

Suspensions were flocculated by high molecular weight non-

ionic, anionic, and cationic polymers. Adsorption of the polymers from water on to the samples was investigated and correlated with the degree of flocculation obtained. The adsorption isotherms were of typical Langmuir-type. The influence of pH and a neutral salt were determined. The effects of methylation and oxidation on adsorption behaviour were also studied.

The results indicated that the mechanism of adsorption of non-ionic polymer occurs mainly through hydrophobic interaction between the polymer molecule and the coal surface. However, polymer adsorption in the presence of a H-bonding competitor suggested that an H-bonding interaction mechanism may play a minor role. Anionic polymer adsorption took place in the presence of a simple electrolyte which reduced the electrokinetic potential and allowed H-bonding to occur. Cationic flocculation of the coal was explained in terms of Coulombic attraction.

Preliminary selective flocculation tests of coal from a coal/quartz mixture showed that it is possible to selectively separate finely divided coal particles from quartz using a non-ionic polyethylene oxide at high alkaline pH conditions.

ACKNOWLEDGEMENTS

I would like to express my sincere gratitude to Dr. H.L. Shergold and Dr. R.J. Gochin, for their help, encouragement and guidance throughout the course of the project.

I further thank Dr. K.I. Marinakis and my colleagues for their frequent assistance and useful discussions.

I am indebted to Turkish Scientific and Technical Research Council for financial assistance provided during the course of the present work.

I also wish to thank Miss M. Cook who deciphered my handwriting and made my manuscript presentable.

CONTENTS

LIST OF FIGURES

LIST OF TABLES

CHAPTER 1. INTRODUCTION

1. INTRODUCTION

1.1 The significance of fines to coal preparation

The quantity of fine-size coal particles processed in coal preparation facilities has risen steadily in recent years. This has been caused by such factors as increased mechanization and working of poorer seams in mines to improve productivity, finer comminution in the preparation plant for impurity liberation and the imposition of anti-pollution legislation.

By present standards the industry has adequate processes for cleaning coarse coal at almost any desired specific gravity. However, in the case of fine coal the most widely accepted process - froth flotation - does not in its present state of development yield products that are comparable in ash content to those normally obtained from coarse coal processes.

Precise laboratory washability studies show that fine-coal processing is considerably less efficient than coarse-coal cleaning processes. Due to this inherent inefficiency of fine-coal processing, the results of existing fine coal systems are in many cases entirely unsatisfactory and any or all of the following problems arise:

i) Valuable coal is lost to reject.

ii) The efficiently cleaned coarse-coal product is contaminated by inefficiently cleaned fines.

iii) The fine-coal present in the reject tends to hang up or even float in static thickeners. As a result of this flocculation costs are excessive and serious handling problems may be created.

iv) Rejected fine-coal contributes to the carbon content of the refuse piles, and if these undergo spontaneous combustion they can create air pollution or even water pollution resulting from the solution of sulphur gases in rain water.

The fundamental difference between fine coal and coarse coal processing lies with those physical mineral properties which can be used to effect a coal/non-coal separation. The coarse coal processes make use of the differences in relative density between various particles. This parameter, as well as allowing comparative simplicity of separating process, also gives a ready means of determining process efficiency. Thus, using a simple float and sink test which involves immersing a sample of raw coal in a liquid of known relative density and then analysing the resultant floating and sinking fractions, data on the theoretically perfect separation can be obtained. Actual process performance can then be related to such a test to give a measure of process efficiency.

This procedure does not in fact use relative density differences directly but rather differences in the settling velocities of similar sized particles in a controlled environment to achieve rapid and efficient separation. Thus, as particle size is reduced, given the same relative density difference, settling velocities will also reduce. Because of this the coarser particles are usually separated into two size fractions, +25 mm and 25 mm - 0.5 mm. The +25 mm particles can be separated in dense medium "static" baths which operate on the float and sink principle with raw coal being immersed in a liquid, or more accurately a suspension, of known and controlled relative density.

When particle size is less than 25 mm settling velocities under gravitational acceleration become too slow. In order to overcome this, these particles are separated in cyclones. In these devices the particles are acted upon by centrifugal forces and separating velocities are increased.

This general technique, unfortunately, is not readily applicable to particles below 0.5 mm in size. There are several reasons for this but the principal one concerns the separating medium. Dense media in coal preparation comprise suspensions of finely ground mineral, most commonly magnetite, in water. As the size of the coal/shale particles to be separated approach the size of the dense medium particles it becomes extremely difficult, after separation, to recover the medium solids from the coal and shale solids.

Thus at present, it is necessary to rely on other methods of separating fine coal. These include froth flotation, oil agglomeration, selective flocculation, etc., but the most important point is that they all rely on differences in coal/non-coal surface characteristics to achieve separation. Such differences are very readily influenced by external factors. For example, the fact that the coal is normally stockpiled prior to treatment can affect process response, as can the pH level or mineral salt content of the process water. The number of possible process variables can be quite high and as a result, there is no ready means of assessing process efficiency.

During the cleaning process extremely fine particles complicate some of the operations, e.g., flotation, dewatering, purification of the circulating waters. The negative effect of extremely fine

particles on the flotation process is largely the result of their ability to form slime coatings on the surface of bigger particles, and their inherently slower kinetics (1). For this reason a desliming step is introduced before many coal flotation processes during which particles smaller than 20 μm are removed. This product is usually considered to be waste material and is left in sedimentation ponds, although it often contains considerable quantities of "value".

1.2 Fields of application of flocculation in coal preparation

Water purity: There are two main reasons for removing fines from circulating and effluent waters in coal preparation plants. First, the accumulation of fines in recycle water cannot be tolerated because of the detrimental effect they have on the washing efficiency of the unit operations in the plant (2), and secondly, the discharge of waste water is forbidden by environmental pollution regulations in most areas. Clarification of these waters is speeded by flocculation.

Thickening: The advantages derived from flocculation in thickening may be:-

i) low solids content of thickener overflow, which means clarified water and greater solids recovery,

ii) rapid sedimentation of solids resulting in increased available capacity of thickener.

Filtration: As a result of their initial permeability and plastic properties, flocculated slurries have improved filtration characteristics. The greater initial permeability results in a lower flow

resistance while the plastic property, which is due to the bonding of particles in flocs, prevents complete break up and thus retains open voids. The advantages gained from flocculation when used in filtration are clearer filtrate, greater capacity, improved filter cake properties but sometimes at the expense of an increase in the water content of filter cake.

Centrifuging: In centrifuging operations, using solid bowl centrifuges, the flocculant solution may be fed to the slurry either at a point just prior to the centrifuge or through a separate feed pipe into the bowl itself. The second method is generally more efficient since the flocs are exposed to mechanical actions for shorter periods. Higher molecular weight synthetic polymers which produce strong flocs are preferred. Flocculation, when applied to centrifuging, tends to reduce solids content of water through better fines removal and it increases centrifuge capacity.

Dewatering over screens: Flocculation with certain polymers has been successfully applied to dewatering slurries on screens to allow the recovery of finer particles on larger-mesh screen surfaces.

1.3 Aim of the project

As outlined in the previous section, flocculation has been applied in coal preparation where it is most often employed for the purposes of water clarification. However, it has not been extensively studied as a possible means of separating the suspensions consisting of fine size particles of coal and refuse.

Recently, the treatment of coal-washery waste by flocculation has been suggested as a method of fine coal cleaning or for recovering

coal from material currently considered as waste (3)(4). However, in all cases the work has been empirical and little is known of the surface chemistry of coal and how it interacts with different flocculants. It is not possible, therefore, to predict the conditions required to flocculate a given coal or waste material from knowledge of its composition.

The aim of this project was to study the feasibility of using flocculation to selectively separate fine coal from refuse. It was believed that improving methods of fine size coal recovery would result in additional recovery of combustible material as well as abatement of environment pollution and solid waste disposal problems.

Knowledge of the surface chemistry of coal and how it adsorbs flocculants, polyvalent metal ions, etc., is a necesary prerequisite to determining the optimum conditions for its flocculation and whether or not coal can be separated from other minerals by a selective procedure. In the latter case information is, of course, also required on the properties of associated minerals. Therefore, in this work the surface chemical properties of coal were determined, which involved measurement of the electrokinetic and acid-base properties of various samples. The results obtained were then correlated with the flocculation and polymer adsorption behaviour of coal with a view of establishing the mechanism of polymer adsorption.

Most of the work has been carried out with anthracite, since it was thought that this represents the "purest" form of coal. Throughout the study the results were compared with those obtained with graphite. The latter was selected as a "model" system because coals display diffuse graphite XRD peaks (5). These have been

attributed to extremely small particles in which the arrangement of carbon atoms is similar to that of graphite. Quartz was chosen as the model impurity mineral for selective flocculation studies since a great deal is already known about its surface chemistry and flocculation properties.

CHAPTER 2. PROPERTIES OF COAL

2. PROPERTIES OF COAL

Coal is not chemically uniform, but a mixture of combustible metamorphosed plant remains that vary in both physical and chemical composition (6). The diversity of original plant materials and the degree of metamorphism affecting these materials are the two major reasons for the variety of physical and chemical behaviour in coal. These widely varying factors also greatly affect the preparation characteristics of coal.

2.1 Classification

Coalification or carbonification is the name given to the development of the series of substances peat, lignite, bituminous coal and, finally, anthracite and rank refers to the degree or stage, reached in coalification by a given coal.

Of the several different ways to classify coals, rank is generally the most common. However, the rank of a coal is not a directly measurable quantity. To define it, it is necessary to refer to a specific physical or chemical property (such as carbon, volatile matter, or moisture contents) which exhibits adequate changes in the course of coalification.

In many countries the classification systems used are based primarily on the content of volatile matter which is the loss of weight of heating coal to about 900°C. Coals with 8% volatile matter (VM) (dry mineral matter free basis) are called anthracites. A very special type with volatile matter content of less than 2% is called meta-anthracite or graphitoid coal. The next classes are, semianthracite or lean coal (8-14% VM), low volatile bituminous coal (14-22% VM) and

medium volatile bituminous coal (22-31% VM). When the volatile matter content is greater than about 30%, it becomes difficult to classify coals on the basis of volatile matter alone and a second parameter is usually applied. In the United States, the calorific value is used for further subdivision into different classes of high volatile bituminous coal, subbituminous, and lignite coals. In Great Britain, the coking value is used as a classification parameter and, in most of the other countries, the swelling index, defining the appearance of the coke button after removal of the volatiles, has been accepted as a second parameter.

Other classification systems based on ultimate and proximate analyses and heating value of the residual coal have also been developed but they have not received widespread acceptance.

Coal seams display two different modes of variation, rank and type. As mentioned previously, the position of a coal in the continuous series ranging from peats through anthracites determines its rank. The different bands of coal which constitute a coal seam are distinctly contrasted in regard to physical properties and chemical composition. These bands are the coal types. The macroscopically recognizable coal types are termed lithotypes. A lithotype classification system has been proposed by Stopes (7). This system recognises two types of bright coal, vitrain and clarain, and designates durain for dull coal and fusain for fossil charcoal. The descriptions for these various constituents and their properties have been reviewed by Thomas (8).

Lithotypes are composed of more or less homogeneous microscopic constituents called macerals. Macerals were defined by Spachman (9) as

organic substances, or optically homogeneous aggregates of organic substances, possessing distinctive physical and chemical properties, and occurring naturally in the sedimentary, metamorphic, and igneous materials of the earth. The macerals found in the different lithotypes have been given by Berry (10) and are shown in Table 2.1

Table 2.1 Heerlen Classification of Macerals

Lithotypes	Macerals
Vitrain	Vitrinite, Collinite, Tellinite
Clarain	Predominantly Vitrinite, some Exinite, Fusinite, Micrinite
Durain	Predominantly Micrinite, some Exinite, Fusinite, Vitrinite
Fusain	Fusinite

2.2 Chemical Properties

The chemical properties are concerned with the characterisitics of coal based upon its chemical constituents. These characteristics are determined to a large extent by the diversity of the original plant materials and the degree of metamorphism which has effected these materials.

The basic elements in coal are carbon, hydrogen, sulphur, oxygen and nitrogen which make up the complex mixture of organic and inorganic chemicals present.

Carbon in coal increases with rank. The percentage of total carbon that occurs in complex, condensed, ring structures also increases with rank. Some coals contain an appreciable amount of inorganic carbonates resulting from secondary deposition of minerals. The carbon content of

coal supplies most of its heating value.

The hydrogen content of coal generally ranges between 4.5 and 5.5%. The hydrogen in dry coal occurs predominantly in saturated or partially saturated ring structures with the carbon.

Sulphur in coal occurs in two forms, organic and inorganic. The organic sulphur appears to be uniformly distributed throughout the coal substance, and its origin is related to the facts that plants contain both protein and nonprotein sulfur and that decaying vegetation evolves hydrogen sulfide. The inorganic sulphur is composed mainly of pyrite and small amounts of iron sulphate.

Oxygen exists in coal in several forms. Hydroxyl, carbonyl and carboxyl groups may be present in lower-rank coals. The water in coal also contributes to the reported percentages of oxygen.

Nitrogen is the only element in coal that is present exclusively in organic combination. The amount present may vary from a small fraction of a percent to about 3%. Bituminous coals generally contain more nitrogen than lignites and anthracites, but there appears to be no regular change in nitrogen content in relation to other variables.

For practical purposes the chemical composition of coal is always defined in terms of its "proximate" analysis, which gives a rough measure of the distribution products obtained from it by destructive distillation, and by its "ultimate" or elemental analysis. Neither offers significant information about coal structure but both give data that, in the light of long experience, can be directly correlated with coal "behaviour".

Proximate analysis determines (a) moisture contents, (b) volatile matter contents, (c) ash, and (d) indirectly, the so-called fixed

carbon contents. Comprehensive reviews of the largely arbitrary experimental methods developed for these purposes have been reported (11) (12). However, in most coal-producing and -consuming countries, national standard techniques are laid down.

Ultimate or elemental analysis includes quantitative determination of carbon, hydrogen, nitrogen, sulfur, and oxygen, which make up the coal substance, and is usually performed with classic oxidation, decomposition, and/or reduction methods.

2.3 Structure

In the analysis of crystalline substances, X-ray diffraction is usually capable of establishing the molecular arrangement, even in extremely complicated molecules, because of the high degree of regularity in the cyrstal lattice. Coal, however, is not a crystalline substance and molecular structure cannot be deduced from X-ray analysis. There is no evidence to suggest that there is a coal 'molecule' in the strict sense, although in some cases it was considered useful to retain the concept.

The chemical structure of coal involves a carbon skeleton, and X-ray analysis has provided information on the arrangement of the carbon atoms. The first X-ray diffraction study showed that all banded coals had a lattice structure similar to graphite. The X-ray patterns of coals indicated the peaks at the position of the graphite bands and these have been attributed to particles in which the arrangement of carbon atoms is that of a graphite crystal, but with extremely small size of elemental crystallites.

The various features of X-ray diffraction patterns of coal have

been continuously reviewed in the literature. Although notable advances have been made, many aspects of the structure are still a subject for discussion. However, the results may be summarized in terms of three types of structure (a) in low-rank coals, an open structure of small, condensed aromatic layers randomly orientated and cross-linked; (b) in medium-rank coals, a 'liquid' structure with fewer cross-links; a moderate degree of orientation and reduced porosity; (c) in high-rank coals, a structure of larger layers with a higher degree of orientation and an orientated pore system.

Infra-red spectroscopy has provided information on the distribution of side-groups and intermolecular bonding. The spectum shows a number of distinct bands, the frequencies of which can be assigned with some confidence to particular groupings such as -OH, $-CH_2$, $-CH_3$, -CO and aromatic -CH. It is probably because of the nature of coal that one of the largest peaks (1600 cm^{-1}) has been the subject of prolonged discussion over its assignment to aromatic C=C, chelated quinone groups or heterocyclic nitrogen. The absorption bands at 3030cm^{-1} and 2920cm^{-1} can be used to compare the amount of hydrogen attached to aromatic carbon or aliphatic carbon respectively.

Other methods of structural analyses, nuclear magnetic resonance, ^{13}C resonances and chemical analyses of the coal and the residue after thermal decomposition have also been reported.

From the information obtained by X-ray diffraction and infra-red spectroscopy, it is generally believed that the structural unit of a coal 'molecule' contains a flat aromatic core surrounded by a methylene system, which is relatively rich in hydrogen and oxygen and is largely made up of methylene groups containing hydroxy, carboxyl, and carbonyl constituents. The molecules are considered to have clusters of between

one and four condensed benzene rings linked together. As coalification proceeds these linkages are partly transformed into aromatic types of bonds.

2.4 Porosity and Surface Area

Coal is microporous. It contains very small pores that limit the size of (reagent) molecules which can pass through them and consequently make coal a natural molecular sieve. This aspect determines the total surface area that coal presents to a reagent and also influences the rate at which access to the surface can be gained in any particular case.

The methods used for calculating surface areas involve measuring (a) heats of wetting, i.e., the temperature rises (ΔT) that accompany immersion of thoroughly evacuated, weighed test samples in a known volume of a suitable liquid (b) isothermal sorption of a gas or vapour by the coal. In the former case, provided there is no chemical interaction between the coal and liquid, the heat of wetting is directly proportional to the extent of the wetted surface, and surface area can be calculated from the heat liberated on wetting unit area of the surface. In the sorption method, the quantity (υ) of gas or vapor sorbed at different relative pressures (P/P_o) is plotted against P/P_o, and surface area is evaluated from υ at monolayer capacity and from the cross-sectional area of the sorbate molecule in its adsorbed state.

The absolute magnitude of the surface area has been the subject of numerous studies. Many different sorbates, under various conditions of temperature and pressure, have been used; rare gases, nitrogen, oxygen, carbon dioxide, hydrocarbons, alcohols, etc., have been sorbed

from the gas or vapor phase, and a wide range of liquids of different molecular sizes and properties have been used in experiments on heats of immersion. Following directly from these measurements, specific surface values have often been deduced in attempts to elucidate coal structure and to explain the behaviour of coals. However, rather poor correlation between the values obtained with the different methods or sorbates used has given rise to much controversy.

Most of the published data have been criticized on specific grounds. Heats of wetting in methanol are now known to be greatly distorted by polar interaction of methanol with oxygen-containing functional groups (notably -OH) at the coal surface. Estimates of surface area from sorption of oxygen, nitrogen, or other gases depend on how the sorption isotherms are determined and evaluated, and often involve assumptions about mechanisms by which the sorbate molecule reaches the surface and remains on it.

Recently, Spencer and Bond suggested that calculation of specific surface values from sorption data, or even to apply the concept of 'specific surface' to coals is not meaningful. They believe that 'sorption uptake' under defined conditions is the correct parameter that should be used to describe the sorptive properties of coals, and specific surface values determined under one set of conditions should not be used to calculate sorption uptakes for different practical conditions (13).

Notwithstanding the efforts devoted to the measurement of the surface areas of coal, it is however still questionable how much significance can be attached to these data, and numerical values of surface area must be treated with considerable caution.

2.5 Surface Properties

2.5.1 Surface charge

When a mineral particle is immersed in an aqueous solution its surface acquires an electrical charge which is caused by the dissociation of surface groups or the preferential adsorption of ions. As the system as a whole must be electrically neutral an equal charge of opposite sign to that on the surface must be present in the surrounding liquid. This gives rise to the electrical double layer.

The ions responsible for the surface potential, Ψ_o, are referred to as potential determining ions, PDI, and they are unique for a particular solid. In the case of ionic solids they are the ions that constitute the lattice. For oxides and silicates H^+ and OH^- ions have long been considered to be PDI, although there still remains a difference of opinion as to how pH actually controls the surface charge.

The surface charge, σ_s, on a solid in aqueous solution is determined by the adsorption density of PDI on the solid surface. In the case of uni-univalent salt, σ_s is given by

$$\sigma_s = F(\Gamma_{M^+} - \Gamma_{A^-}) \qquad (2.1)$$

where F = Faraday constant, 96500 C/mole

Γ_{M^+} = Adsorption density of potential determining cation, moles/cm^2

Γ_{A^-} = Adsorption density of potential determining anion.

At a particular pH value, the net adsorption density of PDI will be zero, this is termed the point of zero charge, PZC. An estimate of PZC can be obtained by determining the concentration of PDI at which

the zeta potential is zero. This condition is called the iso-electric point, IEP, and it equals the PZC in the absence of specific adsorption of any ionic or polar species and of other sources of charge.

Electrokinetic results are generally expressed in terms of the zeta potential which is the potential at the slipping plane when liquid is forced to move relative to solid. Generally the zeta potential is assumed to approximate to that of the Stern plane which is the position of closest approach of hydrated counter ions to the solid surface.

Although the significance of zeta potential and electrical double layer characteristics of minerals on the various processing operations has been adequately emphasized, information regarding the detailed electrokinetic studies on coal is still lacking. Furthermore, there have been wide variations in electrokinetic data quoted in the literature. This could be attributed to various factors, such as the extremely heterogeneous nature of coal, degree of surface oxidation and to some extent sample preparation.

A similarity between the surface characteristics of coal and some oxide minerals was first proposed by Glembotskii (14). On this basis, Campbell and Sun (15) studied the electrokinetic properties of bituminous coal and postulated that the coal surface hydrates and then undergoes pH-controlled dissociation to establish a charged surface in a similar manner to oxide minerals. However, in view of the heterogeneity of coal surface and the relatively large particles used in the measurements (35 x 48 mesh Tyler), it is not certain whether or not the electrokinetic data reflect the properties of the bituminous coal surface. These authors also studied the zeta potential of different

anthractie samples (16) and similar to the results of the previous study on bituminous coal, they emphasized the potential determining role of H^+ and OH^- ions and obtained IEP values between pH 2.5 and 5. These values are comparable to those obtained by other workers (17)(18)(19). Kovachev (20), using an electroosmosis technique, showed that sodium chloride decreased the zeta potential on coal surfaces. He suggested that the electolyte makes the coal particles hydrophobic by decreasing the surface potential. However, Kitchener and Laskowski's work (21) dispute this conclusion. They showed that hydrophobicity need not be related to the magnitude of the surface potential. Some authors (15)(16)(22) also considered that maximum hydrophobicity is obtained at the PZC of the coal and that the reduced floatability obtained under other conditions can be related to the charged condition of its surface. Jossep and Stretton (23), however, showed that a coal which floated most easily had no PZC and that other coals floated best at pH values of greater than the IEP. Similar results were obtained by Celik and Somasundaran (24). There appears to be no simple relationship between the magnitude of the surface potential of the coal and its flotation. Studies of the effect of oxidation on the zeta potential of bituminous vitrain have been made by Wen and Sun (22). The zeta potential - pH curves were shown to move to more negative zeta potentials with oxidation and this resulted in a displacement of the IEP to more acid pH values. The results were attributed to an increase in the amount of oxygen-containing functional groups on the coal surface.

The similarities observed in the electrokinetic properties of coal and those of oxide minerals suggest that the coal surface either

has an outer oxide later or an outer layer which has oxide-like characteristics. This is not surprising because it is well known that coal readily reacts with oxygen. Therefore, it is reasonable to assume that the coal surface behaves like oxide minerals. However, the extent of this similarity and whether or not H^+ and OH^- ions are the only PDI are not known.

2.5.6 Surface Groups

The surfaces of carbons and graphite contain amounts of combined oxygen and hydrogen, which give rise to various types of surface species or compounds. Many attempts have been made using specific chemical reactions, to establish the nature of the surface groups. Special emphasis has been placed on carbon-oxygen complexes. Results so far are rather inconclusive although certain specific groups have been detected. The recent reviews (25) (26) have noted the existence of carboxyl, carbonyl, phenol, quinone, and lactone groups as well as a CO_2 complex considered to behave as a frozen layer of CO_2 (26).

For coals, many different analytical procedures have been employed to determine the major oxygen containing groups. Although agreement between different chemical methods is rather poor, it is generally stated (27) that most of the oxygen in coals is present as carbonyl and phenolic hydroxyl groups and the remainder as ether and carboxyl groups.

It is evident from the literature (28) that the quantitative analysis of functional groups in coal is very difficult. The material is not readily accessible to the reagent. Consequently, the reaction period required is long and the results are sometimes not reproducible. Furthermore, a portion of the oxygen contained in coal is completely

unreactive, while another portion does not become reactive until the coal has been hydrolyzed.

Apart from the chemical methods, investigation of surface groups by physical methods, especially spectroscopy, is apparently difficult with microcrystalline graphite because of its high absorptivity and poor crystallinity with random orientation of the crystallites.

2.5.2.1 Direct Titrations

Boehm (25), using bases of different strength, has suggested that the different acidic oxides on carbon can be determined by a selective neutralization technique. He considered that carboxyl groups are titrated with $NaHCO_3$, carboxyl plus lactone groups with Na_2CO_3, and carboxyl plus lactone plus phenol groups with NaOH. These assignments have been criticized by Puri (26), on the basis that incomplete neutralization of the groups will be obtained because the alkalis are not sufficiently strong and the groups will be extensively hydrolyzed. This is especially true of the phenols in aqueous solutions. On this basis, Studebaker (29) has studied the potentiometric titration of surface oxides in non-aqueous medium. Using sodium aminoethoxide or alcoholic potassium hydroxide, he found indications of carboxyl and phenol groups. However, only two-thirds of the acidity that was determined by NaOH neutralization was titrated in non-aqueous medium.

Several investigators (30) (31) determined the total acidic groups of various coals by indirect titration, i.e., by heating in the presence of an excess amount of alcoholic potassium hydroxide followed by back titration of the excess. Direct titration has been mainly applied to humic acids, an application to coal has been described by Brooks (32) in which a coal suspension in ethylene diamine has been titrated with

a solution of sodium aminoethoxide as a titrant. Only ill-defined end points have been observed suggesting the presence of groups of slightly differing acid strength which could not be differentiated. Van Krevelen (33) emphasized the possibility of decomposition of coals in non aqueous medium.

Although direct titrations have been used to obtain information about the carbon surfaces, the validity of applying such techniques for the identification and estimation of surface groups on coals or carbons is questionable. It is unlikely that a group on a carbon surface will have the same ionization characteristics as the equivalent bulk compound and it is probable that the various groups will not be present as simple, independent and nonassociated structures.

2.5.2.2 Methylation of Surfaces

One of the reactions used in studies of carbon surfaces involves methylation of hydroxyl groups. Diazomethane (CH_2N_2) is a powerful methylating agent and reacts with any ionizable hydrogen on a carbon surface. A hydrogen atom which can ionize from a carbon surface is known as "active" hydrogen and can originate in many groups such as phenols, carboxylic acids, and lactones. By analysis of the methylation products it is possible to determine whether the hydrogen is associated with a carboxyl group or a phenolic group. The reaction of carboxyl groups with diazomethane produces methyl esters.

$$R - COOH + CH_2N_2 \rightarrow R - COOCH_3 + N_2 \qquad (2.2)$$

which can be easily hydrolysed

$$R - COOCH_3 + H_2O \xrightarrow{HCl} R - COOH + CH_3OH \qquad (2.3)$$

whereas phenolic groups react with diazomethane to produce methyl

ethers which are more resistant to hydrolysis.

$$R - OH + CH_2N_2 \rightarrow R - OCH_3 + N_2 \qquad (2.4)$$

Instead of diazomethane, dimethyl sulfate can be used for the methylation (25). If the reaction is allowed to proceed in the presence of an excess of alkali, only phenols are methylated.

Methylation by refluxing with methanol in the presence of dry hydrogen chloride is thought to attack only carboxyl groups.

These techniques have been widely employed to methylate graphite and coal samples (33) (34) (35). Methoxyl determinations before and after hydrolysis of methylated samples have been used to distinguish between carboxylic and phenolic hydroxyl groups. Numerous investigators have presented the bulk content of various groups. However, the role of active hydrogen on the surface properties of graphite or coal has not been determined.

2.5.2.3 Oxidation of Surfaces

The reaction of oxygen and carbon until recently was difficult to elucidate because of the impurities in carbon. Preparation of pure graphite and carbon has made the reaction easier to study although it has been realised that the kinetics of the process are complicated. The different crystallographic directions in the basal plane of graphite are attacked at different rates and the basal plane itself contains considerable crystal defects which become sites of localised attack (36). Minute amounts of foreign atoms can have an enormous effect on the rates of oxidation.

Many investigators have found that the edges of the crystals, flakes, and microcrystallites, oxidize more rapidly than the surface, which consists of basal planes. The rate of oxidation of the atoms

in the basal plane of crystallographically perfect lattices was observed to be negligible. In a review of the rate of oxidation, it was (36) pointed out that the oxidation of the edges is usually four to one hundred times faster than that perpendicular to the basal plane. Henning (37) showed that the edge atoms are at least 10^{12} times as reactive as those in the basal plane. He also stated that about 10% of the basal plane consisted of edge atoms.

Studies into the nature of chemisorbed layer of oxygen on carbon and graphite indicated that carboxylic, phenolic, and quinone groups may be present. The nature of the groups has been reviewed by Boehm (25). Other workers (26) have also determined the presence of carboxylic and tertiary hydroxyl groups.

From the foregoing, it is clear that chemisorbed oxygen on graphite and other carbons occurs mainly at the edge surface. As these edges constitute the main adsorbing surface, the oxygen complexes exert a considerable influence on surface behaviour and surface reactions of carbon.

When the coal is oxidised, a reduction in hydrophobicity will result similar to the effect observed on other carbons. This effect has been attributed to surface oxidation which takes place readily at atmospheric temperature. The initial stages of oxidation have been characterized by chemisorption of oxygen at readily accessible surface sites and by formation of acidic functional groups, in particular, -COOH, =CO, and phenolic -OH. If moisture is present some chemisorbed oxygen will also form peroxide or hydroperoxide complexes.

A phenol theory of coal oxidation (38) advanced a series of

postulates which suggested a reaction sequence, as shown below, beginning with formation of phenols and proceeding through carbonyl compounds (quinones) to acid anhydrides and carboxylic acids.

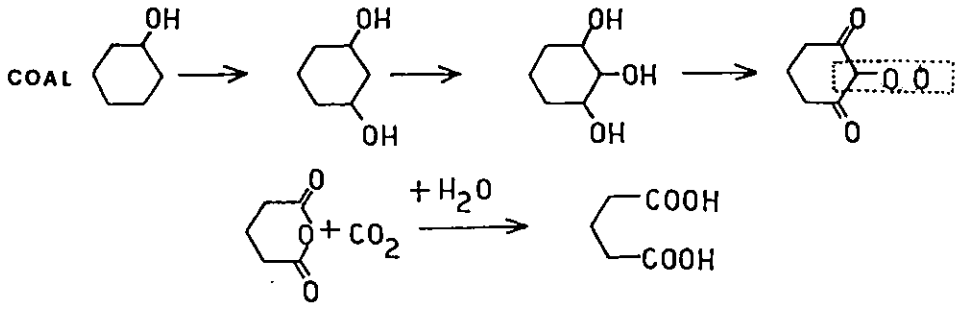

The formation of phenols has been qualitatively confirmed (39). It has been shown that oxygen uptake by various coals and susceptibility of known phenols to oxidation could both be greatly reduced by methylation. Van Vucht et al (40) found an increase in OH groups during the oxidation of coal. These results were also confirmed by infrared studies (41). Dry oxidation studies of subbituminous coal by Jensen et al (13) have shown that phenolic structures appear well before appreciable amounts of the carboxylic acids are detected. From a large number of infrared spectra, it has been shown that the result of oxidation, is (1) an increase in the number C-O, O-H and hydrogen-bonded OH groups (2) the appearance of C=O groups, and (3) the elimination of aromatic C-H bonds. It was concluded that the main reaction during oxidation is the formation of carboxyl groups from C-H groups on aromatic nuclei.

The effect of oxidation on the floatability of various coals has been established. However, in many cases, quantitative measures of the degree of oxidation have not been made. Furthermore, detailed

characterisation of the surface properties of oxidized coals has been lacking.

2.6 Natural hydrophobicity

Gaudin et al (42) proposed that natural hydrophobicity results when at least some fracture or cleavage surfaces form without rupture of interatomic bonds other than residual (van der Waals) bonds. Therefore a hydrophobic surface is one on which saturated molecular bonds are present or predominate so that conditions for water molecule attachment are much less favourable.

Thus in graphite the carbon atoms lie in layers which are in the form of hexagonal lattices. Strong atomic bonds exist between the carbon atoms in the plane of these layers, but the bond between layers is formed by weak molecular forces. This is why graphite can be readily split along the cleavage plane between the layers, and why the surface which coincides with the cleavage plane is hydrophobic. However, the plane perpendicular to the cleavage plane has unsaturated atomic bond forces, causing it to react with water as a hydrophilic surface.

According to Glembotskii (14), the extent to which coals are naturally hydrophobic is closely dependent on their metamorphism. In nature there are two basic processes which affect the flotation properties of coals in opposite ways. Firstly, the organic matter becomes carbonized and its crystalline structure acquires a regular pattern. These processes increase the natural hydrophobic properties of coal. Secondly, the organic matter is oxidized and carbonyl and carboxyl groups are formed, these readily react with water and render

the surface hydrophilic.

Gaudin (43), commenting on the correlation between rank and contact angle, noted that the ash content of a coal influenced its wetting properties, the greater the ash content the less hydrophobic the sample. This is to be expected since silicates and other ash forming minerals are readily wetted.

Taggart et al (44) suggested that the variation in natural hydrophobicity of coals of differing ranks is due to variation in the C:H ratio.

To explain the different floatabilities of various coals Sun (45) has developed a surface components theory which is based on the concept of a balance between hydrophobic and hydrophilic constituents. He correlated bulk chemical analyses with the surface hydrophobicity and proposed a formula to calculate the floatability of a given coal. Although calculated and actual floatability values were in agreement the approach has two defects: firstly such complete chemical analyses are rarely available and since the analyses are based on the bulk sample, surface oxidation can completely destroy the estimate.

Several workers have determined that coals show substantial contact angles in distilled water. The water-receding contact angle is the one of interest in the attachment of air bubbles to coal particles and reported values range from 10 to 20 degrees for anthracites to near zero degree for low rank coals. The advancing contact angle is of interest in the removal of air bubbles from coal particles and with reported values from 60 to 85 degrees is close to the values of the 'equilibrium' angle by which natural hydrophobicity of coals has been characterized.

CHAPTER 3. INTERACTION WITH ELECTROLYTES AND POLYMERS

3. INTERACTION WITH ELECTROLYTES AND POLYMERS

3.1 Stability of suspensions

Suspensions are termed "stable" when the rate of particle aggregation is very slow. Particle aggregation is caused by the universal van der Waals attractive forces which operate between the atoms of the various particles. Forces acting against particle aggregation are consequences of Brownian motion and repulsive interactions between particles with similarly charged electrical double layers.

The theory relating the energy due to overlap of electrical double layers and the London - van der Waals energy in terms of interparticle distance, and their summation to give the total energy is known as the DLVO theory after its founders, Derjaguin and Landau (46), and Verwey and Overbeek (47). The theory considers both the interaction between two parallel charged plates, and between two charged spheres. Mathematically the latter is difficult but a satisfactory general description of stability can be derived from the first treatment.

As two particles, both having diffuse double layer of the same sign approach each other, parts of the diffuse layers overlap. This interaction results in repulsion between particles. The repulsive potential energies at various distances of separation can be calculated (48). The repulsive potential function against distance is of an exponential character and is maximum at zero distance decreasing rapidly at greater distances (Figure 3.1).

The attractive interparticle forces are of atomic origin and are called van der Waals forces, including Debye, Keesom and London forces.

However, only the London attraction has a sufficiently long range to be of importance in coagulation. The Keesom force originates in the interaction of adjacent dipoles and the Debye force from the induction of a dipole in an atom caused by the presence of a dipole in an adjacent atom. The London force however, is due to charge fluctuations in an atom associated with the motion of the electrons; such fluctuations produce a transient dipole moment in the atom, and a phase difference between the transient dipoles of adjacent atoms results in an attractive force between them. All three types of van der Waals forces show a similar dependence upon the interatomic distance, the energy of attraction varying inversely with the sixth power of the distance. However, in the case of aggregates of atoms, e.g., particles, the total interaction energy due to Keesom and Debye forces is not equal to the sum of separate interaction energies because these forces interact with each other. The London energy on the other hand can be obtained by summing the attractions between all the atoms involved.

The total energy of interaction is obtained by summation of the electrical double layer and van der Waals energies, as shown in Figure 3.1. The repulsion is an exponential function of the distance with a range of the order of the thickness of the double layer, and the van der Waals attraction energy decreases as an inverse power of the distance between particles. Consequently, van der Waals attraction will predominate at very small and very large distances. At intermediate distances double-layer repulsion may predominate, depending on the actual values of the two forces.

If the potential energy maximum is large compared with the

thermal energy of the particles, the system should be stable; otherwise the system should coagulate. Therefore, coagulation can be enhanced by reducing the total potential energy through reducing the Stern potential (and zeta potential). Depending on the characteristics of the different types of counter ions involved in colloidal system, the repulsive zeta potential of the particles can be reduced either by the compression of double layer thickness by increasing the ionic strength or by the specific adsorption of counter ions in the Stern layer, with a concurrent reduction in the Stern potential.

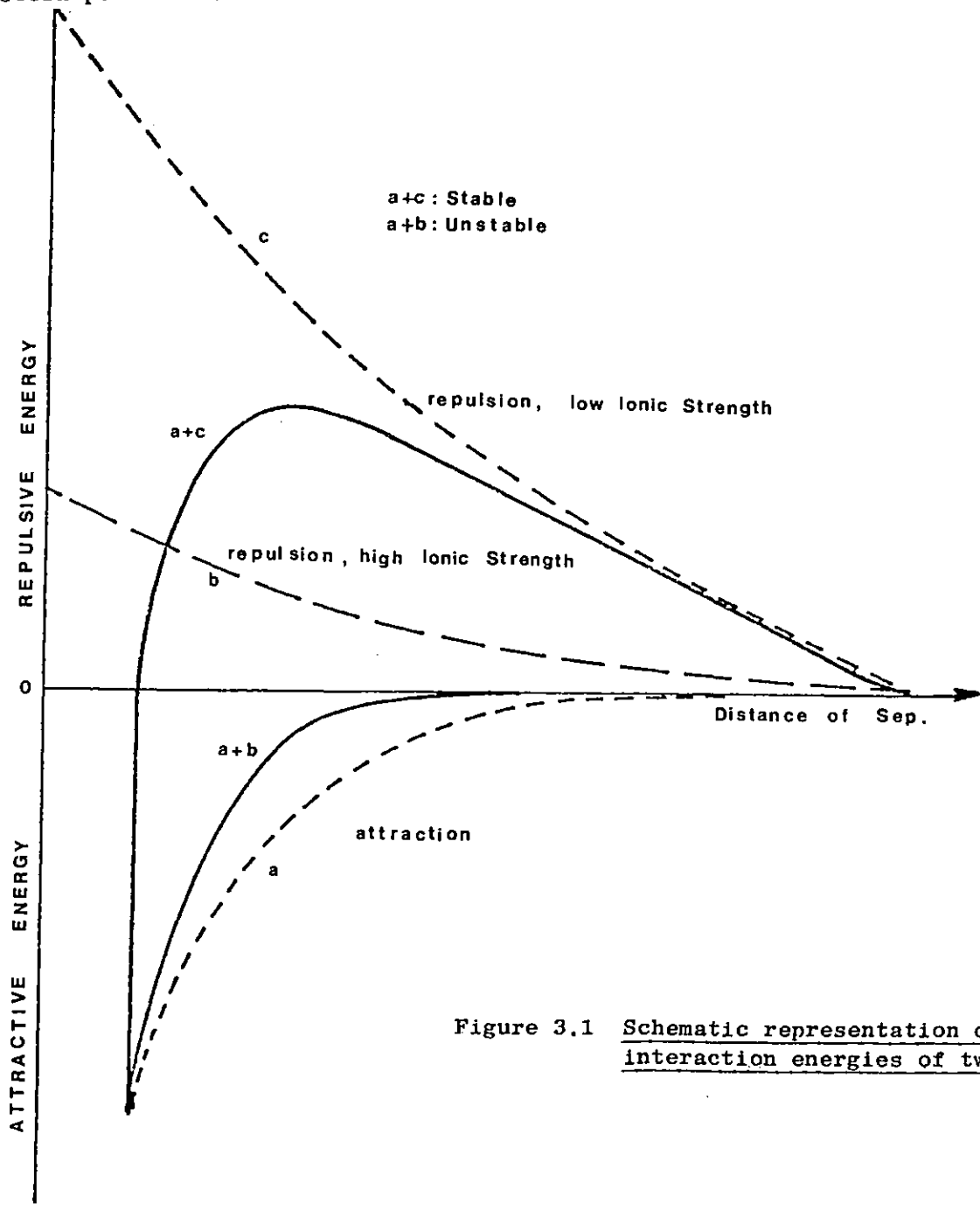

Figure 3.1 Schematic representation of the interaction energies of two particles

3.2 Coagulation by electrolytes

In coal washery slurries, particles usually have a negative surface charge. This surface charge attracts ions of opposite sign from solution. When an electrolyte is introduced into an aqueous suspension the electrolyte molecules dissociate, forming anions and cations. The positive cations will be attracted by the opposite surface charge to the solid surface as counter ions. Hence the concentration of cations in the vicinity of the solid surface can increase considerably upon addition of an electrolyte. Due to the greater number of counter ions in the vicinity of surface the potential drops more rapidly than without electrolyte, consequently the zeta potential is decreased. This sharper drop in potential considerably reduces the repulsive forces and the net potential energy maximum and therefore coagulation may take place.

Various cations have differing effects on the reduction of zeta potential, the valency of the cation being the main factor. The higher the valency, the greater is the reduction of zeta potential at a given electrolyte concentration. The Schulze-Hardy rule (49) expresses the relationship between the ratio of molar concentration of mono-, di-, and trivalent ions required for coagulation as $1:(1/2)^6:(1/3)^6$. Thus divalent ions like Ca^{2+}, Fe^{2+}, Mg^{2+} and trivalent ions such as Al^{3+}, Fe^{3+} are more effective than monovalent ions. Ionic size also will influence the effectiveness of ions as coagulants. Large ions, because of their influence on the thickness of the double layer and thus on the zeta potential will be more effective coagulants than similarly adsorbed smaller ions. Since ionic hydration decreases as the ionic radius increases,

a decrease in ionic hydration should promote the compression of the electrical double layer because the hydration layer reduces electrostatic interaction between the counter ions and the solid surface. So it is clear why the ability to compress the electrical double layer and reduce the zeta potential increases in the series from Li^+ to Ba^{++}.

Since coagulation by electrolytes relies mainly on van der Waals attraction it is most suitable for the aggregation of finely divided solids. The aggregates formed in electrolyte coagulation are usually small and fairly compact. Sedimentation velocities are low and the sediment obtained is not very permeable.

3.3 Adsorption of metal ions at the solid/water interface

The adsorption of metal ions by oxide minerals has been widely studied and it has been established that polyvalent metal cations adsorb on oxides in the pH range where the concentration of first or second hydroxy complex is at a maximum. On quartz, the adsorption was characterised by a reduction in the negative zeta potential and charge reversal, if sufficient metal salt was added.

Although the actual specific mechanism is unclear, there are various proposals for the mechanism of adsorption of metal species at the oxide/water interface. The simple "ion exchange model" considers the reaction of the free metal ion with surface hydroxyl groups to form a coordinate metal-oxygen bond with the release of H_2O and H^+. Fuerstenau and co-workers (50) proposed a mechanism of adsorption involving a condensation reaction. A first or second hydroxy complex is adsorbed initially by a hydrogen bonding, then a water molecule is eliminated leaving a positive site. Healy

and his associates (51) proposed that the relative hydration energies of the hydrated cation and the hydroxylated cation may be used to explain why the hydroxylated metal species is involved in the adsorption process. For highly charged cations the energy involved in removing hydration sheaths, thus allowing the ion to penetrate the Inner Helmholtz Plane, was considered to be so large that the overall value of free energy of adsorption would be positive. Reduction of the charge on the cation by hydroxylation would reduce the solvation energy and a net negative free energy would be obtained. These authors also considered the possibility that the adsorption was an interfacial precipitation of the metal hydroxide occurring at a lower pH than the bulk value. Charge reversal would therefore be obtained between the pH value at which the hydroxide forms, and the PZC of the hydroxide (as the layers build up). Although this theory explains a number of experimental observations it does not readily show why cationic metal species adsorb onto positive oxide surfaces (50). Matijevic and co-workers proposed that the reversal of the zeta potential of silica, at low pH values, in the presence of hydrolysable metal ions is caused by the adsorption of polymeric cationic species(52).These authors suggested that aluminium hydrolyses in solution to form $Al_8(OH)_{20}^{4+}$ species. The adsorption of these species in sufficient concentration on silica surfaces could account for the positive zeta potentials. This theory has only been suggested for the aluminium-silica system, and it may not be applicable to other metal ions, where the formation of polymeric species is uncertain. However, no conclusive evidence has been obtained to show that any one of the above types of

adsorption occurs uniquely on a given system.

Reported studies on the interaction of metal cations with coals are virtually non-existent. Recently, Wen and Sun (22) studied the adsorption of positively charged hydrolysis products of metal ions on bituminous coal by zeta potential measurements. The presence of ferric and aluminium salts changed the zeta potential of coal from negative to highly positive values. They have observed two charge reversal points on the zeta potential - pH curves of coal. This result, similar to that observed with quartz, was explained either by the adsorption of cationic metal hydroxy complexes or the appropriate collodial metal hydroxide.

Since carbon surfaces show many characteristics of an oxide surface, it is reasonable to assume that the adsorption characteristics of metal cations onto coal surfaces would show similarities with those on oxides.

3.4 Flocculation by polymers

The process of aggregation initiated by the action of high molecular weight polymers is known as flocculation. Efficient flocculation can be effected by very low dosages of polymer (in the order of a few p.p.m. in the liquid) and occurs within seconds of mixing the flocculant with the suspension. The large, loosely-textured, fluffy aggregates (flocs) obtained settle rapidly and occupy a large final volume.

These observations indicate that the effect of a flocculant is to form stronger inter-particle bonds than those present in coagulated systems. This requirement is satisfactorily incorporated into the "bridging" theory of flocculation whereby a macro-

molecule adsorbed by one particle extends into solution and is capable of being adsorbed by another particle. This bridge is the basic link in the formation of a large, three dimensional, network of flocs.

3.4.1 Adsorption of polymers at solid/liquid interface

The efficiency of a polymer is largely determined by its adsorption characteristics. The adsorption of polymers is much more complicated than that of inorganic or surface active ions on solids because of their complex macromolecular nature.

Adsorption from aqueous solution in all cases is governed by the interactions between the solid and the adsorbate which, in turn, are influenced by their interactions with the solvent. In case of the polymers, an additional major factor is the configuration of the polymer molecule and the changes in it during, as well as subsequent to, the process of uptake. Alterations in configurations of adsorbed polymer molecules can lead to important changes in the fraction of polymer segments in active contact with the surface of solids. All such changes can also lead to further variations in adsorption density and in the performance of interfacial processes such as flocculation.

Polymers adsorb far more easily than monomers. Adsorbed amounts may be considerable even at extremely low equilibrium concentrations, although at higher concentrations the adsorption density tends to become constant. The adsorption isotherm is then of the high-affinity type (Langmurian).

In many cases the plateau value of the amount adsorbed for polymers is of the order of 1 or 2 mg m^{-2}. Estimates for a close-

packed monolayer of monomer units show that it is impossible to accommodate such amounts of material in direct contact with the surface. This has led early investigators (53) to postulate that only part of the adsorbed chain molecules is directly bound to the adsorbing interface. A sequence of such bound monomer unit is called a 'train'. The remaining units should find a place in sequences with both ends on the surface (loops) or sequences with only one end on the surface (tails). This is schematically pictured in Figure 3.2.

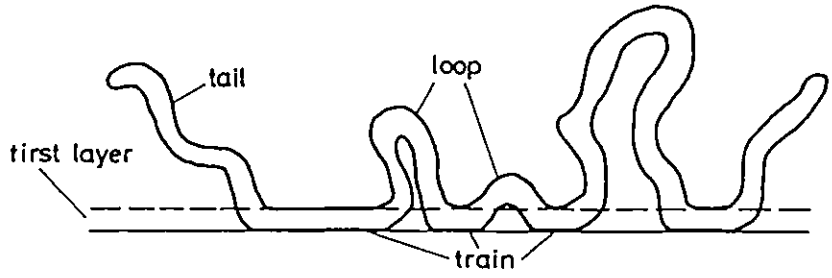

Figure 3.2 Model representation of an adsorbed chain molecule

The loop, train and tail model implies that the adsorbed molecules extend a considerable distance into the solution.

Because of the large number of segments in contact with the surface, it is statistically very unlikely that desorption of all segments will occur simultaneously. However, this fact does not mean that the polymer adsorption is irreversible. By change of conditions, such as pH or addition of a high concentration of a surface competitor, it is generally possible to displace a polymer that would be completely immune to washing with water.

The driving force for adsorption is the reduction in free energy

arising from the binding of train units to the surface. The binding process includes the removal of solvent molecules from the surface. The reduction in free energy upon binding is counteracted by the changes in conformation from a wholely three dimensional coil to an (at least partially) two-dimensional structure. This rearrangement process is accompanied by a considerable loss of entropy per molecule which depends on chain length and chain flexibility. As distinct from smaller molecules, with polymers flexibility is very important and the conformation of polymer molecules and an interface is a key feature in polymer adsorption.

Considerable advances in the theoretical analysis of polymer adsorption have been made in recent years. Reviews of the major aspects of the theories are reported in the literature (54)(55) (56). The main object of these theories has been to predict how certain parameters, e.g., the mass adsorbed per unit area, the fraction of segments in trains, and the thickness of the adsorbed layer depend on the various variables of the system such as polymer concentration, molecular weight, temperature, solvency, etc.

Despite all the advances in the theoretical treatment of polymer adsorption, the formulation of a thermodynamic model describing the adsorption process still presents many problems. These arise partly from difficulty in identifying and defining the various processes involved in the adsorption (for example, the role of the solvent has often been ignored), and partly because of the lack of reliable experimental data.

So far, information about the fraction of segments in trains and

loops has been obtained by using spectroscopic methods such as IR (57)(58), ESR (59) and NMR (60). Direct measurements of the interaction between particles with adsorbed layers, as a function of their distance of separation have reported using a surface balance (61) and using a compression technique with a concentrated latex (62). Knowledge about the net interaction energy between the surface and the segments has been obtained from microcalorimetry (63). Finally, the effective adsorbed layer thickness, an important parameter which offers some insight into the structure of adsorbed layer has been measured by a number of different techniques, namely, ultracentrifugation (64), viscometry (65)(66), ellipsometry (67)(68), spectroscopic methods (69), and electrophoresis (69)(70).

However, classical measurements of adsorption isotherms still form the majority of the reported experimental data on polymer adsorption. Although, in principle, polymer adsorption isotherms are readily determined, the time required to reach a steady state may be considerable. Also reliable, accurate data is often only presented for the plateau region of the isotherm, whereas the interesting region, at least for making comparisons with theory, is the initial, rising part of the isotherm, where lateral interactions between adsorbed polymer molecules are absent. The main problem here is that one is usually faced with measuring trace quantities of polymer in bulk solution. Furthermore, it is difficult and may even be misleading to deduce anything about the state of the adsorbed layer from adsorption isotherms alone. For this reason, a combination of classical adsorption isotherms with

direct observation of layer conformation is a more powerful approach. For practical purposes adsorption isotherms do provide qualitative analysis of the distinct interactions governing the adsorption of the polymer onto a solid surface. Thus by modifying the possible adsorption sites the different responses can be measured and some information can be obtained for various interaction mechanisms involved.

3.4.2 Mechanisms of interaction with polymers

Various polymer-surface interaction mechanisms have been postulated for a number of different mineral-flocculant systems.

a) Coulombic attraction - Adsorption is possible when the polymer and the surface are of opposite charge, resulting in non-specific electrostatic interaction. Addition of an oppositely charged polymer is almost always likely to produce flocculation. It is also suggested that since surfaces are heterogeneous with regard to charge, there can occur areas on the surface with higher, lower or even opposite local charge to the overall surface charge. This means that if the greater part of the surface is negatively charged, there may be small areas of positive charge. Anionic polymer can then be adsorbed onto these relatively small areas even though the net charge of the particle is of the same sign as the polymer.

b) Hydrogen bonding - This is a very common type of bonding exhibited by organic acids, amides, alcohols, amines, etc., which contain a hydrogen atom attached to a strongly electro-negative atom, e.g., O,N,S. In these compounds the hydrogen atom has lost much of its electronic atmosphere, and is ready to accept electrons donated by the surface atoms of the solid. The hydrogen is then shared between

the surface atoms (usually oxygen) and the oxygen and nitrogen in the polymer. Taken individually, this is a relatively low-energy bond (25 kilojoules per mole), but an acrylamide polymer of molecular weight one million, for example, can form up to 14000 such bonds and the total energy of attachment per molecule is enormous. This mechanism has been shown to be responsible for the adsorption of polyacrylamide flocculants on to fresh silica (71) and various clays (72).

c) Activation of solid surfaces - When the polymer and the surface have the same sign of charge electrostatic repulsion prevents polymer adsorption and hence flocculation. In virtually all such cases no adsorption occurs in the absence of added salt. Some critical concentration of electrolyte (often a divalent metal salt) is necessary for adsorption. Although it is possible that some general ionic strength effect is involved, it is more likely that ions such as Ca^{2+} promote adsorption by binding ionic groups on the polymer to charged sites on the particle surface. This effect is analogous to the use of metal ions as activators to promote the adsorption of collectors in some types of mineral flotation.

d) Complex formation - Another possible contribution to the adsorption of polymers could be complex association with transition metal ions in mineral lattices. This kind of interaction has been suggested in the flocculation of copper carbonate by polyethyleneimine (73).

e) Another possibility with ionic crystals is the interaction of dipolar groups on the polymer with the electrostatic field at the crystal surface. Such a mechanism has been postulated for the adsorption of polyacrylamide on fluorite particles (74).

f) Hydrophobic association - This type of interaction may be responsible for the adsorption of non-polar groups onto some surfaces. In the adsorption of polyphenols on graphitised carbon black, it is believed that the hydrocarbon chains of the phenols are probably held to the hydrophobic surface of the graphitised carbon black by hydrophobic interaction (73).

Hydrophobic interaction usually arises from the tendency of non-polar groups of organic molecules to adhere to one another in a polar aqueous environment (75). The free energy change corresponds to the removal of a non-polar group from its aqueous environment and the resulting Van der Waal s attraction between the non-polar group and the hydrophobic surface. In fact, the attraction of non-polar groups, such as hydrocarbon chains, for each other by Van der Waal's forces is small (76) and plays only a minor role in the adsorption process. The major contribution to the energetics of adsorption probably arises from the change in the nature of the hydrogen bonds of the structured water molecules near the non-polar surface (77). The total free energy change for the removal of a nonpolar CH_2 unit from the aqueous phase into a nonpolar environment has been estimated to be 2.5 to 3.3 kilojoules per mole of CH_2 groups (78). As this small figure is compounded by the large number of structural and energetic factors involving molecules, substantial free energy changes are involved in hydrophobic association (78).

3.5 Flocculation of coal

Flocculation has been applied in coal preparation, in a number of solid/liquid separation processes, including thickening, filtration and water clarification.

Coal washery refuse pulps contain appreciable quantities of finely divided clays as well as coal particles which will not settle unless flocculated. Under these conditions the addition of flocculants may be economically justified by the improved operating conditions which result from the recirculation of solid-free water and the avoidance of environmental pollution. These benefits, have been discussed by Dahlstrom (79) and Matoney (80) and their recognition is evidenced by the expanding use of flocculants in coal washeries.

The main problems associated with the use of a flocculant in a coal washery circuit are the selection of effective flocculants from the almost unlimited range of reagents available, and the prediction from small-scale experimentation of the quantity of flocculant required for a particular plant operation. The selection of a flocculant for a particular suspension is largely a trial and error process. The main obstacle to a theoretical approach is inadequate knowledge of the surface chemistry of particles in water and of the specific mechanisms of polymer adsorption.

Since the principal applications of flocculation in the coal industry lie in the area of waste water treatment, the main concern is more with the behaviour of associated minerals than with the coal itself. Matheson and Mackenzie (81) studied the flocculation of sub-micron sized clay particles in coal washery refuse pulps. They showed that the adsorption of anionic polymers on to the negatively charged clay particles is prevented by electrostatic repulsion between ionized carboxyl groups of the polymer and the negative Stern potential. In the presence of Ca^{++} however, flocculation

was obtained. They suggested that Ca^{++} ions reduce the Stern potential and so permit the adsorption of anionic polymers by hydrogen bonding. It was also considered that the ionized hydroxyl groups of the polymer chain become attached by electrostatic forces to Ca^{++} ions adsorbed in the Stern layer. The action of the Ca^{++} ions, therefore, appears to be similar to the calcium activation of silicate minerals for flotation with anionic collector reagents (82).

The evaluation of synthetic organic flocculants in the treatment of coal refuse slurries was carried out by the USBM (83). Poor flocculation of the suspensions with the anionic flocculants was attributed to the high negative surface charge of the particles. It was concluded that anionic polymers actually increased the negative charge so that effective aggregation of the particles was not possible. However, no specific interaction mechanism was suggested and it is not clear how anionic polymers adsorbed on the highly negatively charged particles. In the same study, it was also observed that the best flocculation results were obtained when the anionic polymer was added first, followed by cationic polymer. It is known that a cationic polymer causes the flocculation of negatively charged particles by the electrostatic interaction mechanism and also serves to provide positively charged regions on the particle surfaces on to which the anionic polymer can subsequently adsorb. Therefore, the opposite sequence of polymer additions should be expected to produce the best flocculation results.

Flocculant adsorption on washery waste water solids was studied by Mirville and Hogg (84). An important finding of this work was that polymeric flocculants appear to be very strongly adsorbed on

coals. They showed that the coal particles can adsorb up to ten times as much non-ionic polymer per square cm of surface as the mineral constituents (clay, quartz). This result suggested that the adsorption of non-ionic polymers on waste water solids is completely dominated by the coal.

Apart from water clarification, there have been a few studies in which flocculation was applied to remove fine coal particles, selectively, from the coal-refuse slurries. In a USBM study (4), selective flocculation was applied to minus 400 mesh coal and shale. It was found that fine coal particles selectively flocculated in the presence of associated mineral matter. Low molecular weight non-ionic polymer functioned effectively and alkaline conditions (around pH 11) were found to be most favourable. No explanation was given for the result but it is likely that under the conditions used non-ionic polymer adsorption on the impurities did not occur so that coal particles underwent flocculation whereas impurities remained in the suspension. It was also observed that the flocculated sediment contained entrapped shale, and required further treatment.

In the selective flocculation of coal it is likely that various other particles will settle quicker than the flocculated coal because of density differences. For this reason, Blaschke et at (3) suggested that selective flocculation would be best under conditions where the coal particles were dispersed and impurities flocculated. Although the study was conducted by the method of trial and error, the results showed that under certain conditions flocculation of impurities occurred whereas coal particles remained in the suspension. Unfortunately a fundamental investigation of this result has not been made.

CHAPTER 4. MATERIALS AND EXPERIMENTAL TECHNIQUES

4. MATERIALS AND EXPERIMENTAL TECHNIQUES

4.1 Materials

4.1.1 Characterization of coal and graphite samples

The coal samples used in this work were obtained from various N.C.B. coal fields to represent different ranks. Their sources were as follows:

Table 4.1 Sources of coals used

Rank	Source
Anthracite	Cynheidre, South Wales area
Medium volatile coal	Derwenthaugh, North East area
High volatile coal	Bilsthorpe, East Midlands area

The lithotype samples, namely vitrain, durain and fusain were separated from the $\frac{1}{2} + \frac{1}{4}$" fraction of a sample of anthracite by hand picking. A point counting technique on polished pellets of the anthracite showed that it contained 73% vitrain, 20% durain and 7% fusain.

Most of the coal samples were supplied as -1" lumps and these were crushed and ground to -72 mesh (0.2 mm). Samples of the 0.2 mm material were further ground to -350 mesh (45μm) in a steel vibrating mill (as coal is a relatively soft material, negligible contamination by iron is incurred). This size fraction was used throughout the study. For the potentiometric titrations and, where required, for the electrokinetic measurements 10 g of -45 μm anthracite was conditioned with 100 ml of 10N HCl for 2 h. After this treatment the sample was repeatedly filtered and washed with double distilled water for a few days until the pH of the aqueous

anthracite suspension had reached at least pH 5. The sample was then vacuum dried at room temperature.

Proximate analyses of the coal samples were made according to BS 1016 (85) on the -72 + 100 mesh (-0.2 + 0.15 mm) fractions and results obtained are shown in Table 4.2.

Table 4.2 Proximate analyses of the coal samples

		As received, %			
Sample	NCB Rank Code	Ash	Volatile Matter	Moisture	Fixed Carbon
Anthracite	101	2.26	5.70	0.78	91.26
High volatile	700	3.48	33.50	4.05	38.97
Medium volatile	301	6.56	23.80	0.60	69.04
Vitrain	-	1.19	-	-	-
Durain	-	16.50	-	-	-
Fusain	-	9.85	-	-	-

Ultimate analyses of the anthracite were made by the Analytical Services Laboratory at Imperial College. The results are given in Table 4.3.

Table 4.3 Ultimate analyses of the anthracite

	Carbon %	Hydrogen %	Nitrogen %	Sulphur %	Oxygen %
Anthracite	90.53	2.97	1.35	0.80	4.35

XRF analyses of the coal samples, also carried out by the Analytical Services Laboratory, showed that the other main elements present were Aℓ (0.5 - 0.05%) and Fe (0.05 - 0.5%). Trace amounts of K, Na, Mg, Ca, Si, S and Cl were also detected.

The XRD patterns derived from the coals were very diffuse but examination showed that there are broad peaks in positions related to those of the sharp peaks given by crystalline graphite. Broader peaks are commonly associated with small crystalline size. Where a sequence of graphite peaks is replaced by one broad, asymmetrical peak, it is suggested (5) that in coals there are small layer planes present of the graphite type, but they are stacked without regular order from one to the next.

Infrared spectroscopy was used to obtain an information on the surface groups. Discs of the coal powders which were made up with spectroscopically pure KBr were used. The spectra were obtained with a Perkin Elmer 599B Infrared Spectrophotometer shown in Figure 4.1. Infrared spectra of the high and medium volatile coals generally showed the absorption bands which were characteristics of coal material (86). However, the absorption bands present in these coals were essentially absent or considerably reduced in the spectra of anthracite and its lithotypes.

A volumetric gas adsorption apparatus was used to measure adsorption isotherms. For nitrogen at $-196^{o}C$, five adsorption measurements in the range 0.05 - 3.0 relative pressure, $P/_{Po}$ (where: P, the equilibrium pressure; and Po, the saturation pressure of the adsorbate at the adsorption temperature) were taken to calculate the surface area using the BET equation which gave a value of 7.8 $m^2\ g^{-1}$ for anthracite.

Ash from the anthracite sample used in electrophoretic mobility measurements was obtained by the radio frequency ashing technique (87) which was carried out at low temperature ($100^{o}C$) so that

Figure 4.1 Infrared Spectra of coals

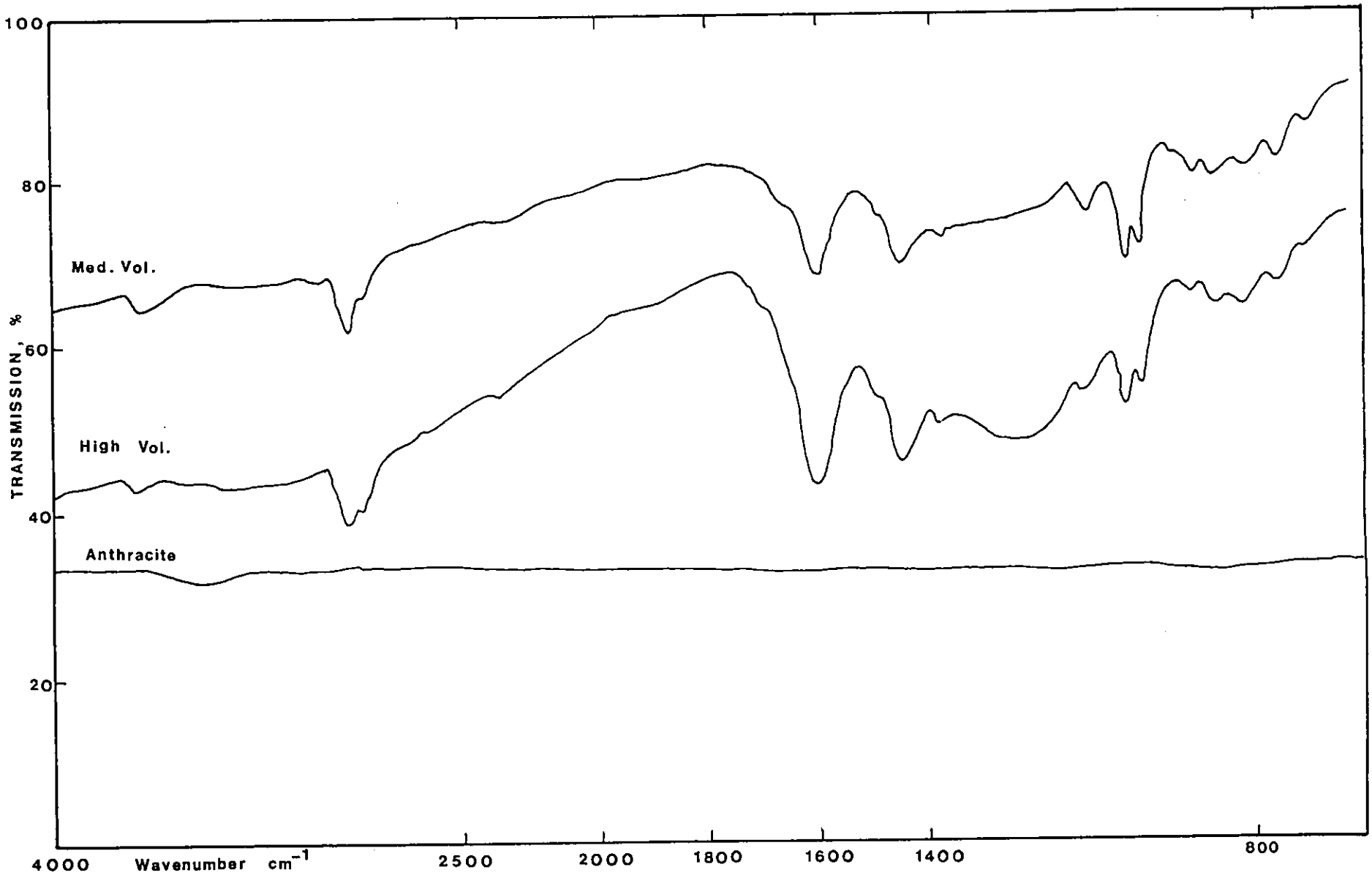

mineral matter in ash was left unaltered.

Hydrophobicity of the anthracite was qualitatively assessed by using a simple vacuum cell. An aqueous suspension was saturated with nitrogen and then the pressure above it reduced. Bubbles preferentially nucleate on hydrophobic surfaces and the ease with which particles were carried to the surface indicated whether or not the anthracite sample was strongly hydrophobic.

Natural graphite, supplied by Hopkin and Williams Ltd., was screened into various size fractions and the carbon content of each fraction determined. The -52 + -72 mesh (-0.3 + 0.2 mm) material containing 98.5%C was ground in a steel vibrating mill to -350 mesh (45 μm). This size fraction was used throughout the study. Preliminary XRF analysis of the graphite showed traces of Fe, Ni and Cu. consequently the sample was leached with dilute HCl to remove impurities (at least from the surface) and washed thoroughly with double distilled water, dried under vacuum and kept in a stoppered bottle. The analysis of the final graphite sample is shown below.

Table 4.4 The analysis of the graphite

	% Wt
Fixed carbon	98.5
Volatile matter	0.5
Ash	0.8
Moisture	0.1
Fe	< 0.05
Ni	< 0.05

The specific surface area of the sample was 3.7 m^2 g^{-1} which was

measured by a BET nitrogen adsorption technique.

Quartz samples used in the selective flocculation tests were obtained from "optically clear" Brazilian quartz rock crystals, which had previously been crushed and leached in hot concentrated HCl. The crystals had then been washed with double distilled water and dried at 100°C. This material was dry ground in a vibrating agate mill and stored in glass stoppered bottles. A semiquantitative XRF analysis showed that the main element present was Si, but there were trace quantities of Ca, K and Fe. The specific surface area of the sample was 1.25 $m^2\ g^{-1}$. Specific surface area was measured on a Quantachrome Corporation "Monosorb" surface area analyser which uses a single point adsorption method.

4.1.2 Chemicals

The chemicals used in this study are presented in Table 4.5 with their purity and sources. In general the solutions used were prepared by weighing out a predetermined amount of the chemical and diluting it with double distilled water. When ageing was a problem, fresh solutions were prepared daily.

Chromic acid for cleaning glassware was prepared by dissolving 7 g of sodium dichromate in a small amount of water then adding 100 ml of sulphuric acid.

High purity water was used throughout the study. It was prepared in a glass still using PTFE sleeved butt joints. Distilled water was passed through a mixed bed ion exchange resin, followed by an activated charcoal bed and then redistilled. The purified water was stored in a pyrex vessel vented to atmosphere via an

activated charcoal filter. The conductivity of this water was 1.0 x 10^{-6} ohm^{-1} cm^{-1}, and showed very short bubble persistence times, so that it was assumed to be essentially surfactant free.

Table 4.5 Chemicals used in the project

Inorganic	Grade	Source
Hydrochloric acid	AristaR	BDH
Sulphuric acid	AristaR	BDH
Sodium hydroxide	AristaR	BDH
Sodium chloride	AnalaR	BDH
Calcium chloride	AnalaR	BDH
Ferric chloride	AnalaR	BDH
Aluminium chloride	99.999%	Koch-Light
Copper chloride	AnalaR	BDH
Potassium bromide	IR spec.pure	BDH
Sodium dichromate	AnalaR	BDH
Sodium carbonate	AnalaR	BDH
Sodium bicarbonate	AnalaR	BDH
Organic		
Tannic acid	AnalaR	Hopkin and Williams
Hydroxyquinoline	AnalaR	Hopkin and Williams
Acetone	Puriss	Koch-Light
Diethyl ether	Pure	BDH
Hyamine 1622	-	BDH
N-methyl n-nitro-N'-nitrosoquanidine	Purum	Fluka
Sodium ethoxide	Pure	Cambrian

4.1.3 Polymers

The non-ionic polymer selected for this study was a high molecular weight polymer of ethylene oxide"Polyox-Coagulant". It is a commercial product from Union Carbide, supplied by BDH. Polyethylene oxide (PEO) is a linear polymer with a molecular weight in excess of 5 million. The chemical composition of the polymer molecule can be represented by:

$$(- CH_2 - CH_2 - O -)_n$$

where n refers to the number of monomer units in the polymer chain.

The polymer solutions of this product were prepared with water free of CO_2 and O_2 (distilled water boiled and purged with N_2). Potentiometric titrations showed that the PEO did not contain acid or basic groups and, therefore, did not acquire charge due to dissociation. Therefore, it should be referred to as non-ionic.

Two other non-ionic polymers supplied by BDH, polyvinyl alcohol (125.000 mol. wt.) and polyvinyl pyrrolidone (700.000 mol. wt.) were also used in some flocculation experiments.

A commercially pure polyacrylamide (PAM) of molecular weight approximately 5.5 million (Cyanamer P250) was provided by the American Cyanamid Company and used as received. Pure PAM itself is virtually non-ionic but it had been previously established by potentiometric titration that commercial PAM may contain about 1% of carboxylic acid groups (71). In this study, influence of this small proportion of carboxylic acid was assumed to be negligible and no attempt was made to convert all carboxylic acid into amide groups.

An anionic polymer of molecular weight several millions (23/12 Na Ac) was obtained from Allied Colloids Ltd. According to the

manufacturer, it was a 23% hydrolysed polymer, presumably prepared by alkali hydrolysis of PAM, the structure probably being

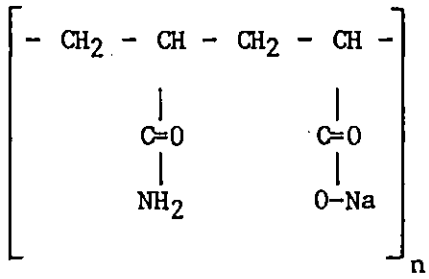

A Cationic polymer (C110) of molecular weight several millions was supplied by B.T.I. Chemicals. It was probably formed by co-polymerization of acrylamide monomer with quartenary ammonium compounds and the structure may be represented by

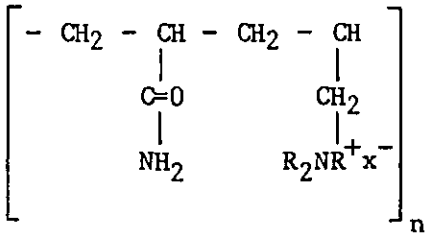

4.2 Experimental methods and techniques

4.2.1 Pretreatment of samples

4.2.1.1 Methylation

Methylation of the anthracite and graphite was carried out with diazomethane (CH_2N_2). This chemical is very toxic and explosive, and so great care must be taken during its preparation. The diazomethane was generated from the reaction of N-methyl n-nitroso N' nitrosoquanidine with NaOH by the technique of Fales et. al. (88), using a special micro-apparatus supplied by Pierce and Warriner (UK) Ltd.

0.5 g of the sample to be methylated was placed in the outer tube with 3 cm^3 of diethyl ether, which had been dried by sodium. 0.5 cm^3 of water and 0.1 g of N-methyl n-nitroso N' nitrosoquanidine were placed in the central tube. The whole apparatus was sealed and placed in an ice bath, in a fume cupboard behind a blast shield. 0.6 cm^3 of 5 M NaOH solution was injected through the septum by a glass syringe fitted with a hypodermic needle. The mixture was allowed to react for up to 2 days. During this long reaction period, additional N-methyl n-nitroso N' nitrosoquanidine was added several times to maintain an excess of free diazomethane in the adsorption chamber. After the reaction period, a yellow colour was always observed in the etheral solution, indicating the presence of unreacted diazomethane. The excess diazomethane and ether were evaporated by applying a vacuum from a water pump. The dry sample was kept in a desiccator until required.

4.2.1.2 Oxidation

The anthracite and graphite samples were subjected to dry oxidation with air and oxygen.

5 g of anthracite of graphite was placed in a quartz tube which was placed in a horizontal furnace. Air or oxygen was passed over the sample at a flow rate of 100 $cm^3\ min^{-1}$. The sample was heated at a rate of $10^oC\ min^{-1}$ to the desired temperature and then kept at that temperature for a specified period of time. Gas flow was then stopped and the sample cooled to room temperature in a flow of nitrogen.

The degree of oxidation has been assessed by infrared spectra of oxidised sample. As can be seen from Figure 4.2 that oxidation

Figure 4.2 Infrared spectra of oxidized anthracites

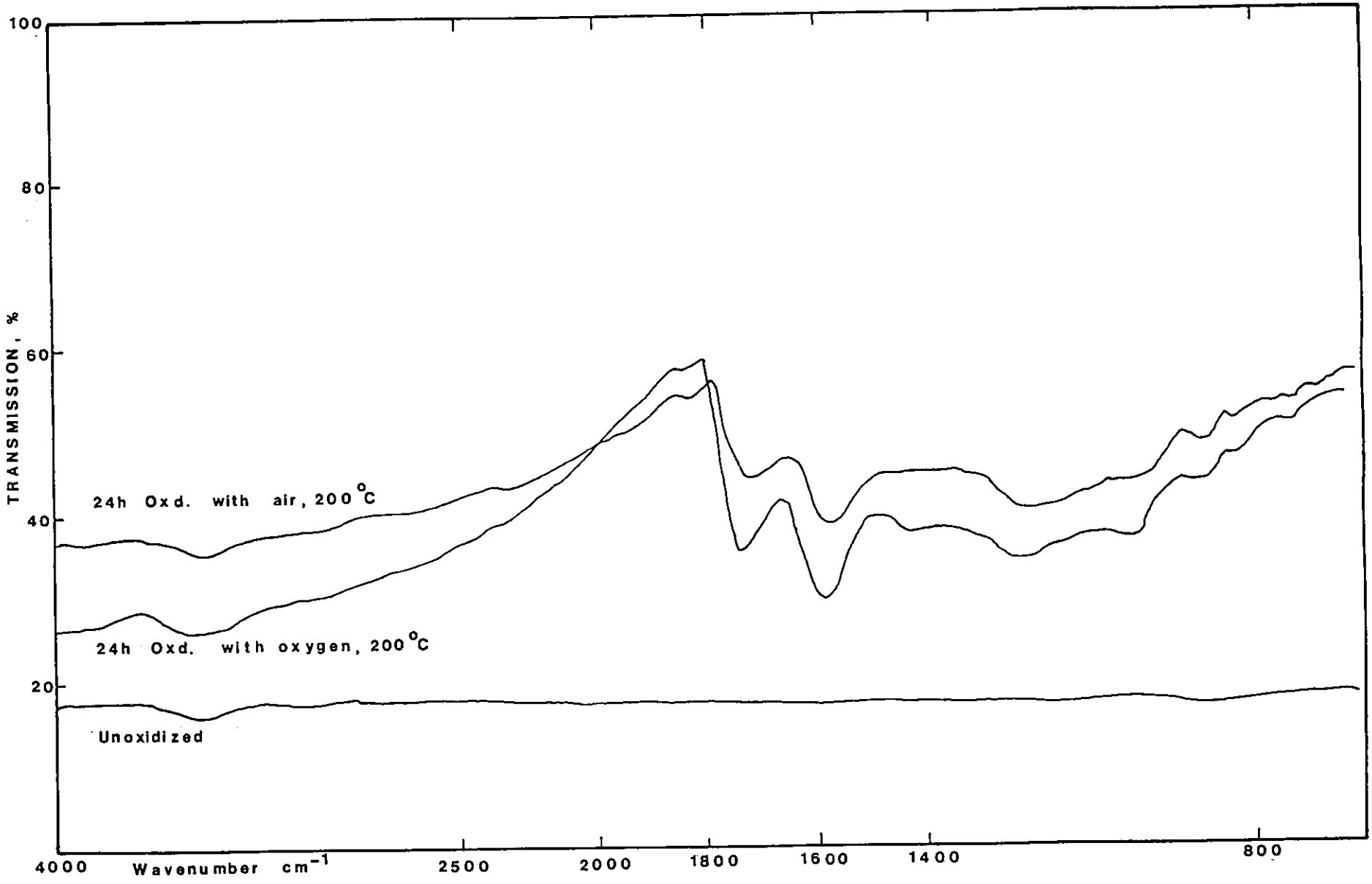

of the anthracite with oxygen has clearly introduced OH and C=O groups at 3400 cm^{-1} and 1700 cm^{-1}, respectively, which suggests the probable formation of COOH functional groups in the oxidized sample. Oxidation of the graphite sample, under the same conditions used for anthracite, had no effect on the spectra obtained.

4.2.2 Electrokinetic measurements

The electrokinetic mobilities of anthracite and graphite particles were determined with a Rank Bros. microelectrophoresis apparatus (Mark II), using a flat quartz cell. A standard suspension was prepared by dispersing 0.05 g of the sample in 50 ml of double distilled water. 1 ml of the standard suspension was added to 100 ml electrolyte solution and the pH adjusted until a constant value was reached, which usually occurred within 10 min. The suspension was then placed in the cell, and the palladium electrodes were inserted. The cell was placed in a water bath, maintained at a constant temperature of 25°C.

The electrophoretic mobilities were measured by timing the motion of individual particles travelling over a fixed distance against a calibrated eyepiece graticule. The applied potential was varied to produce a traverse time between 6 and 9 secs. Timing of fast particles introduces timing error and slower times increases errors due to Brownian motion, inter-particle collisions and convection currents within the cell. Velocities were determined for 10 particles at both stationary levels, and the polarity of the electrodes alternated after each determination to reduce errors due to 'gassing' and polarization. The electrophoretic mobility used in calculations was taken as the mean of 20 determinations. The relative

error was 3 to 5%.

The mobility (u) was calculated from the equation:

$$u = \frac{v}{V/L}$$

where v = velocity ($\mu m\ sec^{-1}$)

V = applied potential (Volt)

L = effective interelectrode distance (cm)

The value of L for the cell was determined for each measurement from the following equation,

$$L = \frac{v}{i} \cdot K.A$$

where i = current

v = applied potential

A = cross sectional area of the cell

K = specific conductivity of the solution (measured with a Portland conductivity meter).

4.2.3 Potentiometric titrations

Potentiometric titrations of NaOH against anthracite and graphite suspensions in HCl were conducted in a flat-bottomed 50 ml pyrex beaker with a rubber stopper. A miniature combined pH electrode supplied by Pye-Unicam connected to a Pye-Unicam PW9418 pH meter was used to measure the pH. The suspension was stirred with a teflon-covered magnetic stirrer. The vessel was purged with oxygen-free nitrogen prior to the measurements, and a constant flow was maintained throughout.

In nearly all the tests 10^{-2} M NaOH was titrated into 25 cm^3 of the 10^{-3} M HCl with a supporting electrolyte of NaCl. The diff-

erence between a blank titration and that obtained in the presence of 1 g of anthracite or graphite was taken as the net abstraction of H^+ or OH^- ions.

Preliminary rate studies were made by allowing the system to come to equilibrium after an addition of NaOH. The change in pH of the suspension was followed with time. For instance, upon addition of an aliquot of NaOH to a suspension at pH 7 the pH was seen to change abruptly to 10 and then drifted slowly with time until an apparent equilibrium at pH 7.3 was attained after 6 hours. A two-step adsorption process was clearly observed, an initial fast increase in the adsorption followed by a much slower adsorption rate. It was thought that the slow adsorption process can be inhibited by the rapid titrations, so that measurements of the pH was made within 15 min after the titrant addition.

Direct surface titrations were performed by titrating 10^{-3} M NaOH in to 1 g of anthracite or graphite powder dispersed in 25 ml double distilled water. Similar titrations were also conducted on methylated samples.

Direct titrations using Na_2CO_3, $NaHCO_3$ and sodium ethoxide were also carried out. It was thought that the end points of these reactions might give an indication of the groups of different acidities present on the surfaces. The results are presented in Appendix I.

4.2.4 Flocculation and stability tests

In all flocculation experiments an arbitrary, but standardized, routine was followed. The tests were carried out in a vertical cylindrical glass tube (diameter 4.5 cm, length 20 cm) fitted with

side outlet at its midpoint.

Highly dispersed suspensions were introduced to the cylindrical glass tube and stirring was maintained at 1000 r.p.m. for 5 min, with a motor driven glass stirrer. At the end of this period a very dilute flocculant solution was slowly added from a 1 ml pipette. The stirring was continued for a further 2 min at the same speed and then reduced to 100 r.p.m. for 1 min, to promote floc growth, then stopped. After standing 2 min the suspension withdrawn from the side outlet and its optical transmittance was rapidly determined. The optical transmittance mesurements were made in a EEL absorptiometer with a neutral density filter, using distilled water as a blank.

The above procedure was also followed in the stability tests where known weights of sample in contact with given volumes of metal salt solutions (200 ml) were dispersed with the aid of ultrasound ("Soniprobe", type 7530A Dawe Instrument Ltd.). The dispersions were placed in the cylindrical glass tube and after given periods of stirring and settling samples were withdrawn from the side outlet and their optical transmittances determined.

4.2.5 Polymer adsorption measurements

Adsorption experiments were carried out in 100 ml glass stoppered Erlenmeyer flasks. Preliminary adsorption tests showed the adsorption of polymers at the anthracite/water or graphite/water interface was rapid, and that no great difference in adsorption was obtained between equilibration periods of 30 min and 12 h. In further tests, therefore, 0.5 g of anthracite or graphite was put into a 100 ml flask with (50-V) ml double distilled water and shaken

vigorously to wet the sample. V represents the volume of the polymer stock solution needed for the desired initial concentration when diluted to 50 ml. Next, the polymer stock solution was added to flask and shaken for 1 h.

After adsorption, the solid was separated from the solution by centrifuging at 3200 r.p.m. for 20 min. Then 25 ml of the supernatant liquid was taken and analysed for residual polymer concentration. The adsorption density was deduced from the difference between initial and residual polymer concentration. The reversibility of adsorption was established by using different amounts of sample in the adsorption tests.

A nephelometric method which was developed by Attia and Rubio (89) for the direct determination of non-ionic polymers in dilute solutions was used to determine the residual PEO concentrations. The method is based on the precipitation of PEO with tannic acid.

The required volumes of PEO stock solution were added to 50 ml flasks already containing 5 ml of tannic acid (0.1%) and 40 ml of NaCl (0.5 M). The solutions were adjusted to 50 ml with double distilled water. The flasks were shaken for about one minute by inverting end over end, and were then allowed to stand for 15 min before measuring the turbidity with a nephelometer head in conjunction with a galvanometer (Univalog type 20/DR, Evans Electroselenium Ltd.). In the measurements the sample of highest PEO content was used to adjust the galvanometer reading to 100 on the linear scale, with distilled water (i.e., zero PEO content) the galvanometer reading was adjusted to zero. Then, the reading was noted for each sample solutions of known PEO concentrations. Typical measurements

were plotted against PEO concentration to produce the calibration curve given in Figure 4.3.

For an anionic polymer (e.g., partially hydrolysed PAM), the residual concentration was determined by a similar technique to that of Crummet and Hummel (90) in which the polymer was precipitated by addition of Hyamine 1622 (p-diisbutylphenoxyethoxyehtyl dimethyl-benzyl ammonium chloride).

1 ml of a 4% solution of Hyamine 1622 was fed continuously over a period of 1 min to 25 ml of polymer solution, the mixture being vigorously agitated by a magnetic stirrer. Careful standardization of these conditions appeared to be essential for the formation of reproducible turbidities, determined with a Perkin Elmer 200 spectro-photometer at 400 μm using a 40 mm cell. A calibration graph is shown in Figure 4.4

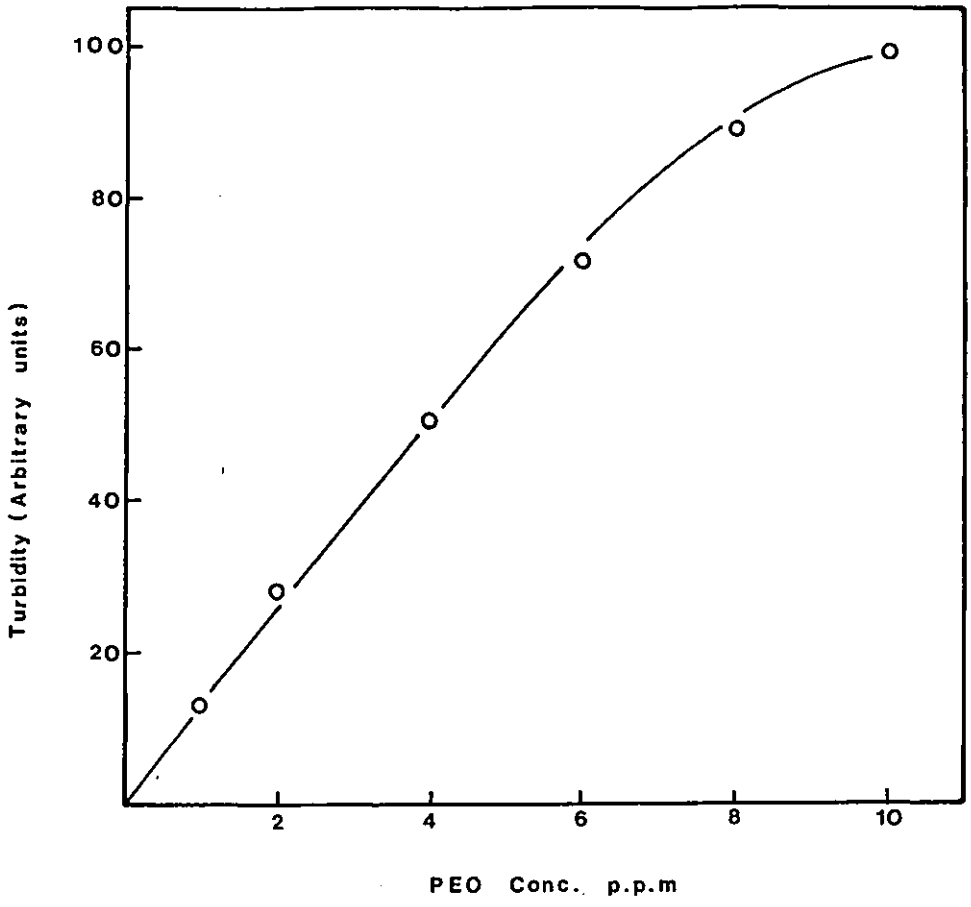

Figure 4.3 Calibration graph for PEO- tannic acid nephelometric analysis

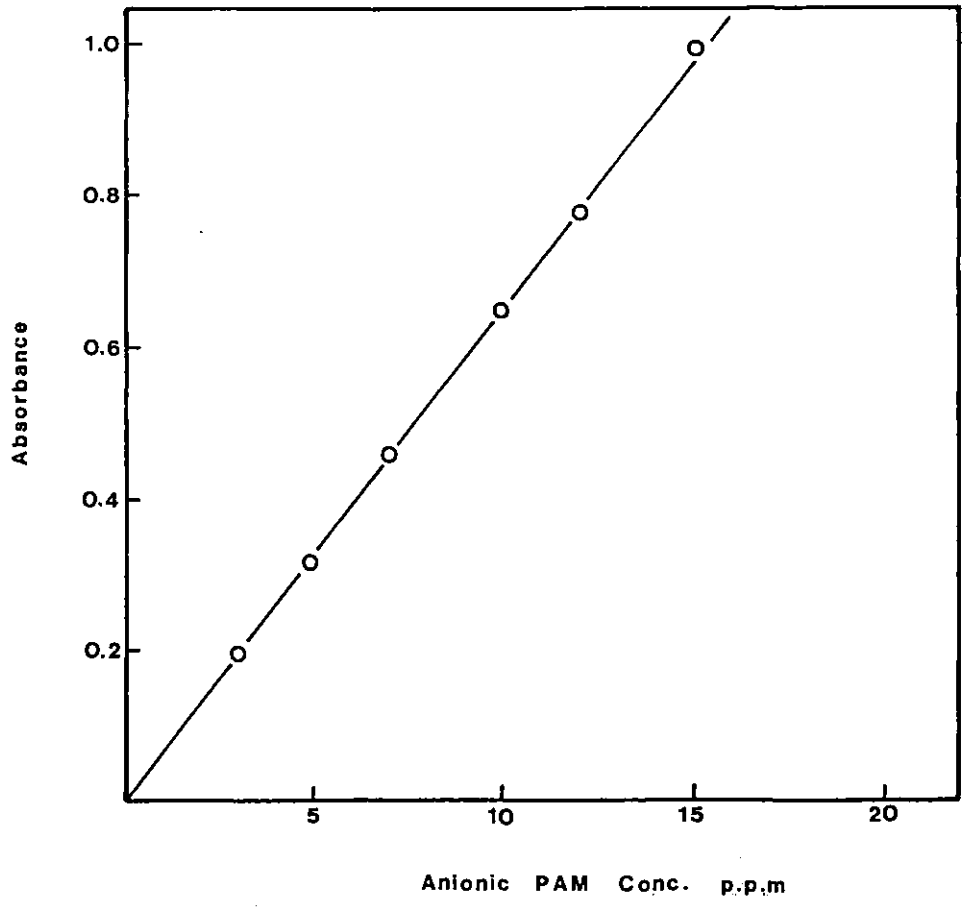

Figure 4.4 Calibration curve for an anionic PAM

CHAPTER 5. ELECTRICAL DOUBLE LAYER PROPERTIES OF COAL/WATER INTERFACE

5. ELECTRICAL DOUBLE LAYER PROPERTIES OF COAL/WATER INTERFACE

5.1 Introduction - The electrical double layer at the solid/liquid interface

When a mineral particle is placed in an aqueous solution, electrical charges develop at the particle-water interface because of the dissociation of surface groups or the preferential adsorption of ions. To maintain electroneutrality this charge must be balanced by an equal and opposite charge in the solution in the vicinity of the particle surface.

Helmholtz considered the charge balance to be a parallel plate condenser with the charges on the particle surface forming either the positive or negative plate and the opposite charges (counter ions) in solution comprising the other plate. This oversimplified model was improved by Gouy who introduced the concept of the diffuse double layer, to which Chapman applied Poisson's equation to determine the potential distribution with distance in the diffuse layer.

According to Gouy-Chapman theory, the distribution of ions in the diffuse part of the double layer is obtained by applying the Maxwell-Boltzmann law

$$n_+ = n_o \exp [-ze\,\Psi/kT] \text{ and } n_- = n_o \exp [+ze/kT] \qquad (1)$$

where n_+ and n_- are the respective concentrations (ions cm^{-3}) of positive and negative ions at points where the potential is Ψ, e is the electronic charge, k is the Boltzmann constant and n_o the corresponding bulk concentration of each ionic species.

The charge per unit volume under these conditions will be given by

$$\rho = ze\,(n_+ - n_-)$$

$$= 2ze\ n_o \sinh \frac{ze\Psi}{kT} \qquad (2)$$

but ρ is related to Ψ by Poisson's equation, which for a flat double layer takes the form

$$\frac{d^2\Psi}{d\ x^2} = \frac{-4\Pi\rho}{D} \qquad (3)$$

where D is the dielectric constant.

Combining (2) and (3) gives the fundamental equation for a flat double layer

$$\frac{d^2\Psi}{dx^2} = \frac{8\Pi ze\ n_o}{D} \sinh \frac{ze\Psi}{kT} \qquad (4)$$

Integration of this equation using limits $\Psi = \Psi_o$ when $x = 0$ and $\Psi \to 0$ $d\Psi/_{dx} \to 0$ as $x \to \infty$ gives a somewhat complicated solution. However a simpler solution results when Ψ_o is small, i.e., $ze\ \Psi_o \ll 2\ kT$ or $\Psi_o \ll 25$ mV.

Under these conditions

$$\Psi = \Psi_o \exp(-\chi x) \qquad (5)$$

for a flat double layer, which shows that at low potentials the potential (Ψ) decreases exponentially from the surface potential (Ψ), with distance (x) from the charged surface. $1/\chi$ is referred to as thickness of the double layer and is inversely proportional to the ionic strength. The surface potential is related to the surface charge (σ_o) by an equation, which at low potentials, simplifies to

$$\rho_o = \varepsilon\chi\Psi_o \qquad (6)$$

The surface potential, therefore, depends on both the surface charge and (through χ) on the ionic strength of the medium.

The Gouy-Chapman theory of the diffuse layer suffers from a number of defects, the most notable being the assumption that the ions can be considered as point charges. This leads to the calculation of impossibly high ionic concentrations near to the charged surface.

Stern introduced a correction for the finite size of the ions in the first ionic layer adjacent to the charged surface. He also considered the possibility of specific ion adsorption giving a compact layer of counter ions attached to the surface by electrostatic and van der Waals forces strong enough to overcome thermal agitation. The double layer is, therefore, considered to be divided into two parts - a compact Stern layer in which the potential changes from Ψ_o to Ψ_δ and a diffuse layer where the potential drops from Ψ_δ to zero. The Gouy-Chapman theory, therefore, applies to the diffuse part of the double layer and Ψ_δ should be substituted for Ψ_o in the relevant equations.

Further improvements to Stern's theory have been developed by Grahame. He divided the Stern layer into two planes called the Inner and Outer Helmholtz planes. The OHP lies at the distance of closest approach to the surface of hydrated ions, and still belongs to the diffuse double layer. The IHP is the plane in which specifically adsorbed and presumably dehydrated ions are found. Figure 5.1 outlines schematically the various regions of the double layer and corresponding variation of potential with distance from the surface in the absence and presence of specific adsorption.

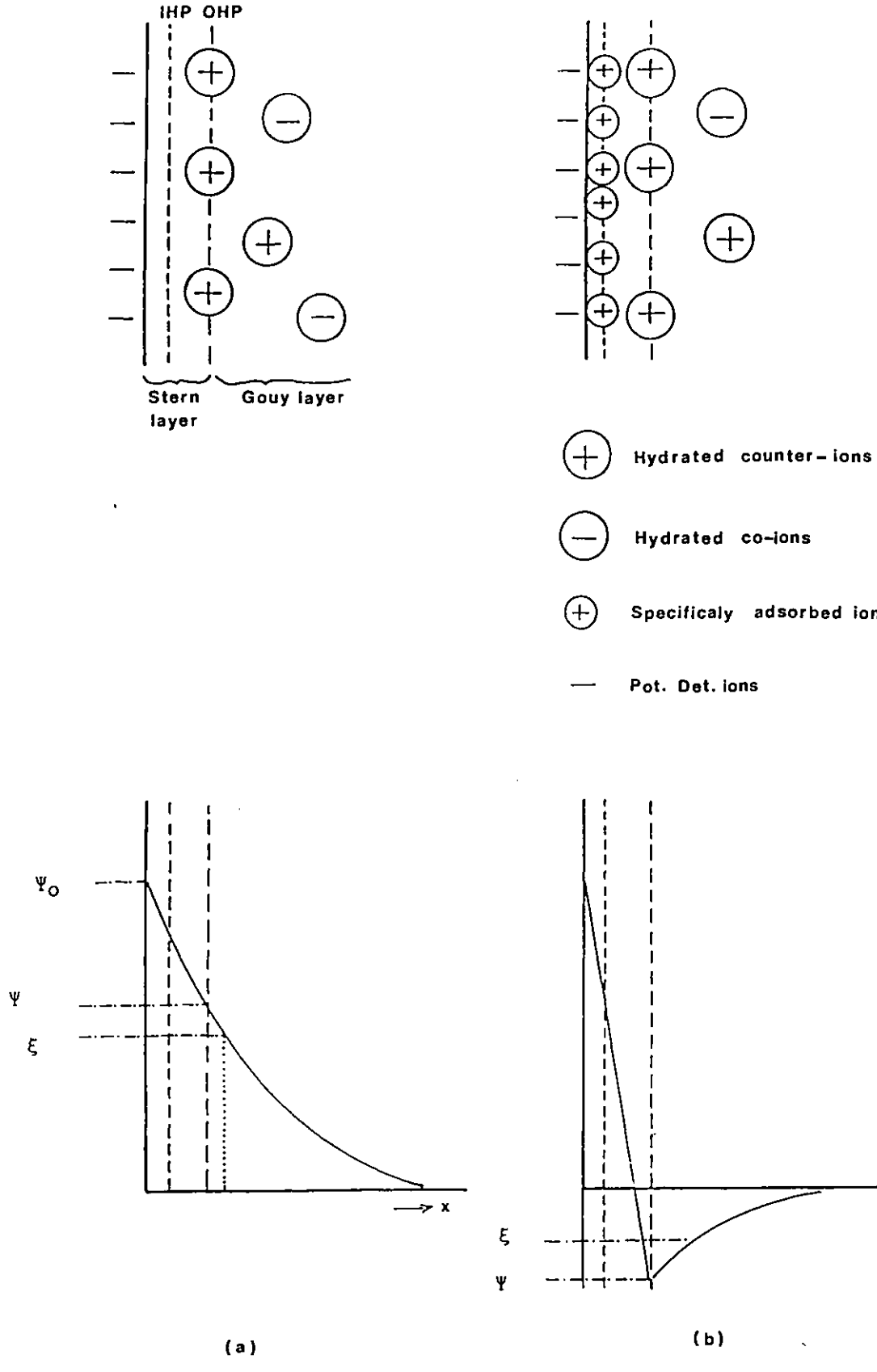

Figure 5.1 Stern-Grahame model of the solid/water interface, in (a) the absence and (b) the présence of specific adsorption

The sign and magnitude of the Stern potential is of considerable importance in colloid chemistry, because it is one of the parameters which controls the stability of colloidal dispersions. In spite of its great importance this parameter cannot be measured directly and its value is generally assumed to be approximately the same as the electrokinetic or zeta potential which is the potential at plane of shear situated just outside the Stern plane.

There are several methods available to measure the zeta potential of mineral particles but the most widely used is that of micro-electrophoresis. In this technique the particles are observed by microscope as they migrate to an oppositely charged electrode. By timing the particles as they travel over a fixed distance, it is possible to calculate their velocity and hence their zeta potential.

The velocity of the particle is given by the Helmholtz-Smoluchowski equation

$$V = \frac{\varepsilon \xi E}{4\pi\eta} \qquad (7)$$

where V = velocity (cm s^{-1})

ε = dielectric constant

E = applied potential (e.s.u/cm)

ξ = zeta potential (e.s.u.)

η = viscosity (0.01 poise)

However, the use of this equation is limited, because of the conditions that the thickness of the double layer should be small compared with the radius of the particle (i.e., $\chi a \gg 1$) and the particle must be insulating with negligible surface conductance.

Hückel, introducing a correction for electrophoretic

retardation gave another equation

$$V = \frac{\varepsilon \xi E}{6\pi\eta} \qquad (8)$$

which can be used for low values of χ a.

Henry showed that both equations are limiting forms of the equation

$$V = \frac{f \varepsilon \xi E}{\pi \eta} \qquad (9)$$

where f is a function of the quantity χ a, whose value depends on the shape of particles.

When the external electric field is applied, a moving charged particle is subjected not only to electrophoretic retardation, but also to electric relaxation. This concept was introduced by Overbeek et. al. (91) in their studies of electrophoretic mobility of a colloidal particle. They also calculated the effect of other factors such as, particle shape, Brownian movement, the viscoelectric effect, particle conductivity.

Despite the attention given by many workers to the calculation of zeta potentials from mobility data and the considerable improvements that have been made to the validity of equation (7), there is still considerable uncertainty of what correction factors should be applied in different situations. In view of these difficulties, electrophoretic mobilities were used throughout this work. Nominal values of the zeta potential were, however, obtained when required by application of equation (7) in form

$$\xi = 12.83 \text{ Electrophoretic mobility}$$

5.2 The electrophoretic mobilities

The dependency of the electrophoretic mobility (e.m) of anthracite on pH is shown in Figure 5.2. The IEP of anthracite occurred at pH 3.5, and above this value the e.m became more negative with increasing pH, up to pH 9. With graphite the e.m - pH curve showed the same trend except that less negative e.m values were obtained.

The effect of increasing NaCl concentration on the e.m of graphite at different constant pH values (Figure 5.3) showed that at a constant pH, the e.m is unaffected by increasing NaCl concentration up to 10^{-3}M. The e.m of anthracite in the presence of different concentration of NaCl is also given in figure 5.4. As can be seen, the position of IEP was not affected by changes in the concentration of this metal salt. Therefore, NaCl appears to behave as an indifferent electrolyte for both graphite and anthracite. At higher ionic strengths a decrease in the negative e.m values to zero would be expected.

Figure 5.5 indicates that the IEP's of high volatile and medium volatile coal occur at pH values 4.0 and 4.5 respectively. Comparison with the IEP of anthracite which occurred at pH 3.5 suggests that a decrease in the rank of the coals produced a shift in the IEP towards less acidic pH values. Generally, anthracite has a higher negative charge than the other coals.

The IEP values of the lithotypes (Figure 5.6) were found to be very close to the IEP of the anthracite from which they were separated. All lithotype samples gave negative e.m values above pH 4 and negative values increased with an increase in pH. Vitrain has a substantially higher negative e.m than that of fusain and durain and

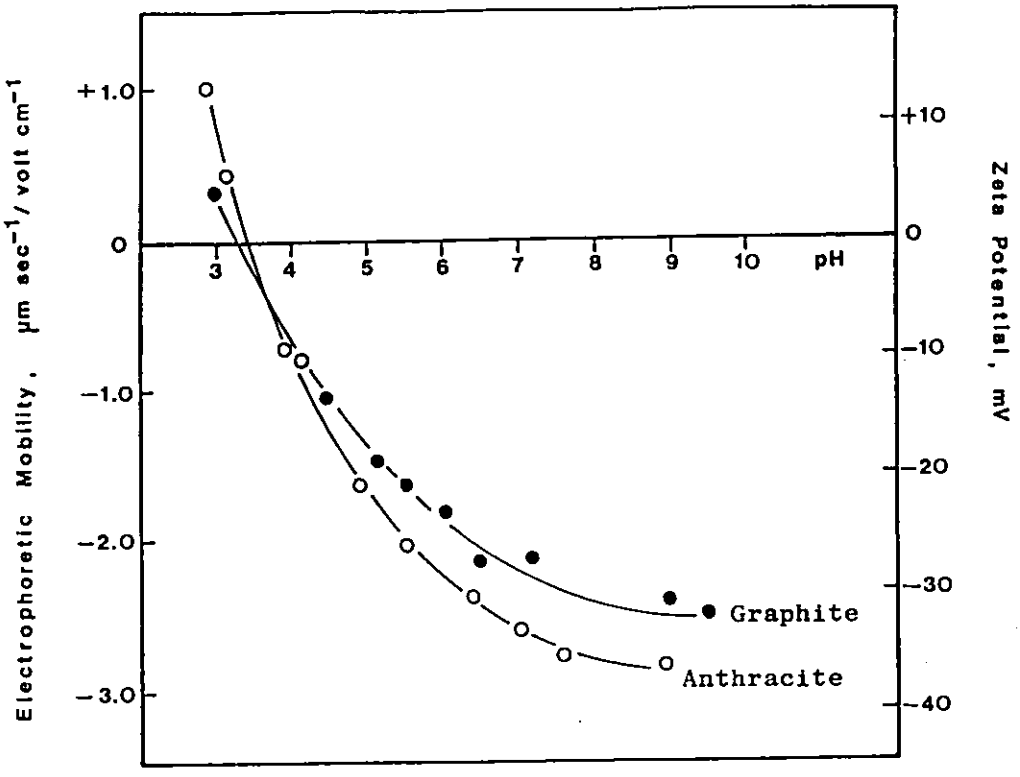

Figure 5.2 Electrophoretic mobility of anthracite and graphite as a function of pH (ionic strength 10^{-3})

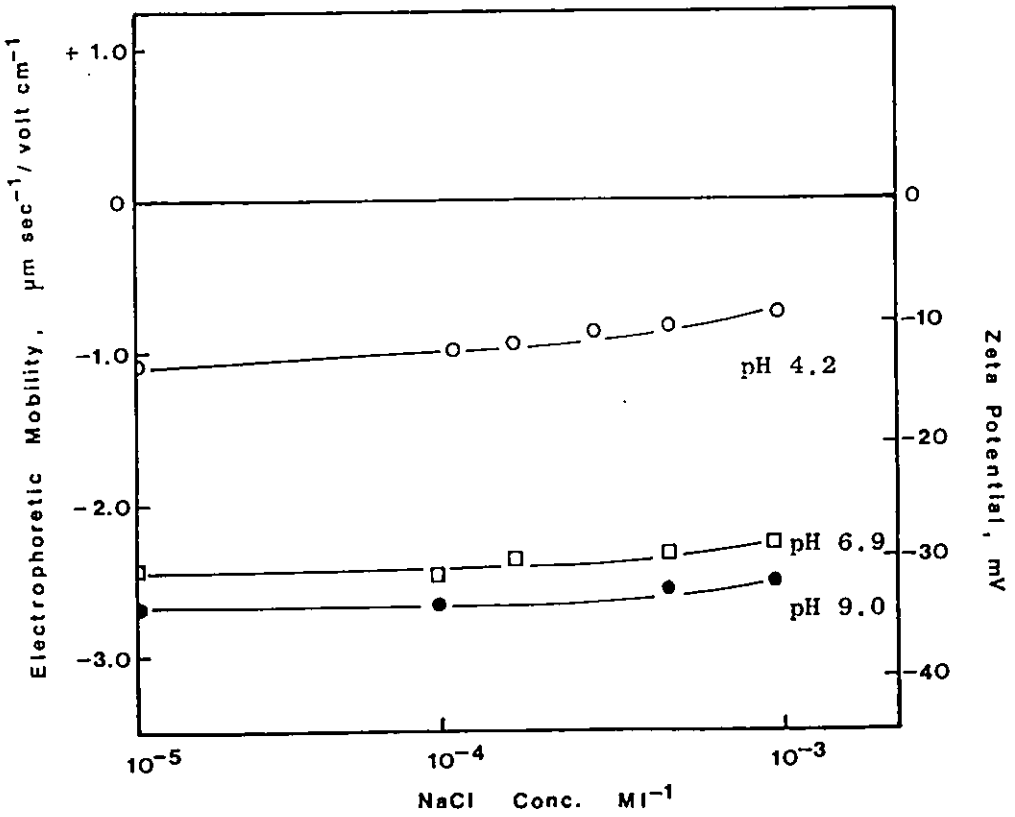

Figure 5.3 Variation in graphite electrophoretic mobility with NaCl concentration

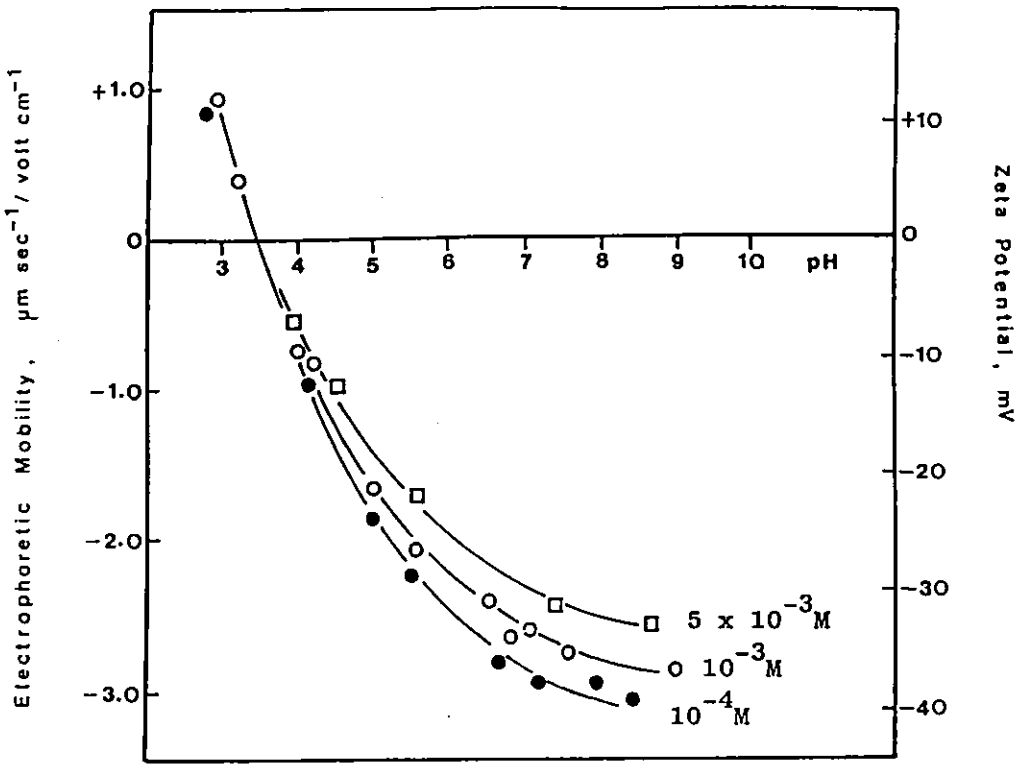

Figure 5.4 The effect of NaCl on the electrophoretic mobility of anthracite

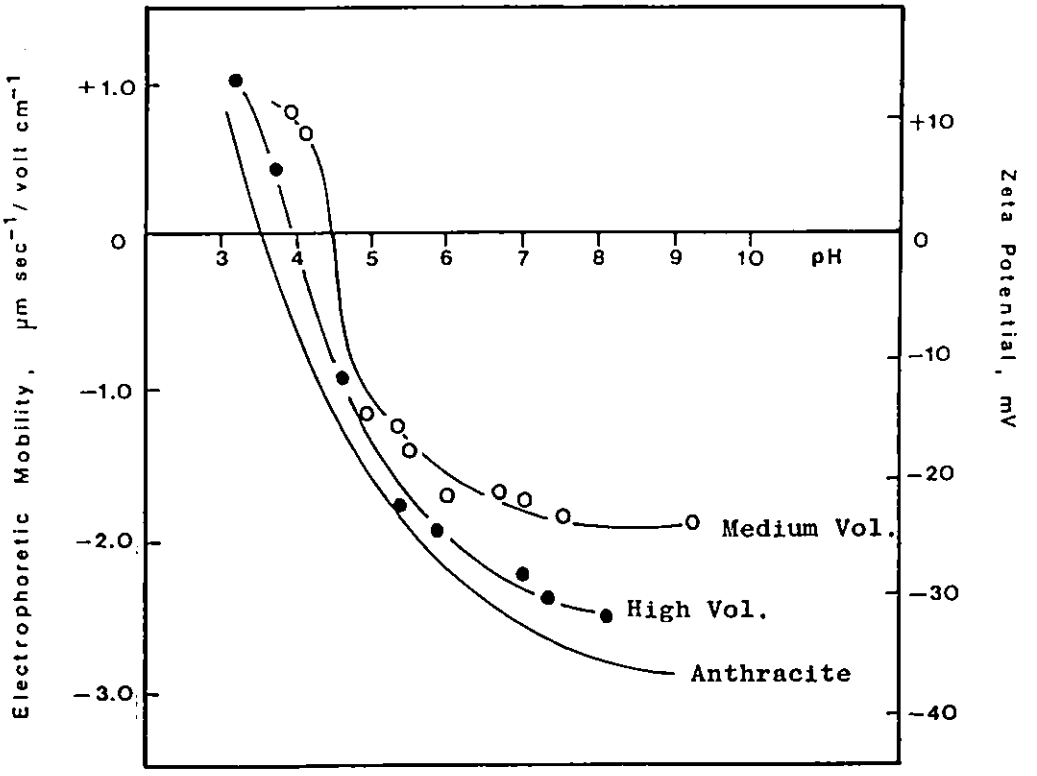

Figure 5.5 The effect of pH on the electrophoretic mobilities of three different coal samples

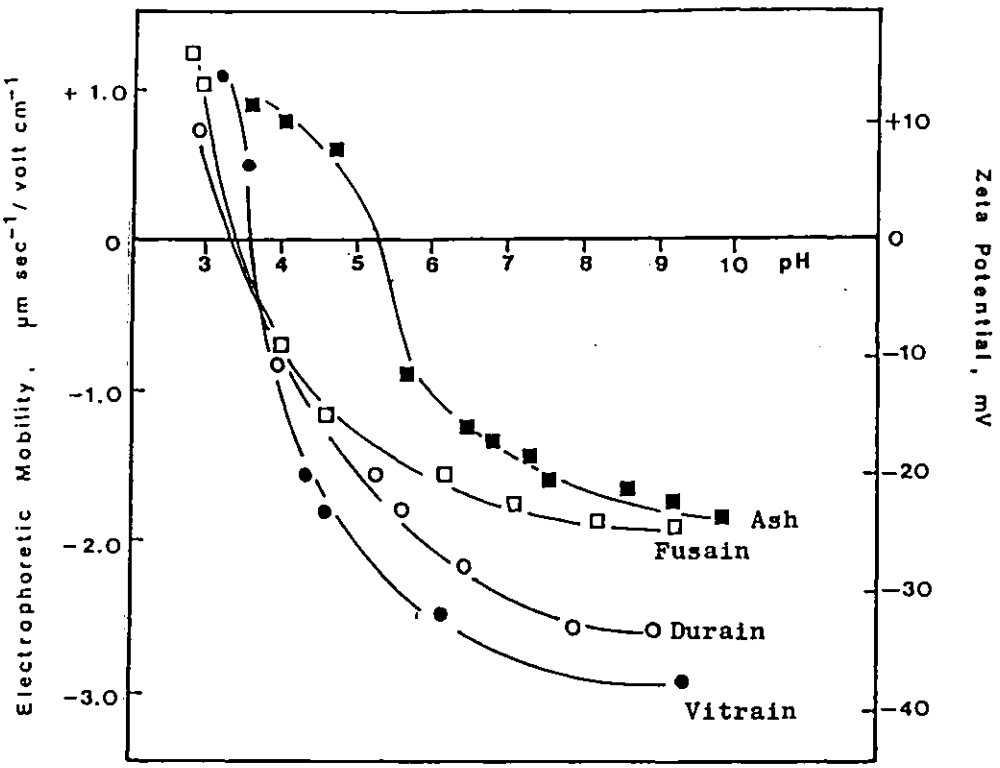

Figure 5.6 The effect of pH on the electrophoretic mobilities of lithotypes and ash

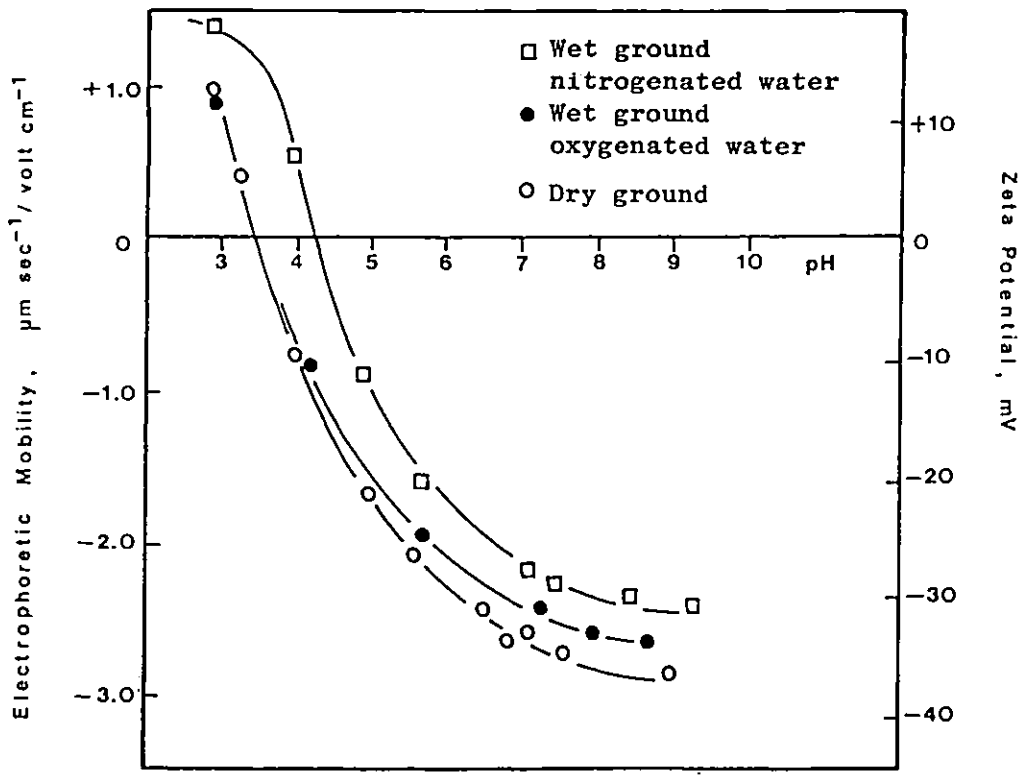

Figure 5.7 The effect of grinding on the electrophoretic mobility of anthracite

it appeared that vitrain has the greatest effect on the resulting anthracite curve because it comprises the greatest percentage (73%) of anthracite. In the same figure the more basic IEP of ash is probably due to presence of large amounts of aluminium and iron whose salts have IEP's in the pH range of 6 to 8.

The effect of dry and wet (in nitrogenated and in oxygenated water) grinding on the e.m of the anthracite is shown in Figure 5.7. The highest negative e.m values were obtained for dry ground anthracite. Wet grinding of the anthracite in oxygenated water gave a slight increase in negative mobility values than from those obtained with a sample ground in nitrogenated water. The latter had an IEP at pH 4.3.

Methylation of anthracite and graphite gave rise to slightly more negative e.m values over the pH range studied than that of unmethylated samples (Figures 5.8 and 5.9).

The effect of oxidation was studied on anthracite and graphite which were subjected to dry oxidation with air and oxygen, at temperatures between 100°C and 200°C, for different periods of time. As can be seen from Figure 5.10 oxidation of samples with air, at 100°C, had a marked effect within the first 24h but thereafter the increase in negative mobility was not great. The IEP of anthracite decreased from pH 3.5 for an unoxidized sample to pH 2.6 for a sample oxidized in air for 24h. No IEP could be determined for the anthracite oxidized in oxygen because high negative e.m values were obtained even in acidic pH values (Figure 5.11). The results also showed that the e.m of an extensively oxidised anthracite is almost independent of pH.

When the same conditions used to oxidize the anthracite were

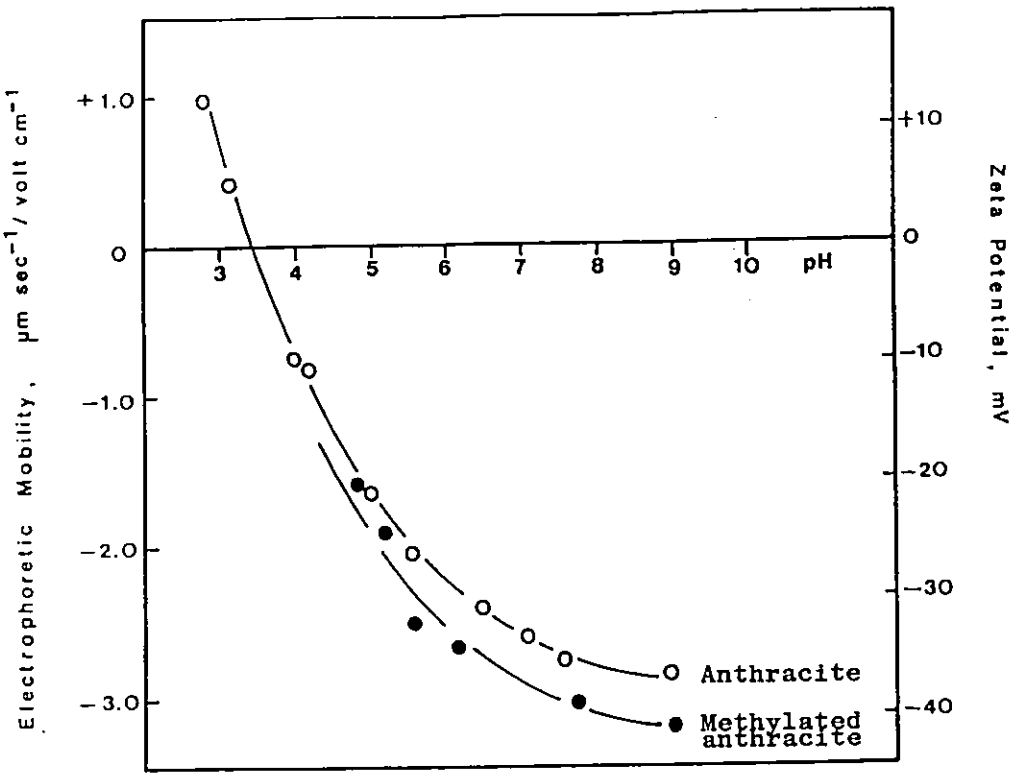

Figure 5.8 The electrophoretic mobilities of methylated and untreated anthracite

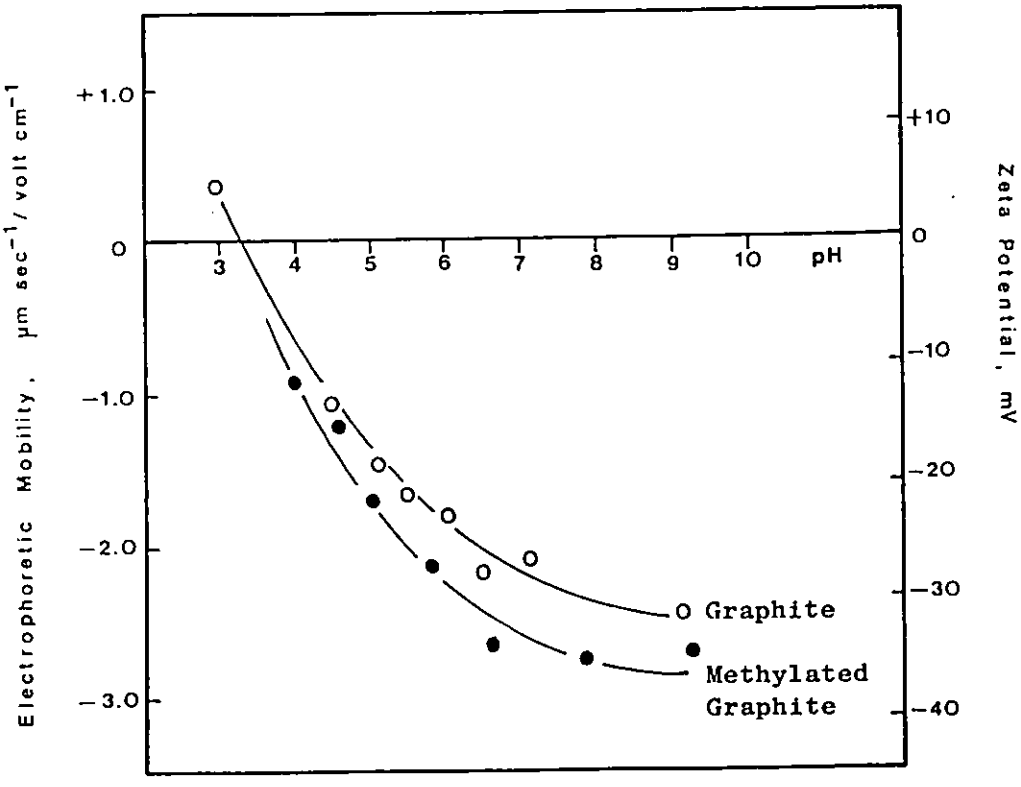

Figure 5.9 The electrophoretic mobilities of methylated and untreated graphite

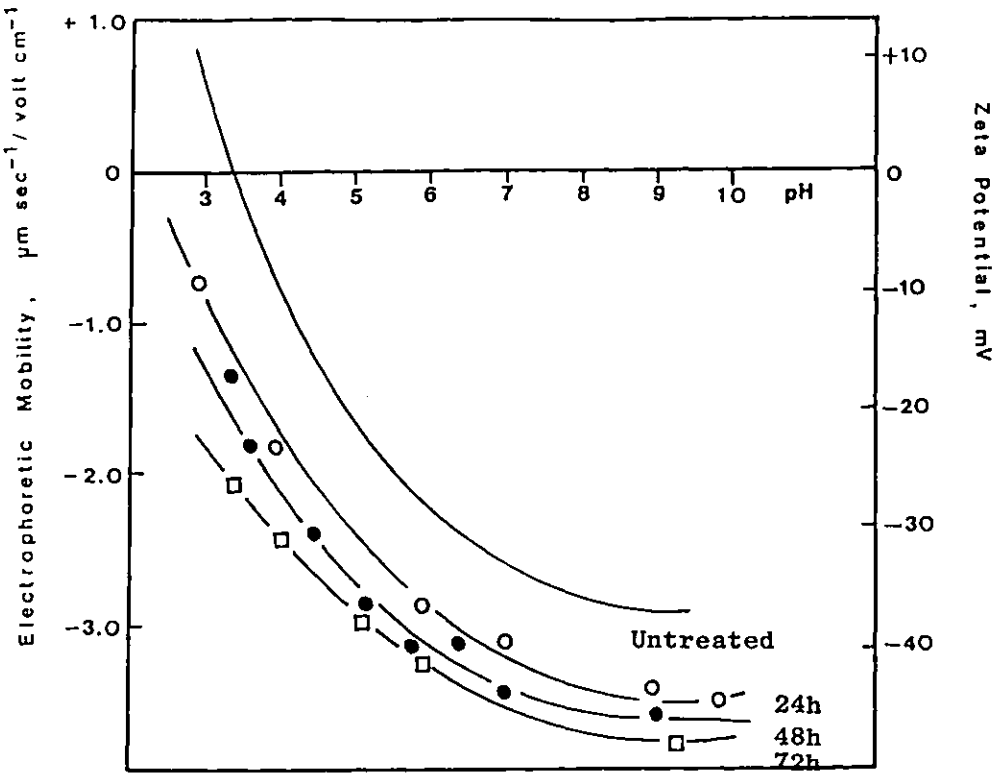

Figure 5.10 The effect of oxidation of anthracite on the electrophoretic mobility (Oxidation with air, at 100°C

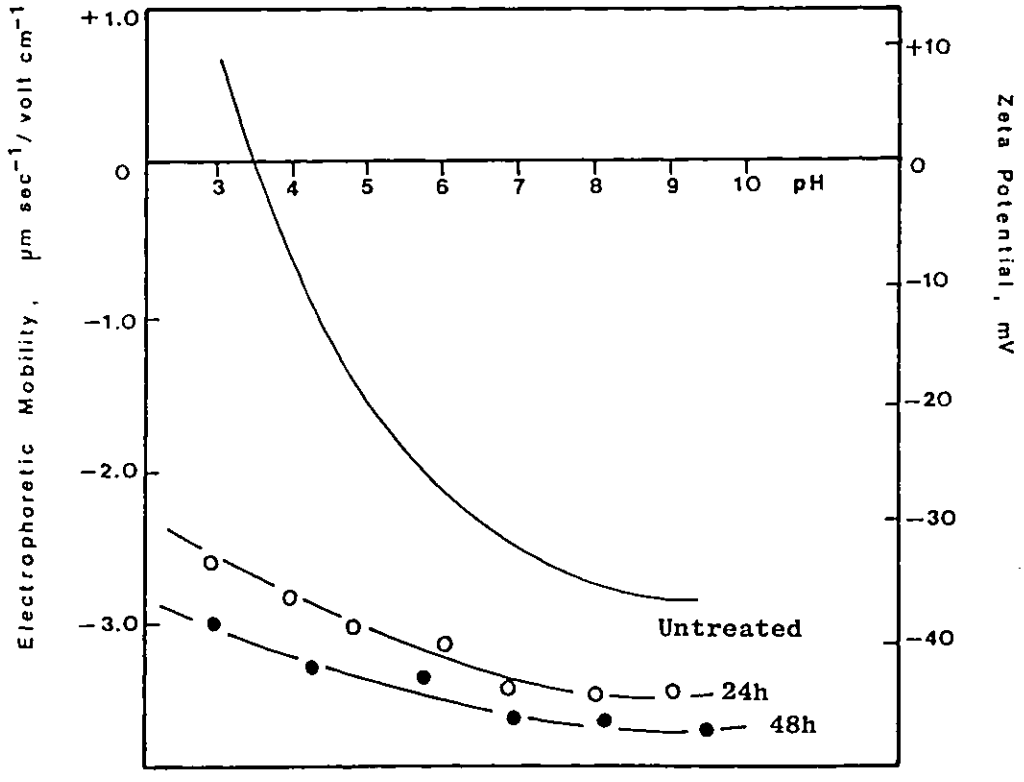

Figure 5.11 The effect of oxidation of anthracite on the electrophoretic mobility (Oxidation with oxygen, at 100°C

applied to graphite, no change in the e.m of oxidized graphite was observed from that of unoxidized graphite. This result was expected, since acidic groups will be only bound to peripheral carbon atoms of each layer (37) and this area is considerably less than the total area.

Acid washing of the samples has not caused any significant changes in the electrokinetic behaviour of the coal and graphite.

5.3 Adsorption of H^+ and OH^- ions

The net abstraction of OH^- ions by anthracite is shown in Figure 5.12, as a function of pH at three different ionic strengths. The OH^- ion abstraction increased with increasing pH and ionic strength. At pH values between 3 and 5 the slope of the abstraction - pH curves, at ionic strength of 0.1, increased sharply suggesting the presence of acidic groups of the carboxylic type on the anthracite surface. Similar results were obtained for graphite and are shown in Figure 5.13.

In principle, it is possible to obtain the PZC from the intersection points of the abstraction - pH curves at various concentrations of an indifferent electrolyte. This method may not be applicable to this coal, but it should be useful for a comparison of coal with oxides. As can be seen from the figures, the indication is that the PZC given by the condition $\Gamma_{OH^-} - \Gamma_{H^+} = 0$ (assuming that H^+ and OH^- are potential determining) is probably below pH 3.

The reversibility of the OH^- abstraction was tested by titrating the anthracite suspension at constant ionic strength with OH^- ions to pH ≈ 9.5 and reversing the titration with H^+ ions. The

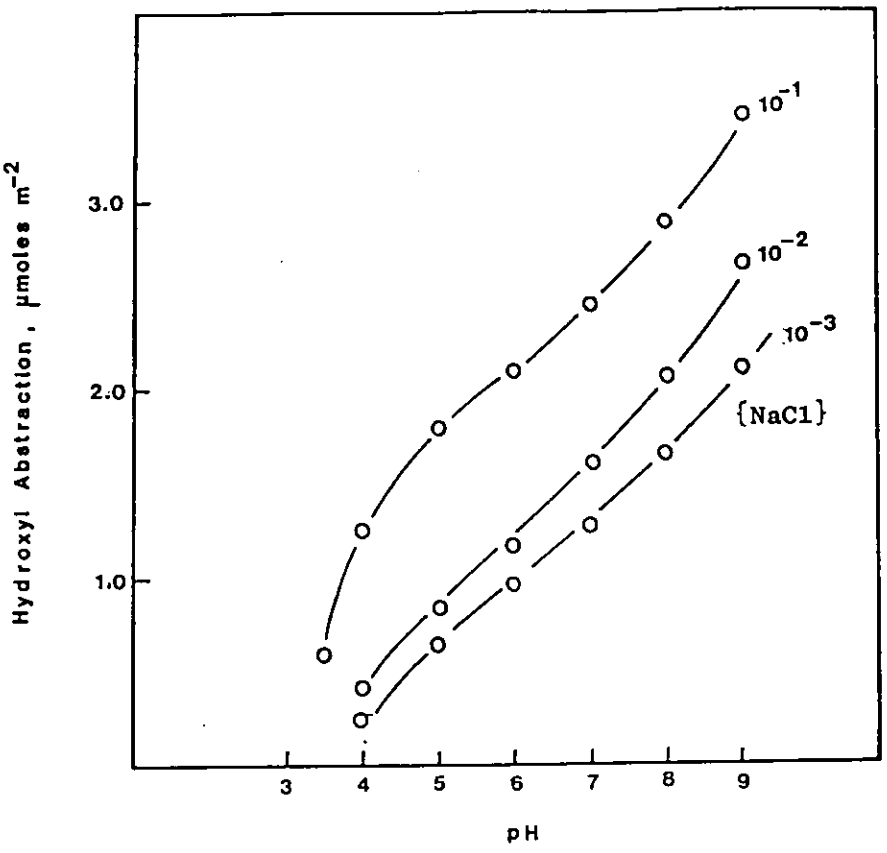

Figure 5.12 The abstraction of OH^- ions by anthracite as a function of pH and NaCl concentration

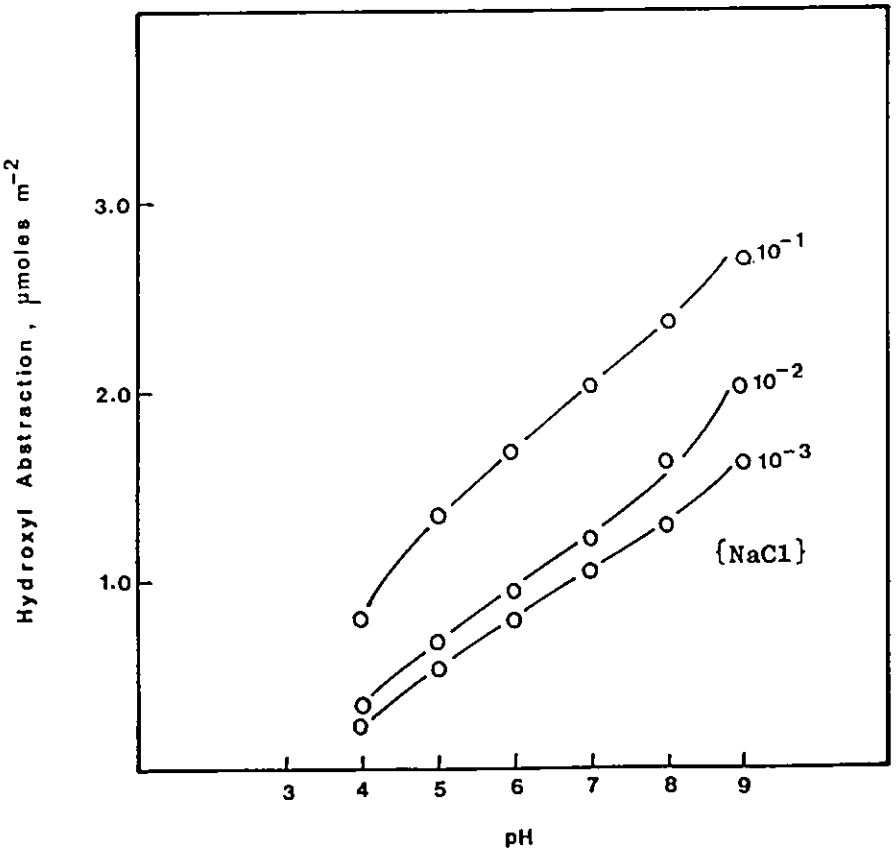

Figure 5.13 The abstraction of OH^- ions by graphite as a function of pH and NaCl concentration

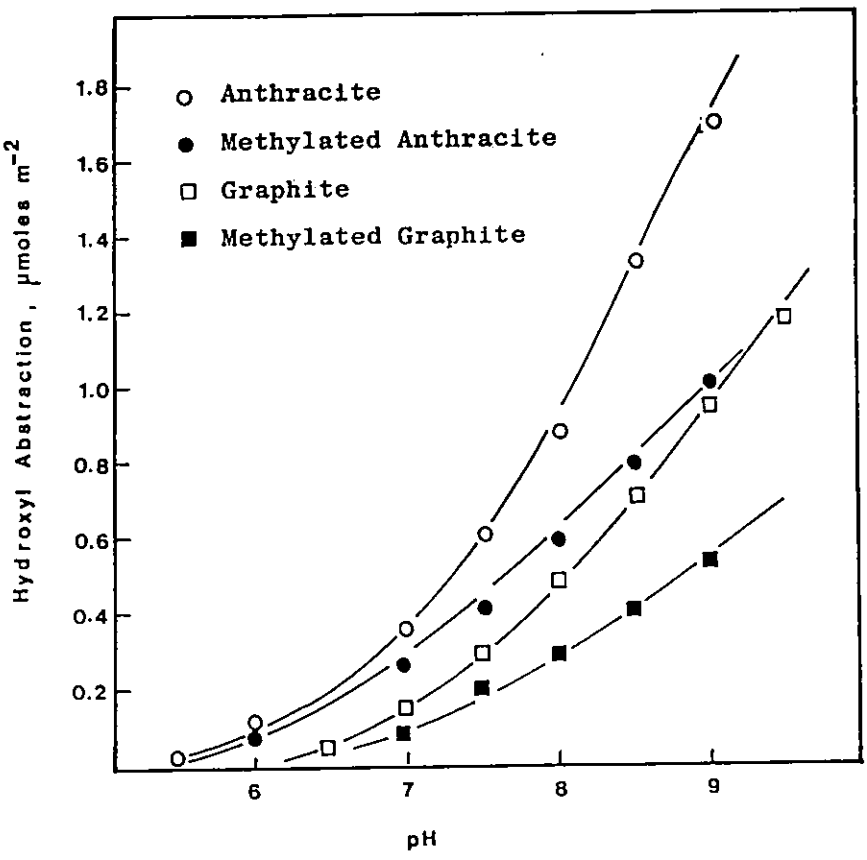

Figure 5.14 The abstraction of OH^- ions by methylated and unmethylated samples

deviations were observed which became less pronounced the more slowly the titration was carried out. These deviations could be attributed to microporous structure of anthracite.

The effect of solid concentration was studied by titrating different quantities of anthracite in the same total volume and at the same ionic strength. It was found that the change in the amount of OH^- abstracted/gramme of anthracite was not very significant, indicating that there is practically no effect of solid concentration on the OH^- ion abstraction.

Figure 5.14 shows the OH^- ion abstraction of methylated anthracite and graphite. Although the abstraction decreased considerably, it did not become zero after methylation of the surfaces by diazomethane, which should have complexed all the active hydrogen.

5.4 Discussion

According to Shaw (92), the mechanism of surface charge formation should be evident from the shape of the curve characterizing the pH dependence of e.m. The experimental e.m - pH curves obtained reflect the amphoteric nature of the surface groups present on both anthracite and graphite. Combination of the OH^- abstraction results with the e.m data shows that, as the e.m becomes more negative, the consumption of OH^- ions increased. This indicates that the surface hydroxyl groups ionized (at high pH), to give a negative surface, and protons in solution. Therefore, the higher negative values of the e.m may be due to the dissociation of acidic (probably carboxylic and phenolic) surface groups:

$$R - COOH \rightleftharpoons R - COO^- + H^+ \xrightarrow{NaOH} R - COO^- + Na^+ + H_2O$$

Extrapolation of the adsorption isotherms in Figure 5.12 indicates that the PZC was below pH 3. Differences between the IEP and PZC values of oxides are attributable to surface impurities, or the specific adsorption of ions. For anthracite, since it was established that NaCl behaves as an indifferent electrolyte (Figure 5.4), the higher pH values of the IEP compared to that of PZC cannot be due to the specific adsorption of Na^+ ions. The difference between these values is most likely due to cationic impurities.

The presence of cationic impurities also explains the positive e.m of anthracite and graphite. However, the formation of carbonium ion has been suggested (93) to explain the positive e.m values of graphite below the IEP. Although the existence of such a structure is only circumstantial, it is known that the carbonium ion is stable in tertiary form with the positive charge distributed to three neighbouring carbon atoms (94). Another possibility includes the formation of protonated tertiary alcohol groups which only dissociate slowly when the pH is increased. Whether or not such situations might occur at the graphite surface is not known.

Calculation of the ionized acidic sites required to give an e.m of -3.0 $\mu m\ sec^{-1}/volt\ cm^{-1}$, using the Helholtz-Smoluchowski and Gouy-Chapman equations assuming no specific adsorption effects, suggests that at pH 9 less than 3×10^{-8} moles m^{-2} would be sufficient, which is less than the experimentally obtained OH^- abstraction (2×10^{-6} moles m^{-2}). Therefore, much more negative e.m values would be expected for anthracite than those obtained. Similar results have however, been reported for oxide minerals. Examples are given in work by Onoda and de Bruyn (95) on hematite, by Bolt (96) on

colloidal silica, by Li and de Bruyn (97) on quartz, by Tadros and Lyklema (98) on porous SiO_2 and by Breeuwsma and Lyklema (99) on hematite where a considerable surface charge was obtained, although the electrokinetic potentials were not particularly high.

To explain the high surface charge Lyklema suggested that the surface may have a porous or gel layer into which both PDI and counter ions can penetrate so that more charge can be accommodated per unit area. It is reasonable to assume that the porous structure of anthracite may be responsible, to some extent, for the apparent inconsistency between the OH^- abstraction and e.m data. Most of the charge measured by titration could be inside the pores whereas the e.m results reflect the properties of the surface sites. However, this suggestion may not be appropriate for graphite or for crystalline oxide surfaces.

According to Bérubé and de Bruyn (100) the high surface charge of TiO_2 and other oxides is a result of close counter ion approach to the plane of PDI, which adsorb within a highly structured, chemisorbed water layer immediately adjacent to the oxide surface. Figure 5.15 shows a schematic representation of an oxide surface, modified from that of de Bruyn and co-workers. The chemisorbed water layer may adsorb or release protons to form the charged surface sites.

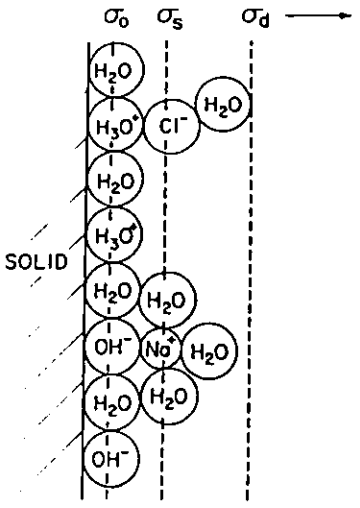

Figure 5.15 Schematic representation of an oxide interface showing possible locations for molecules comprising the planes of charge.

The molecules in this layer represent the σ_o - plane and electrolyte ions may approach this plane to form the σ_s - plane. Because of the intervening water layer, an approaching ion may have a chemisorbed water molecule as part of its hydration layer. This allows a close approach to the σ_o - plane. A similar mechanism can be postulated for the high surface charge of anthracite and graphite.

No significant correlations were observed between coal rank and the e.m results. Wen and Sun (22;) suggested that the lower the rank of coal, the greater the amounts of oxygen-containing functional groups. These groups are acidic in character and are negatively charged in water. Therefore, the negative value of the e.m of coals was expected to increase with decreasing rank. This was not obtained. Arbiter et. al. (101) suggested that electrokinetic properties of strongly hydrophobic solids are primarily or completely determined

by the aqueous phase. The double layer is entirely on the water side of the interface; the sign of the charge and its magnitude are determined by the composition of the aqueous phase with little or no influence from the solid. Because the solid does not specifically adsorb ions, it does not participate in determining the potential. Instead, polarizability of solute ions fixes the composition and electrical properties of the interface. From this conclusion, it appears that e.m variations with pH for coals were a result of the combined effects of various constituents of mineral matter present in the coals.

After methylation, the negative e.m of anthracite and graphite slightly increased. Since diazomethane would react with any ionizable hydrogen in the surface groups and replace it with a methyl group, an increase in the negative e.m was not expected. The results were surprising but are similar to those obtained with silica (21) and diamond (102). It was postulated here that cross-linking siloxane groups on methylated silica could cause a zeta potential, due to the interaction of water with the lone pairs of electrons on the oxygen atoms. Ether-like oxygen on methylated diamond surface was suggested to be responsible for the zeta potential of the methylated diamond. Whether or not similar groups could give rise to the observed e.m of the methylated anthracite and graphite is difficult to assess.

The results also showed that there is still a substantial OH^- abstraction on methylated samples. A similar effect was observed by Boehm (25), who suggested that the last adsorption of OH^- ions was due to very weak acidic groups which are not readily methylated. However, it is most likely that the OH^- abstraction of methylated

anthracite is due to incomplete methylation. Because of the microporous structure of anthracite, it is probable that the sites, containing active hydrogen, inside the pores are not readily accessible to diazomethane. Also it was found (25) that methylation was somewhat incomplete on silica when etheric diazomethane solutions were used. More methoxy groups were formed with gaseous diazomethane. However, polymethylene was formed as a by product and explosions occurred. This method has not been tried in this project.

The e.m of anthracite oxidized with oxygen was found to be almost independent of pH. These results are consistent with those obtained by Wen and Sun (22) on bituminous vitrain and suggest that H^+ and OH^- ions are not potential determining for an extensively oxidized sample. Another possibility is that e.m does not reflect changes in surface potential because of viscoelectric effects and movement of the slipping plane. For high values of surface potential, the field in the double layer may be large enough to produce a very significant viscoelectric effect (103). It has also been suggested that the insensitivity of the zeta potential to the concentration of PDI's is attributable either to a reduction of the dependency of the zeta potential on the charge density in the outer plane or a substantial adsorption of counter ions in the Stern layer (104). There is also the possibility of a limitation to the density of ionizable groups on the surface. The fact that the adsorption of hydroxyl ions did not decrease at high pH values indicates that the latter two possibilities are unlikely, and that, the first suggestion may account for the behaviour of the e.m of oxidized coal.

CHAPTER 6. INTERACTION OF METAL IONS AT THE COAL/WATER INTERFACE

6. INTERACTION OF METAL IONS AT THE COAL/WATER INTERFACE

6.1 Influence of metal ions on the electrophoretic mobilities

The electrophoretic mobility (e.m.) of anthracite was determined in the presence of different concentrations of $CaCl_2$ (Fig.6.1). The position of the IEP was not affected by changes in the concentration of this salt. The negative value of the mobility decreased at higher concentrations with the trend of e.m. values indicating that their sign may reverse above pH 11. This result suggested that calcium is at least partly specifically adsorbed on the anthracite surface.

The effect of pH on the e.m. of coal samples in $FeCl_3$ and $AlCl_3$ solutions at different concentrations are shown in Figures 6.3, 6.4, 6.5 and 6.6. In acidic media, high positive mobility values were obtained, but as the pH of the solutions was increased a reversal in sign from positive to negative occurred and the mobilities became progressively more negative, levelling off at higher pH values. It was also observed that the IEP values of the coal samples occurred at lower pH values as the trivalent metal salt concentrations were reduced. The general trend of these results is similar to those observed with quartz (105). The high volatile and medium volatile coals appeared to be more positive than the anthracite at low pH values. This difference might suggest that positively charged species are adsorbed to a greater extent on the high volatile and medium volatile coals, or alternatively more negative species are released from these coal surfaces than from the anthracite.

The e.m. of anthracite in the presence of $CuCl_2$ (Fig. 6.2) was much less dependent on pH than in its absence and found to be positive over the pH range 3-9. At a given pH value the e.m. became

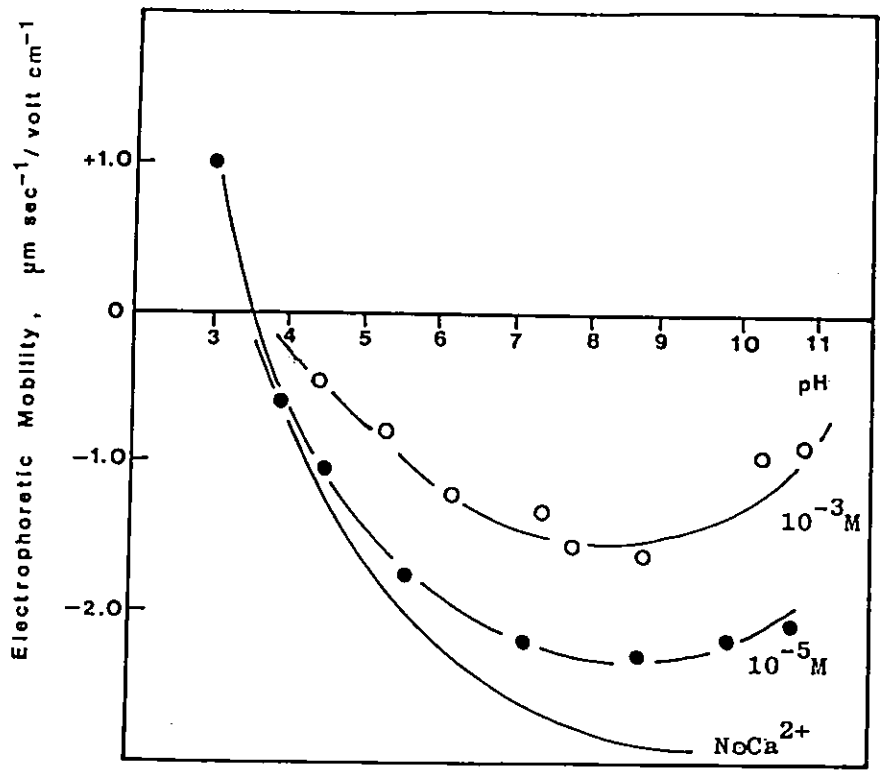

Figure 6.1 The effect of Ca^{2+} ions on the electrophoretic mobility of anthracite

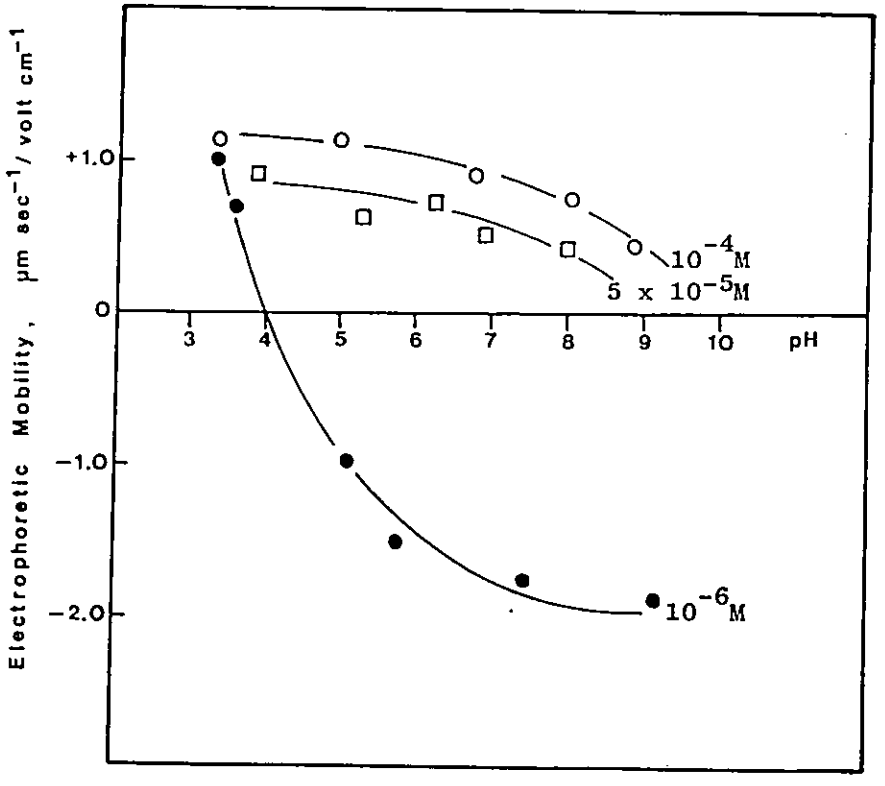

Figure 6.2 The effect of Cu^{2+} ions on the electrophoretic mobility of anthracite

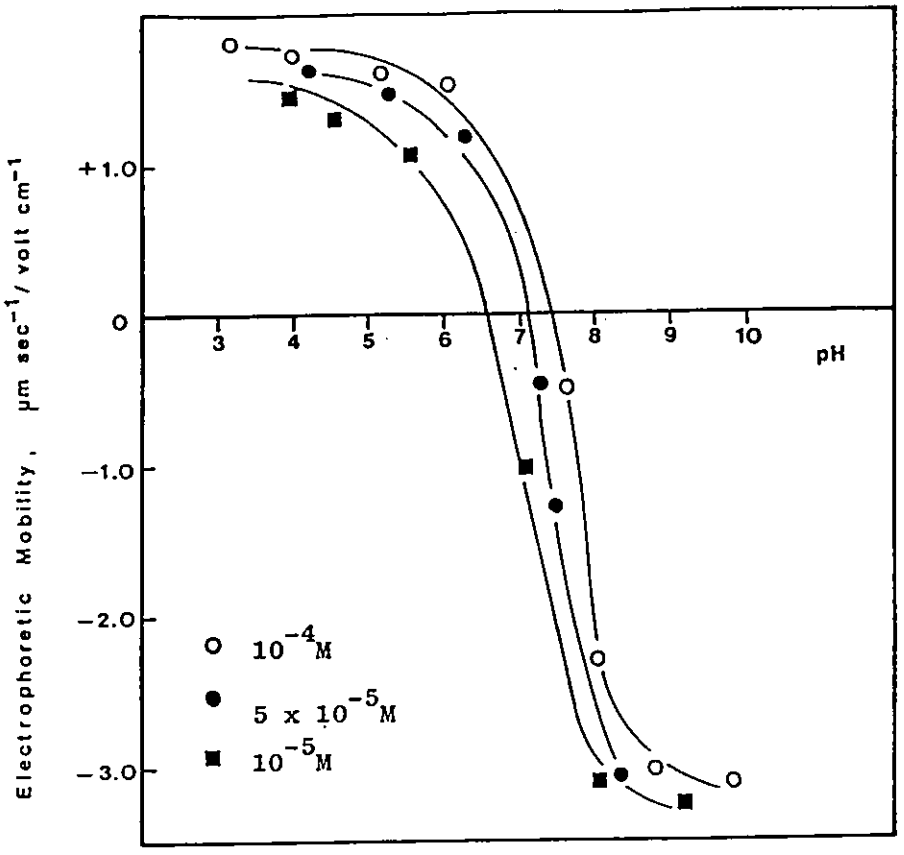

Figure 6.3 The effect of Fe^{3+} ions on the electrophoretic mobility of anthracite

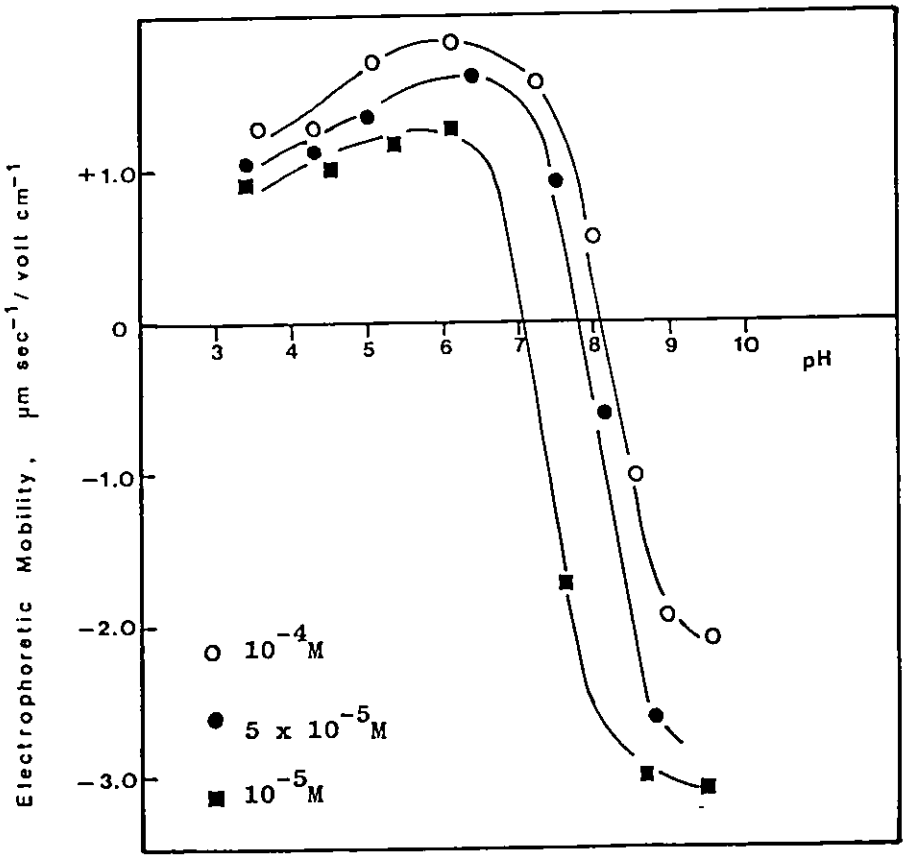

Figure 6.4 The effect of Al^{3+} ions on the electrophoretic mobility of anthracite

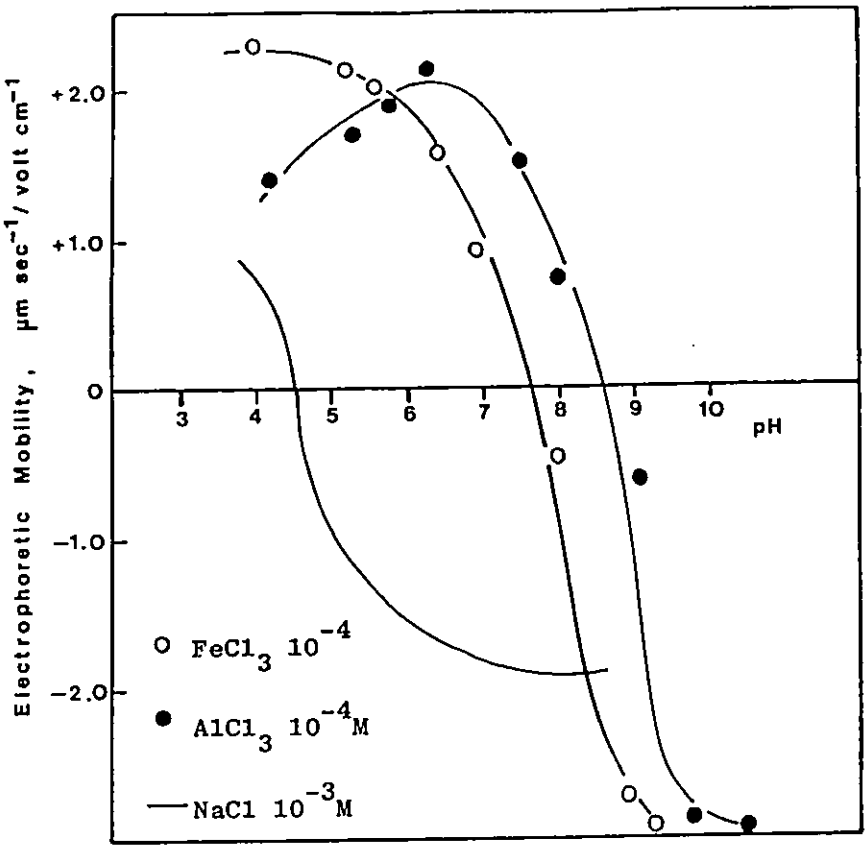

Figure 6.5 The electrophoretic mobilities of medium volatile coal in $FeCl_3$ and $AlCl_3$

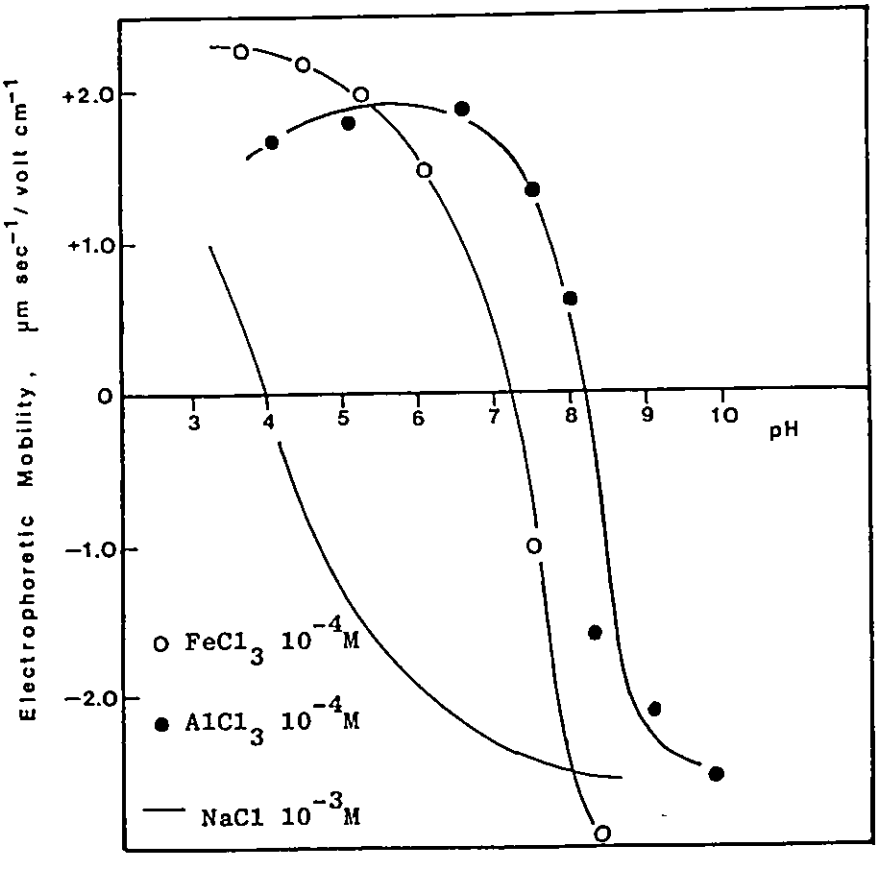

Figure 6.6 The electrophoretic mobilities of high volatile coal in $FeCl_3$ and $AlCl_3$

more positive with increasing $CuCl_2$ concentration up to 10^{-4} M. With 10^{-6} M $CuCl_2$ the e.m. curve was similar to that found in the absence of $CuCl_2$ except above pH 4 where less negative mobility values were obtained.

Ions in aqueous solution became hydrated, usually coordinating four or six water molecules. As the pH of the solutions changes, then the ionization of the water molecules surrounding the ion will also change. Taking aluminium as an example, the following equilibria can be written (106).

$$[(Al^{3+})(H_2O)_6] \rightleftarrows [(Al^{3+})(OH^-)(H_2O)_5]^{2+} + H^+ \quad K_1 \qquad (1)$$

$$[(Al^{3+})(OH^-)(H_2O)_5]^{2+} \rightleftarrows [(Al^{3+})(OH^-)_2(H_2O)_4]^+ + H^+ \quad K_2 \qquad (2)$$

$$[(Al^{3+})(OH^-)(H_2O)_4]^+ \rightleftarrows [(Al^{3+})(OH^-)_3(H_2O)_3] + H^+ \quad K_3 \qquad (3)$$

$$[(Al^{3+})(OH^-)_3(H_2O)_3] \rightleftarrows [(Al^{3+})(OH^-)_4(H_2O)_2]^- + H^+ \quad K_4 \qquad (4)$$

These equilibria are an over simplification because it is known that with aluminium particularly many different polymeric species are also formed (107). At aluminium concentrations as low as 10^{-5} M, hydroxyl bridges are formed between the hydrated aluminium ions producing soluble species with an OH/Al ratio up to 2.5. Equilibria data on the formation of all of these species are not available and, therefore, it is not possible to calculate the dependency of their concentrations on the pH nor their effect on the solubility of aluminium hydroxide. However if the formation of polymeric species is ignored, at concentrations of $AlCl_3$ greater than 10^{-4} M precipitation of $Al(OH_3)$ will

occur in the pH range 7-8 as the concentration is increased so the pH range for precipitation becomes greater.

Manipulation of above equilibria together with mass and charge balances enables the concentration of the various aluminium species to be calculated as a function of pH for a given total aluminium concentration. Using this method the concentration distribution - pH diagrams were calculated for 2×10^{-3} M solution of calcium, and 10^{-4} M solutions of copper, aluminium and iron salts. The results are presented in Figures 6.7, 6.8, 6.9 and 6.10, and details of the calculations given in Appendix II.

Comparison of the e.m. data obtained for coal with the solution equilibria of the metals shows that, with the exception of calcium, adsorption of all the metal cations studied results in e.m. reversal, and that this occurs in pH ranges in which the most predominant metal species are the hydroxide and the first or second hydroxy complex. However, it is not clear which of these species is adsorbed by the anthracite surface.

Calcium chloride was the only salt used which did not achieve an e.m. reversal in the pH range studied, 3 to 11. As can be seen from the species distribution diagrams for this metal (Fig. 6.7), the only species present below pH 11 are Ca^{2+} and $CaOH^{+}$. The hydroxide is not expected to precipitate until approximately pH 13 in a solution of 10^{-3} M l^{-1} $CaCl_2$. If Ca^{2+} was the adsorbed species one would expect a tendency for mobility reversal to occur at lower pH values. Therefore, it appears that adsorption must be related to the presence of $CaOH^{+}$ in solution or the formation of $Ca(OH)_2(s)$ in the pores of anthracite (above pH 13).

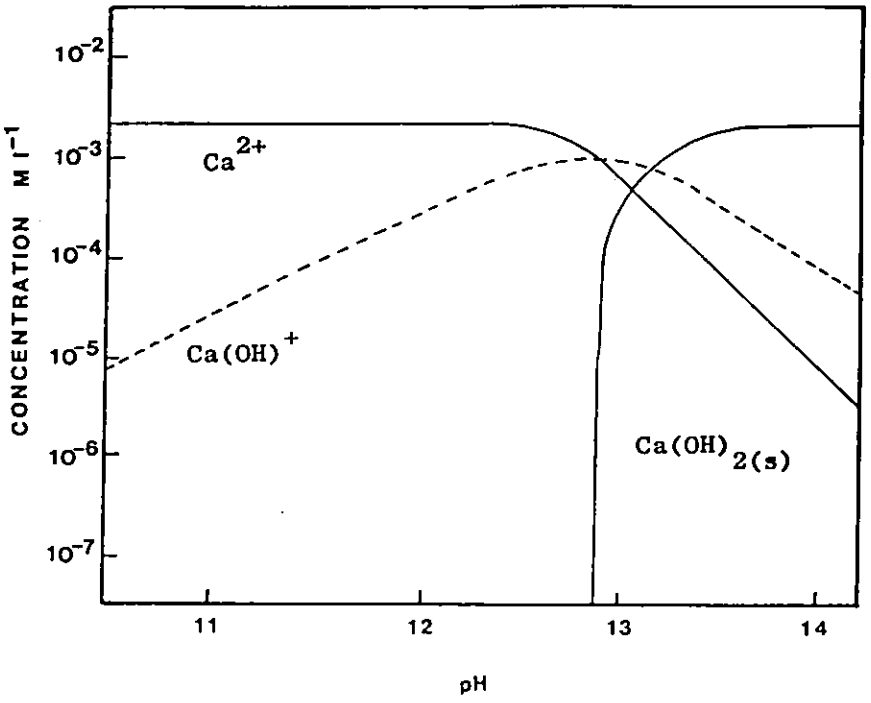

Figure 6.7 The variation of species concentration with pH in a 2×10^{-3}M $CaCl_2$ solution

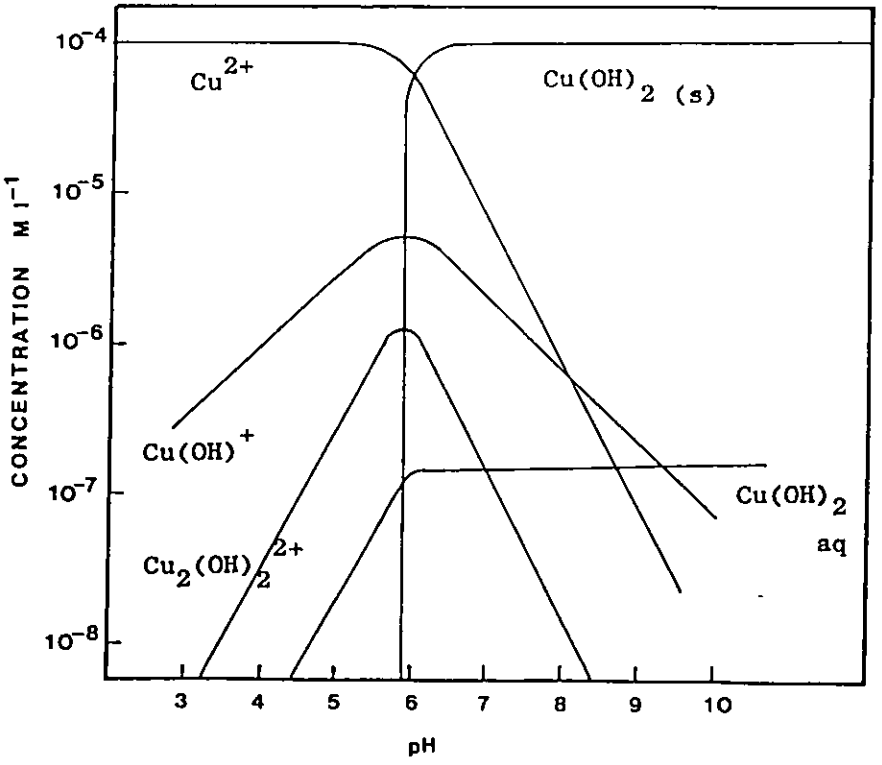

Figure 6.8 The variation of species concentration with pH in a 10^{-4}M $CuCl_2$ Solution

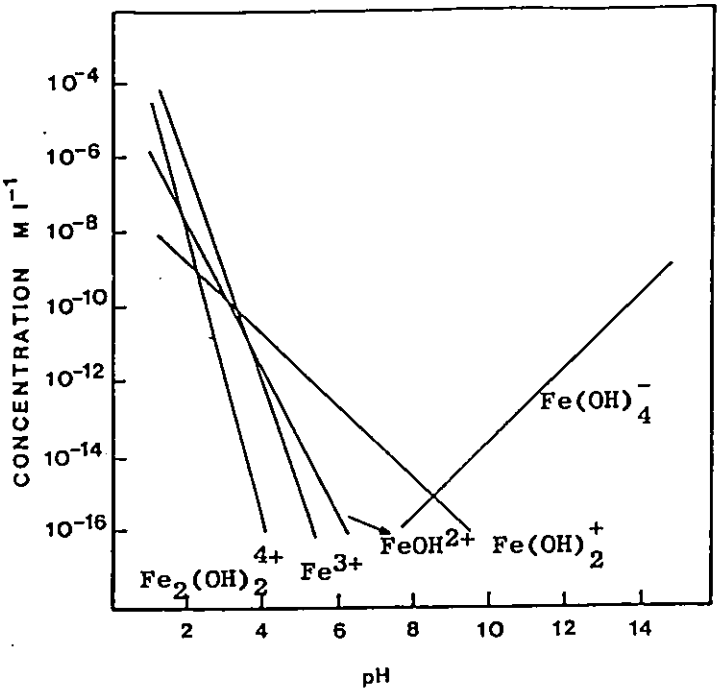

Figure 6.9 The changes of the concentration of various iron hydroxy-complexes with pH

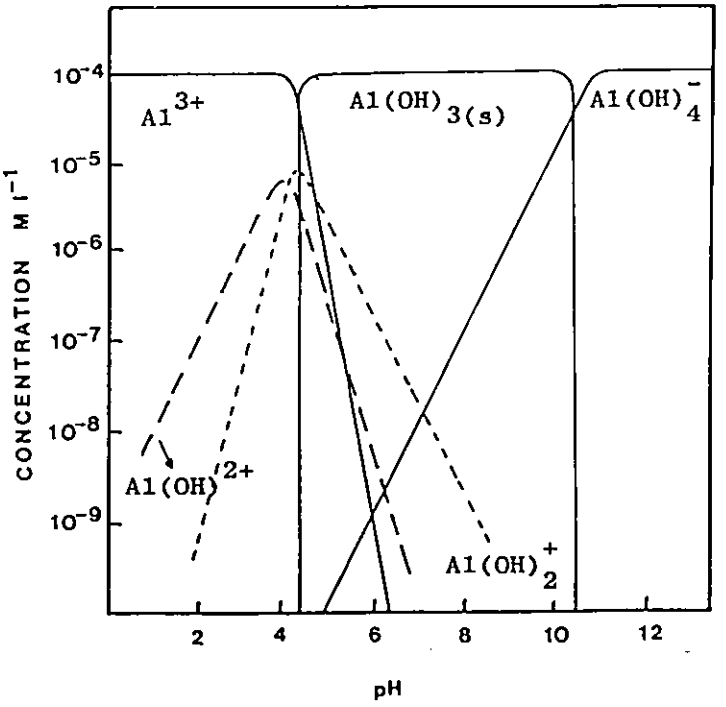

Figure 6.10 Logarithmic concentration diagram for 10^{-4}M $AlCl_3$

The e.m. of anthracite in the presence of 5×10^{-5} M and 10^{-4} M $CuCl_2$ tends to zero at approximately pH 9. This is consistent with the theory of Healy (51), who proposed that colloidal metal hydroxide species are adsorbed, and that the zeta potential then becomes equivalent to that of the adsorbed metal hydroxide. The IEP of $Cu(OH)_2$ has been given as pH 7-9.5. The result indicates that the anthracite surface is behaving as a $Cu(OH)_2$ surface. At low pH values, where Cu^{2+} predominates, the e.m. of anthracite is not affected by an increase in $CuCl_2$ concentration. It would appear that the unhydroxylated cation is not the adsorbed species. Similarly the presence of 10^{-6} M $CuCl_2$ has little effect on the e.m. of anthracite, only slightly reducing the negative mobilities above pH 4 where positively charged hydroxy species, and a solid hydroxide phase are present.

In the presence of $FeCl_3$, high positive charge on the anthracite particles up to pH 7 can be interpreted as being the result of adsorption of positively charged amorphous $Fe(OH)_3$ colloids to the negatively charged anthracite surface. Consideration of the species distribution diagram shows that the first, $FeOH^{2+}$, and the second, $Fe(OH)_2^+$ hydroxy complexes are also present but their concentrations are very small (Fig. 6.9).

Lengweiler and co-workers (108) have measured the mobility of $Fe(OH)_3$ in a 0.01 N solution of $NaClO_4$. Their data shows that $Fe(OH)_3$ is positively charged at pH 3.5, isoelectric at a pH of approximately 6.7, and reaches an approximately constant negative value above pH 8.0. The mobility - pH curve of these authors shows both positive and negative values of mobility in the pH range 6.2 to 7.2.

Below a pH of 7.2 amorphous $Fe(OH)_3$ colloids are positively charged suggesting that Coulombic adsorption of this colloid to the anthracite surface may occur over this pH range. Hydrogen bonding between OH groups of the $Fe(OH)_3$ colloid and the OH groups at the anthracite surface would also provide a mechanism of adsorption of amorphous $Fe(OH)_3$.

Comparison of Fig. 6.3 with Fig. 6.10 shows that aluminium species are adsorbed over the pH range used. At low pH values, anthracite became only slightly more positive with increasing $AlCl_3$ concentration. At higher pH values, anthracite experienced e.m. reversal. It is difficult to determine which species were responsible for the observed effect. However, at high $AlCl_3$ concentrations, it is probable that $Al(OH)_3$ was formed on anthracite surface and the e.m. reflects that of $Al(OH)_3$. This is also consistent with the theory proposed by Healy (51).

In the immediate vicinity of the anthracite surface it is possible that the localised concentration of metal species and hydroxide ions will exceed the solubility products so that precipitation can occur. Alternatively it can be argued that the stability constants of solution near a charged surface will be altered due to the effect of the charge on the "structuring" of the water and hence the dielectric constant (109). The latter is estimated to change the constants in such a way that the formation of the hydroxide would be favoured. A similar theory, which refers to field induced surface precipitation has been proposed by James and Healy (51) to explain the adsorption of polyvalent metal cations at oxide-water interfaces. These authors found that metal hydroxide formation on

an oxide surface can occur at least 2 pH units below that required for precipitation in bulk solution. This suggestion may explain the results obtained in this study.

The actual specific adsorption mechanism of polyvalent metal ions on anthracite is not clear. The results suggest that the formation of metal hydroxide on the surfaces is the main mechanism. However, it is difficult to disregard the involvement of cationic metal species. The specific adsorption of unhydroxylated cations cannot be understood unless a chemical bond is formed between the cation and a suitable surface site. Adsorption of the hydroxylated ions may be easier to explain because of the possibility of hydrogen bond formation with suitable surface sites. Whatever the mechanism it must also explain the dehydration of the adsorbing ion thereby allowing entry into the Stern Layer.

The adsorption characteristics of polyvalent metal cations onto coal surface do show great similarity to results previously documented for the adsorption of hydrolysable metals onto oxide and silicate surfaces. The mechanisms proposed to describe adsorption and to account for charge reversal in these systems have been given in Chapter 3. The results obtained in this part of the study suggest that the model proposed by James and Healy (51) provides the best description of the adsorption of metal ions on the coal surfaces.

6.2 Stability studies in the presence of metal ions

The stabilities of both anthracite and graphite as a function of pH, in the presence of 10^{-3} M NaCl, is given in figure 6.11. In both cases unstable suspensions were observed at a pH range 3 to 4 where the i.e.p. values of anthracite and graphite were obtained.

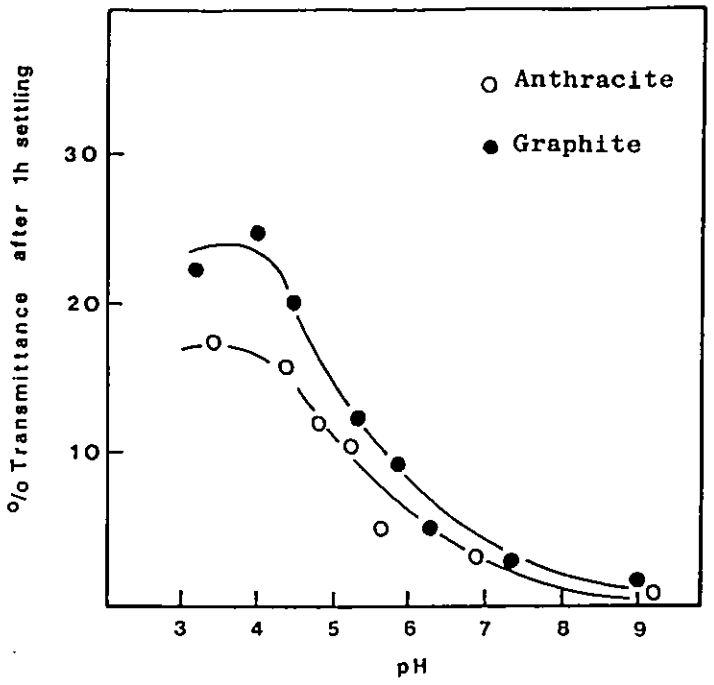

Figure 6.11 Stability of anthracite and graphite in the presence of 10^{-3}M NaCl as a function of pH

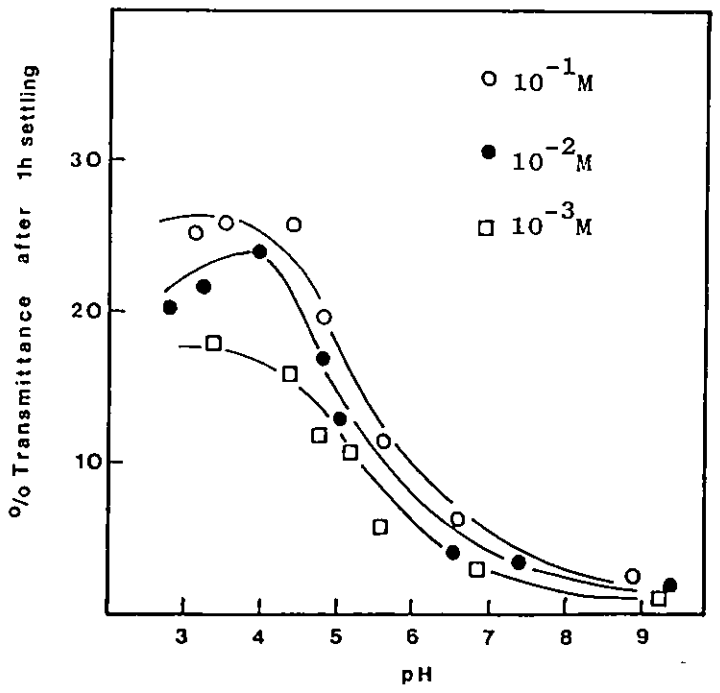

Figure 6.12 Stability of anthracite as a function of pH in the presence of various NaCl concentrations

Increasing the pH above pH 4 gave rise to stable suspensions which were associated with the increase in the negative mobility values. Figure 6.12 shows the effect of NaCl concentration on the stability of anthracite at different pH values. At a given pH the increase in the concentration of the NaCl gave rise to slightly less stable suspensions. The stability appeared to be dependent on the ionic strength and it increased with pH and decreased with the concentration of NaCl. Therefore, it might be concluded that anthracite and graphite follow a DLVO colloid behaviour.

Stability of anthracite suspensions in the presence of various $CaCl_2$ concentrations is given in Figure 6.13. Increasing the $CaCl_2$ concentration decreased the stability. However, higher concentrations above 10^{-3} M produced similar stability results. At higher concentrations of $CaCl_2$ the stability was almost independent of pH, in the pH range of 4 to 8. This result is consistent with the electrophoretic mobility data where anthracite had a zeta potential of around -10 mV between pH 4 and 8 and this low value accounts for the instability.

Figure 6.14 shows the stability of anthracite in the presence of different $FeCl_3$ concentrations. The more unstable suspensions were observed in the pH range where the electrophoretic mobility of anthracite reversed its sign.

Similar to the $CaCl_2$ - anthracite system, increasing the $FeCl_3$ concentration above 10^{-5} M did not markedly affect the stability. This result may be explained by coating of metal hydroxide nucleated on the surface. As the coating approaches full coverage, the particles behave like the metal hydroxide itself. So that once full

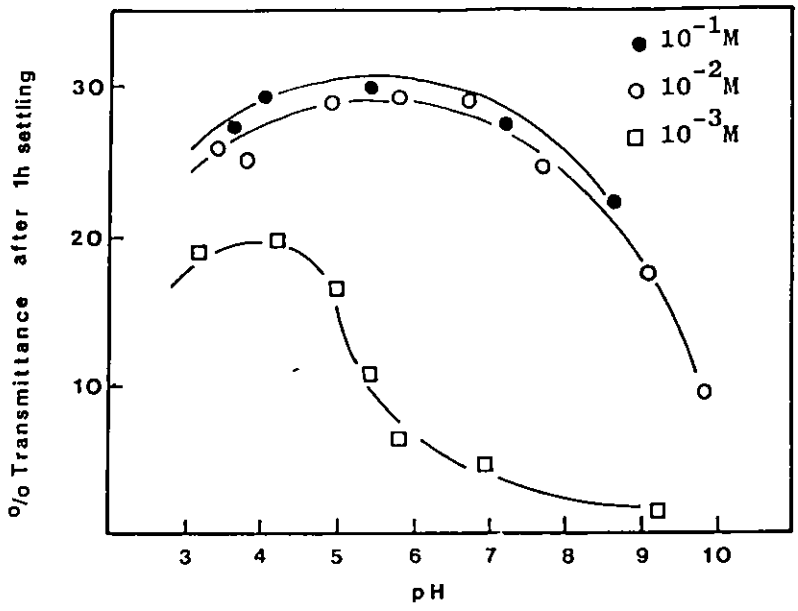

Figure 6.13 Stability of anthracite as a function of pH in the presence of various $CaCl_2$ concentrations

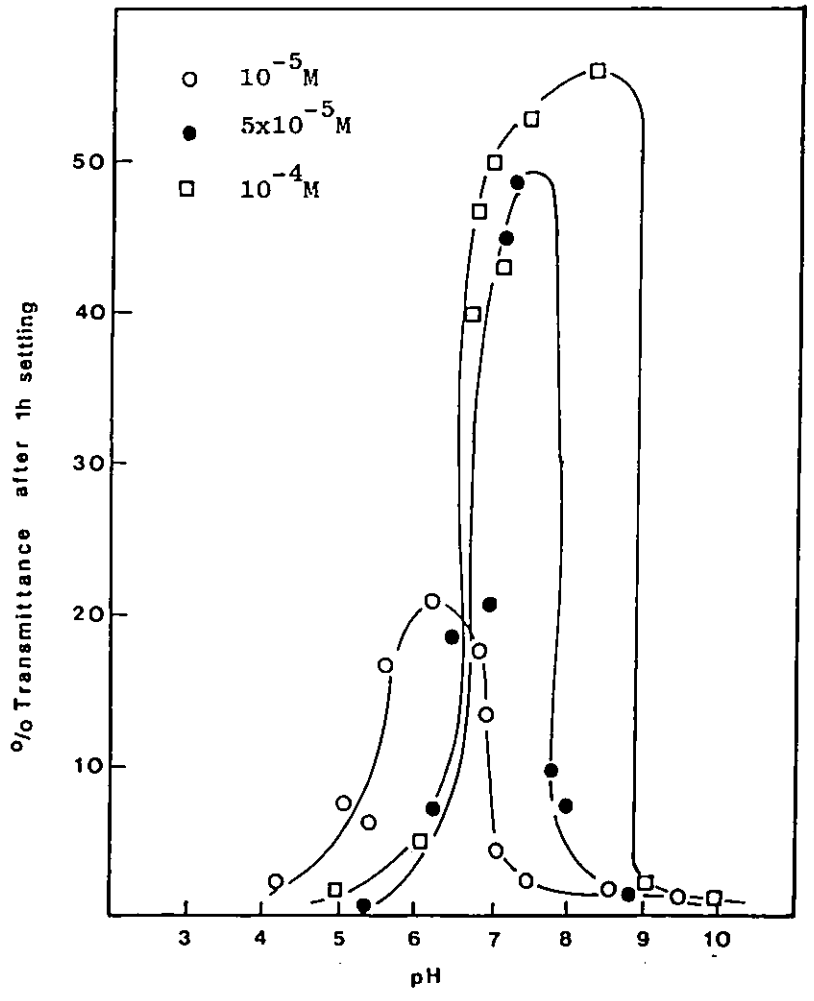

Figure 6.14 Stability of anthracite as a function of pH in the presence of various $FeCl_3$ concentrations

coverage
of metal hydroxide on the surfaces was obtained, increasing the concentration of metal salt does not produce any effect on stability. The results also show that $FeCl_3$ was more effective than NaCl and $CaCl_2$ in producing very unstable suspensions.

CHAPTER 7. FLOCCULATION AND POLYMER ADSORPTION

7. FLOCCULATION AND POLYMER ADSSORPTION

7.1 Determination of optimum flocculation conditions

Efficiency of flocculation: According to Kitchener(110) a thorough description of the progress of aggregation, would require a record of the initial particle size distribution and the distribution of aggregate sizes as a function of time, however, this has never been accomplished because of experimental difficulties. None of the classical techniques for measuring coagulation or flocculation offers a quantitative measure of the condition of a concentrated slurry containing a wide range of particle sizes. Consequently, for particular objectives, empirical test methods have been devised without being able to extract fundamental data from the parameters measured.

A series of tests have been adapted to measure the different properties which can be used to estimate the degree of flocculation of suspensions: (a) Optical transmittance of the supernatant liquid. (b) solid content of the supernatant. (c) The rate of sedimentation of floc boundary. (d) Height of the settled bed. (e) Permeability of a filter-cake formed under standard conditions(111). (f) Capillary suction time(112). (g) Apparent viscosity at a fixed shear-rate. The applicability and limitations of these parameters and correlation between them have been investigated by various workers (74)(113). However, the final selection of one or more parameters to express the degree of flocculation remains arbitrary, depending on the particular system used for flocculation. Since any proposed test of effectiveness of flocculation need only meet the requirements of reproducibility, sensitivity and convenience, the optical transmittance of

the supernatant liquid was used as a measure of the efficiency of flocculation throughout this study.

Concentration of polymer: It has already been established that the flocculation of a suspension cannot be increased indefinitely. Beyond a certain "optimum concentration" the use of additional flocculant is detrimental. This effect has been related to the ability of adsorbed macromolecules to form a bridge to other particles. This is so reduced at high surface coverage that stabilization of a suspension can occur. The results given in the next section (Fig. 7.3) shows the optimum flocculation concentrations of various polymers.

Addition of polymer: For the most efficient use of the flocculant it should be uniformly distributed throughout the suspension. If localised excess concentrations occur, then some particles may be undertreated while others may adsorb an excess and pass into stabilized state. This is most likely to occur when a concentrated solution of flocculant is used or the suspension is inadequately stirred during addition, or both. For instance, Figure 7.1 clearly shows that the flocculation of 1% anthracite suspensions with PEO addition from a 500 p.p.m. solution is less efficient than from a 50 p.p.m. solution.

The effect of agitation: In a slowly coagulating colloidal suspension collision frequency between particles is determined by Brownian motion (perikinetic flocculation). Brownian motion has little effect, however, on the diffusion of larger particles and it is necessary to apply agitation to the suspension to attain a convenient rate of flocculation (orthokinetic flocculation). Figure

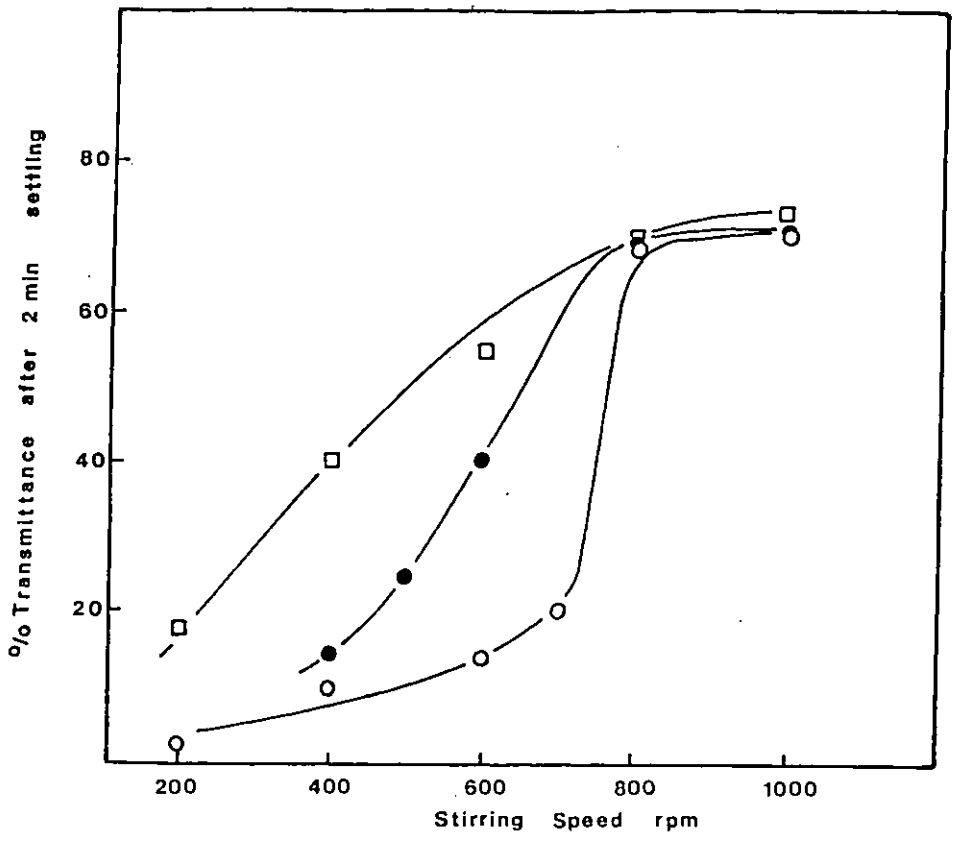

Figure 7.1 Effect of PEO addition from different stock solutions and agitation on the flocculation of anthracite

1% solid content, PEO Conc. 7.5 p.p.m.

2 min. stirring at given speed followed by 1 min. gentle stirring at 50 rpm.

o PEO addition from 500 p.p.m. stock solution

● PEO addition from 50 p.p.m. stock solution

□ PEO addition from 50 p.p.m. stock solution
2 min. stirring at given speed followed by 5 min. gentle agitation at 50 rpm.

7.1 shows the effect of various stirring speeds on the flocculation efficiency, lower initial agitation rates are seen to be detrimental whereas extension of the flow stirring period can be beneficial. This is due to the production of larger flocs and also the promotion of a "scavenging" action where individual particles are "swept up" and united with the large flocs.

Solid concentration: The percentage of solids in a suspension can effect the optimum polymer/solid ratio because it influences the number of interparticle collisions. As can be seen from Figure 7.2 decreasing the solid concentration decreased the optimum polymer/solid ratio. However, Linke and Booth (113) showed that over a practical range of pulp densities (4-50%), the changes in optimum concentration were small.

7.2 Flocculation by polymers

Figure 7.3 shows the optical transmittance of the supernatant liquid of flocculated anthracite suspensions as a function of polymer concentration, at certain pH values. Non-ionic PAM, cationic polymer and anionic PAM all appeared to be very effective in flocculating the anthracite. PEO produced slightly lower flocculation efficiencies, but no anthracite flocculation was obtained with PVA and PVP at any pH. In the presence of 10^{-1}M NaCl, however, both polymers produced flocculation with an efficiency similar to that obtained with PEO (Fig. 7.4).

The flocculation efficiencies of anthracite flocculated with PEO and non-ionic PAM were found to be independent of pH over the pH range 2 to 11 (Fig. 7.5). The flocculation result obtained at a constant anionic PAM concentration of 10 p.p.m. at different pH values is also

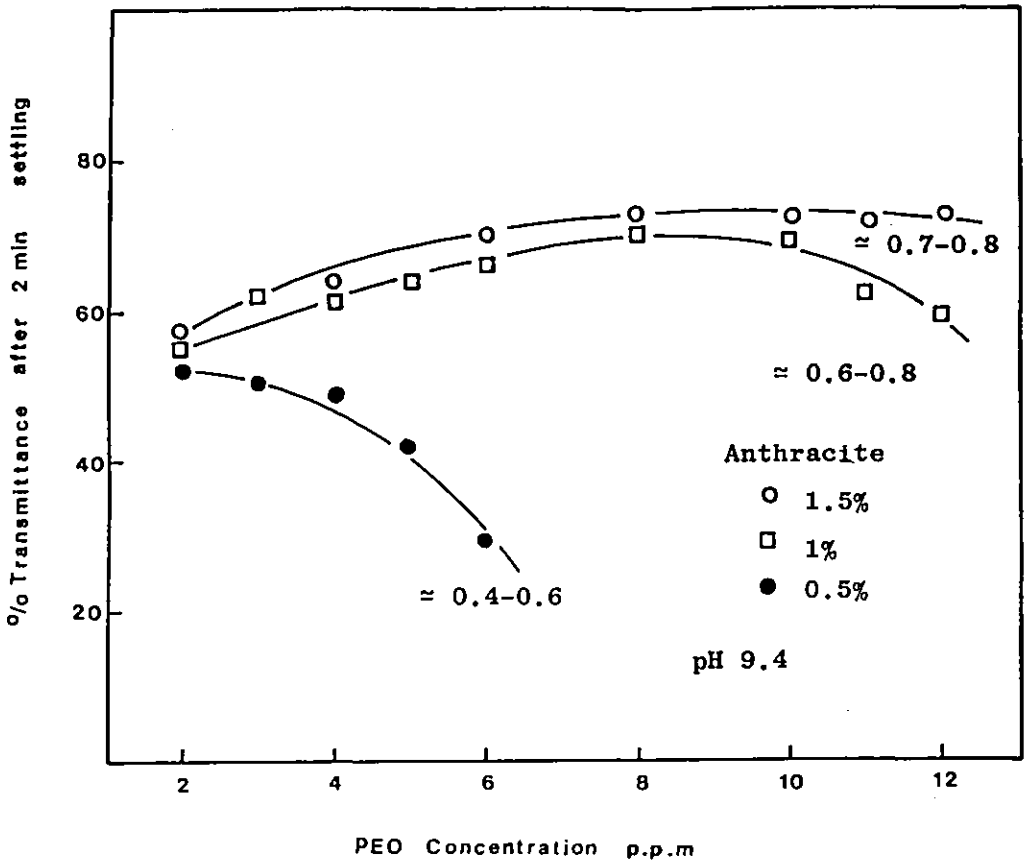

Figure 7.2 Effect of solid concentration on the flocculation of anthracite (Figures show the ranges of the optimum polymer/solid ratios)

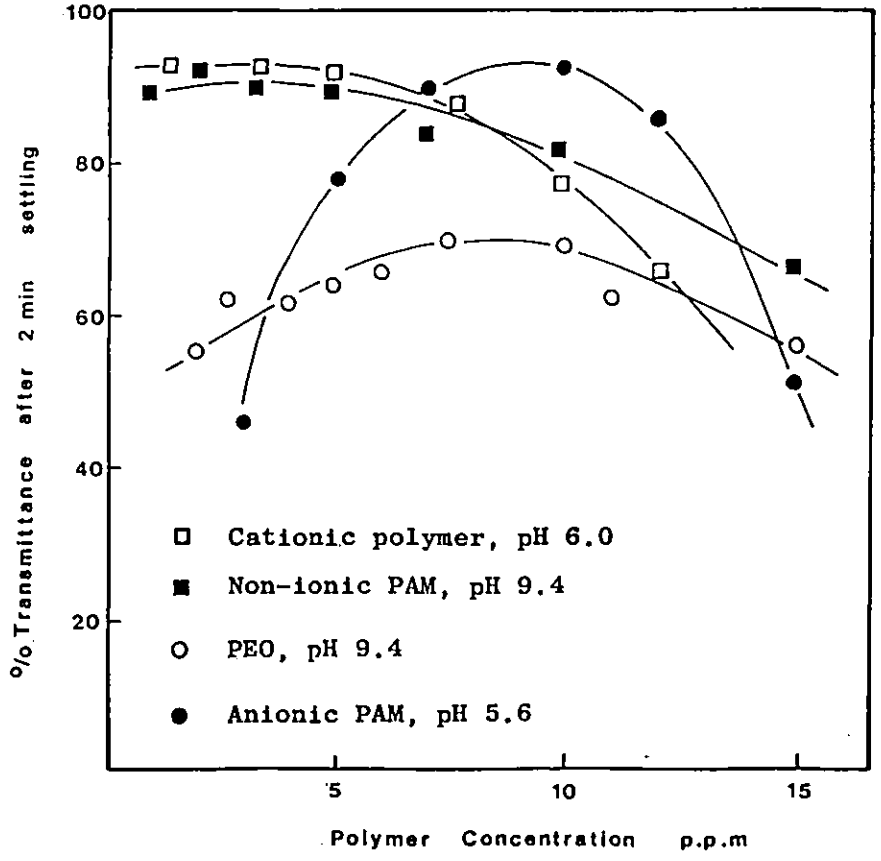

Figure 7.3 Flocculation of anthracite by various polymers

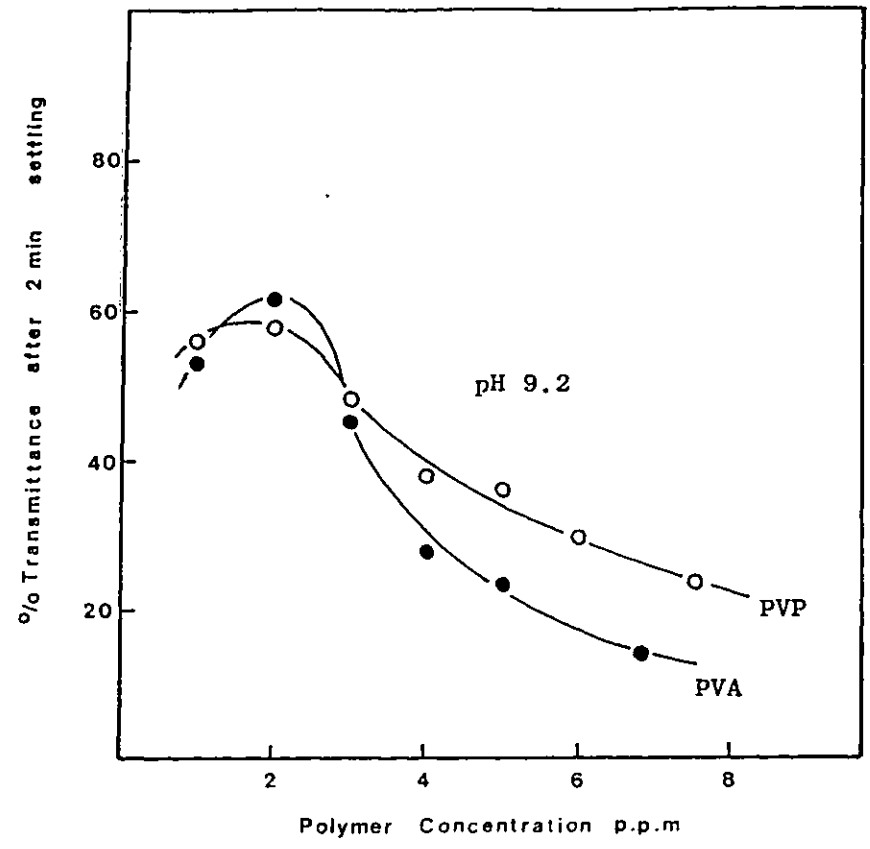

Figure 7.4 Flocculation of anthracite by PVP and PVA in the presence of 10^{-1} NaCl

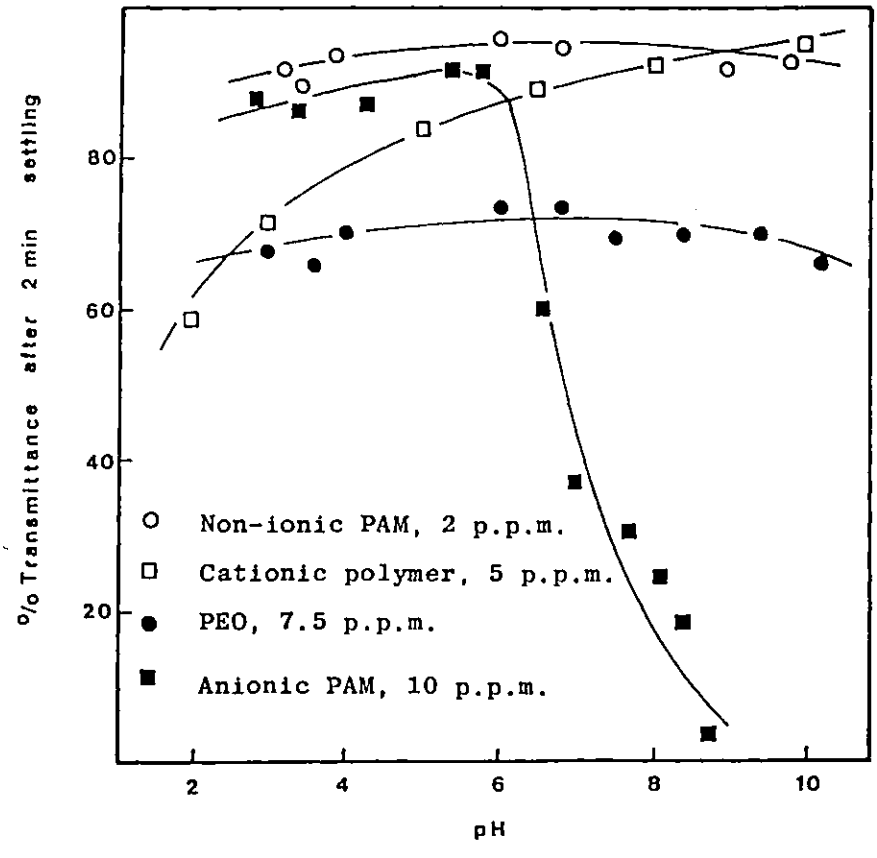

Figure 7.5 Effect of pH on flocculation of anthracite by various flocculants

given in the same figure. Anionic PAM did not produce flocculation of anthracite at pH values above pH 8 in the absence of added NaCl. However, below neutral pH values where the anthracite had a zeta-potential value of about -20 mV flocculation was obtained without the addition of NaCl.

With the cationic polymer high flocculation efficiencies of anthracite were obtained above pH 5, decreasing the pH below this value decreased the efficiency.

Influence of NaCl on PEO flocculation of anthracite is given in Figure 7.6. Increase in the concentration of the NaCl over a narrow range has an effect on the flocculation. The change in the concentration of the NaCl from 10^{-3} M to 5 x 10^{-3} M considerably increased the flocculation efficiency.

Simple non-ionic organic compounds, such as hydroxyquinoline, acetone and ethanol, which would be capable of entering H-bonding were employed in "competitive" tests with the non-ionic polymers to establish the mechanism of attachment of polymers on the anthracite surface. The results showed that flocculation of anthracite was not influenced by the addition of H-bonding agents up to very high concentrations (10^{-5} M hydroxyquinoline, 10^{-3} M acetone) at a constant PEO and non-ionic PAM concentrations of 7.5 and 2 p.p.m., respectively.

When the tests were carried out on oxidized anthracites, the flocculation efficiency did not significantly change from that of unoxidized sample using anionic PAM. Non-ionic PAM flocculated even extensively oxidized anthracite (48 h oxidation with oxygen at 200°C) but flocculation efficiency decreased. PEO, however, did not produce flocculation of even slightly oxidized anthracite (12 h

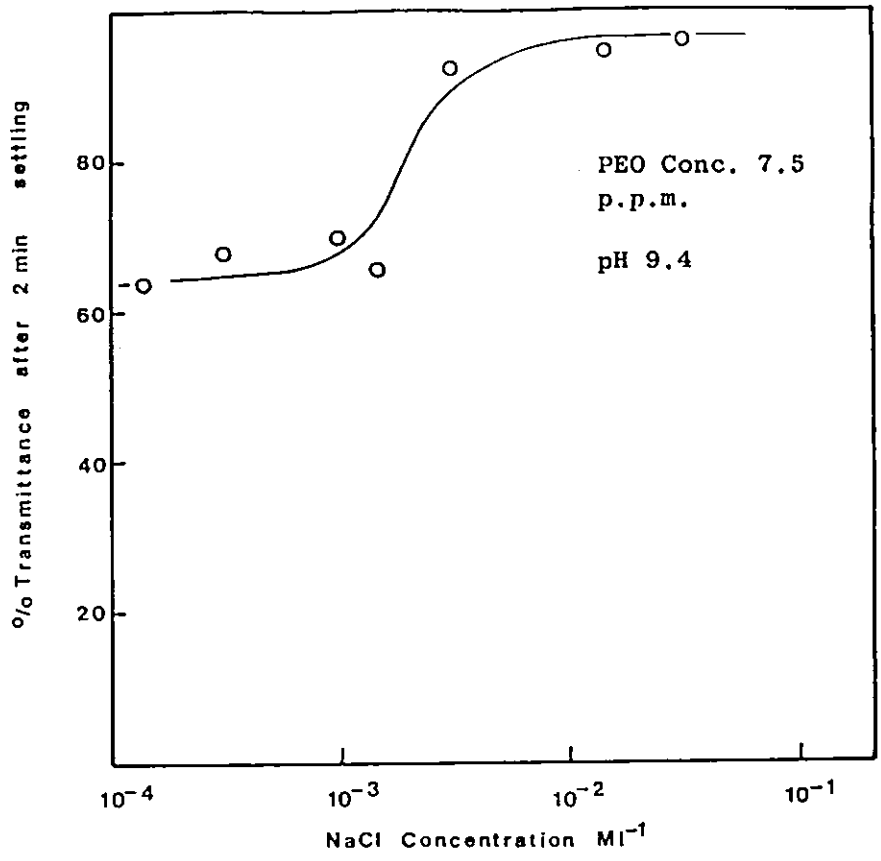

Figure 7.6 Effect of NaCl on the PEO flocculation of anthracite

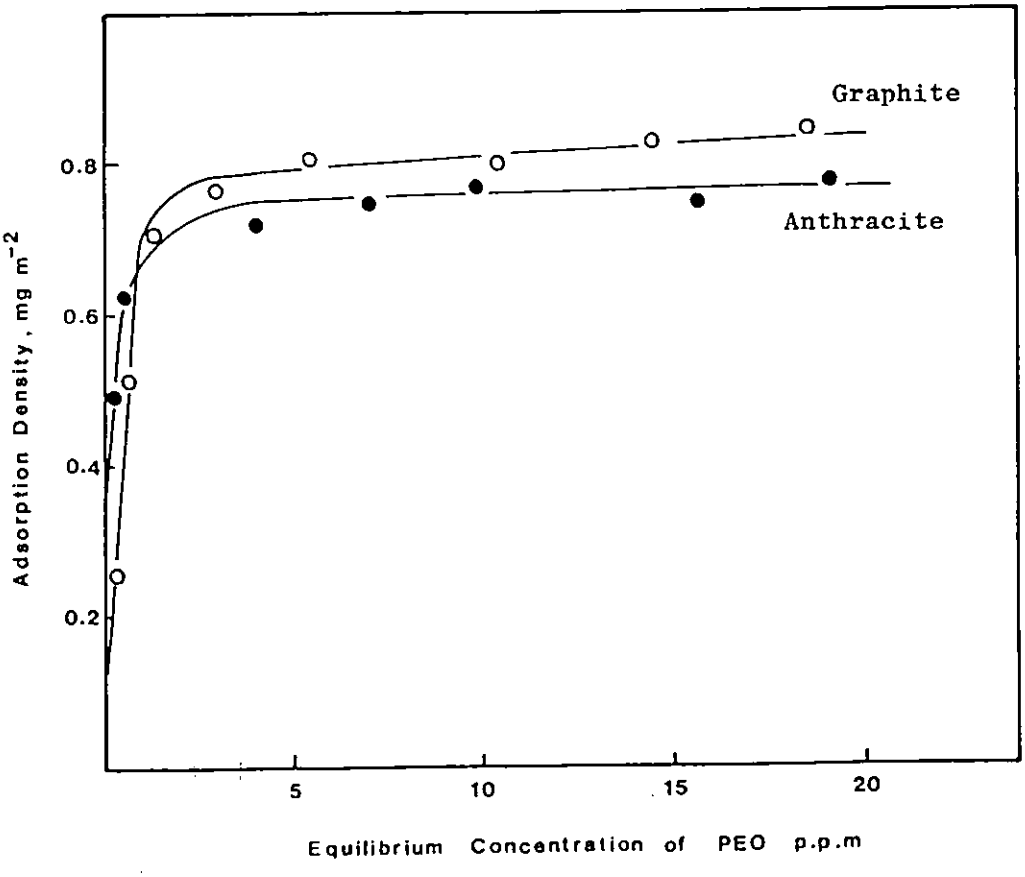

Figure 7.7 Adsorption isotherms for PEO on anthracite and graphite at pH 9.1

oxidation with air at 100°C). Also it was found that the presence of $FeCl_3$ and $AlCl_3$ up to 500 p.p.m. did not influence the flocculation efficiencies of the anthracite suspensions using PEO at alkaline pH.

7.3 Adsorption of polymers

It was not possible to measure the adsorption of PEO on either anthracite and graphite under conditions comparable to those used in the flocculation tests. From Figure 7.4 it is seen that the maximum flocculation efficiency was obtained with the addition of about 10 p.p.m. PEO. At this concentration the PEO was strongly adsorbed and it was not possible to determine an equilibrium concentration because it was below the limit of detection. Therefore, in the PEO adsorption tests much higher initial polymer concentrations were used than those in the flocculation tests. The adsorption density of PEO on both anthracite and graphite is given in Figure 7.7. The amount of PEO adsorbed per gram of anthracite and graphite was divided by the BET surface area. On this basis, it appeared that the amount of PEO adsorbed was slightly higher on graphite than on anthracite.

Figure 7.8 shows that the specific adsorption of PEO on anthracite is independent of pH. This result is consistent with the flocculation data where no significant pH effect was obtained.

The adsorption density of PEO on anthracite in the presence of various hydroxyquinoline concentrations is given in Figure 7.9. The amount of PEO adsorbed is almost independent of the hydroxyquinoline concentration. The presence of this H-bonding agent also slightly decreased the adsorption of PEO on anthracite.

Figure 7.10 shows the adsorption of anionic PAM on both anthra-

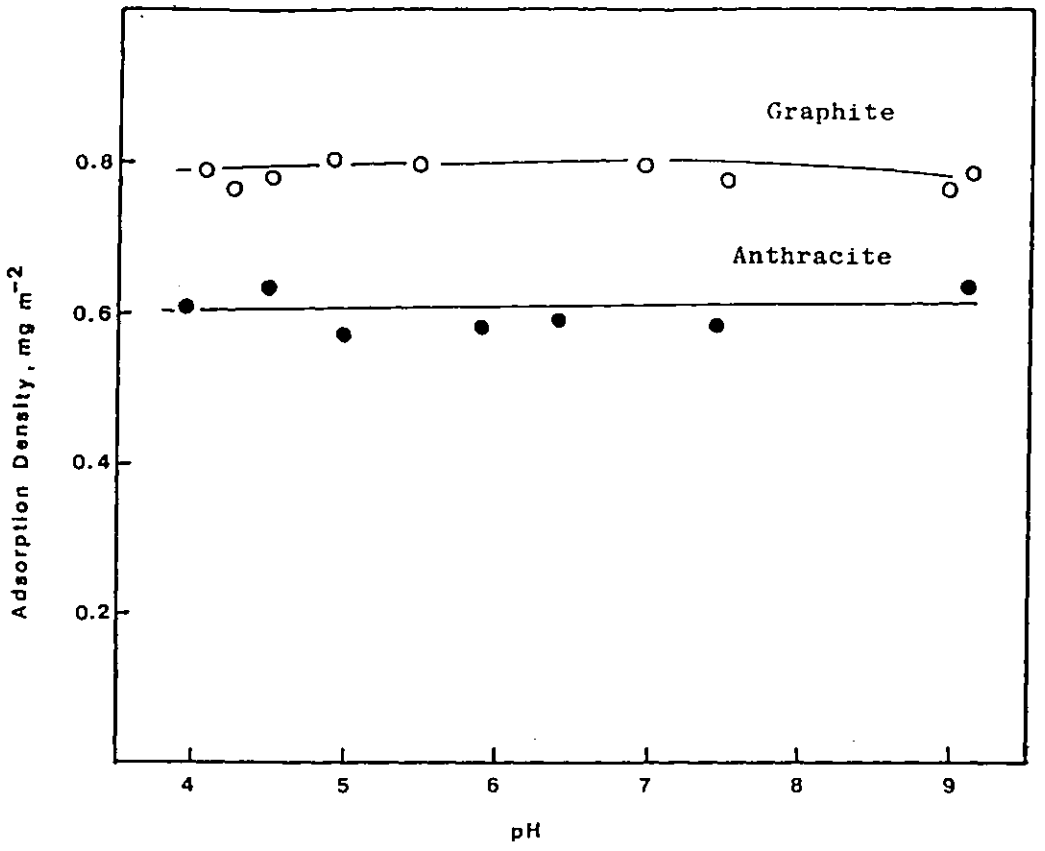

Figure 7.8 Adsorption of PEO on anthracite and graphite as a function of pH (In. PEO conc., 50 p.p.m. for anthracite, 40 p.p.m. for graphite)

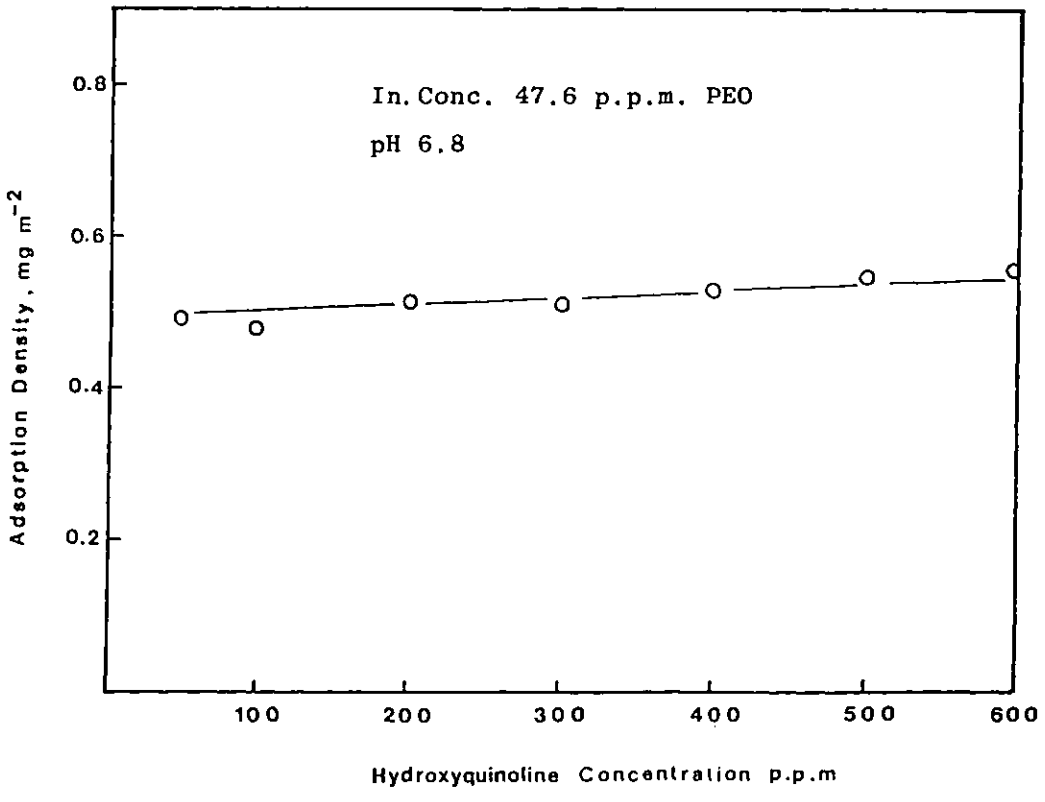

Figure 7.9 Effect of hydroxyquinoline on the adsorption density of PEO on anthracite

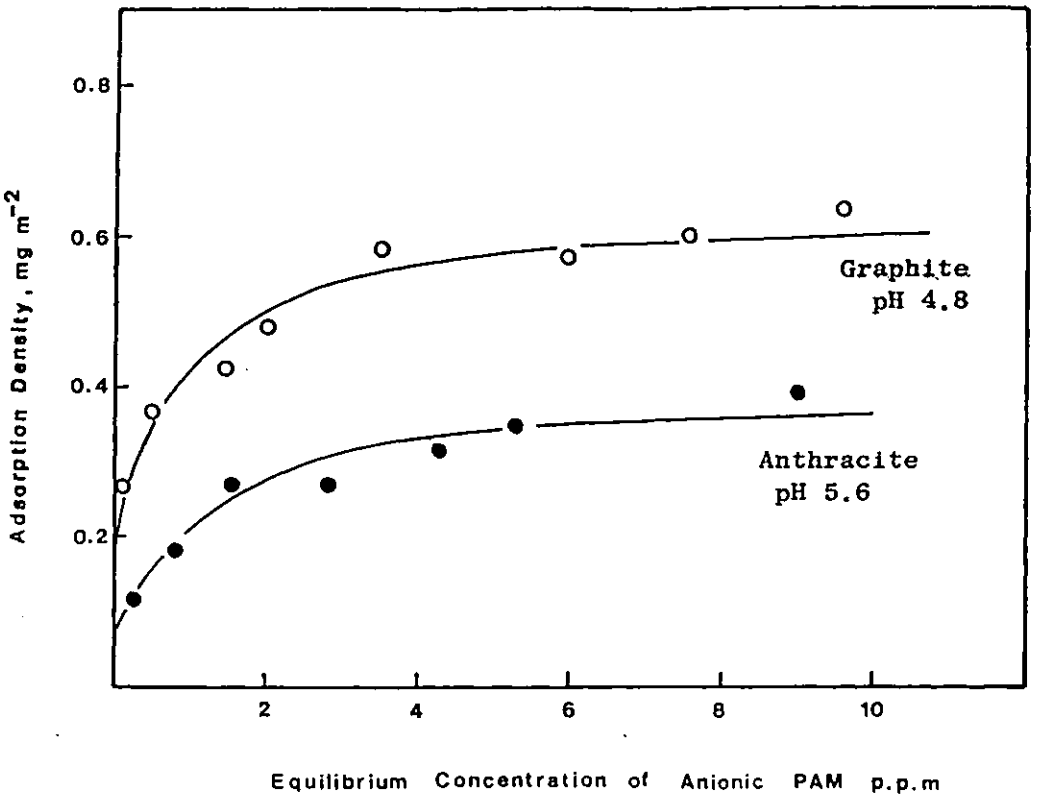

Figure 7.10 Adsorption isotherms for anionic PAM on anthracite and graphite

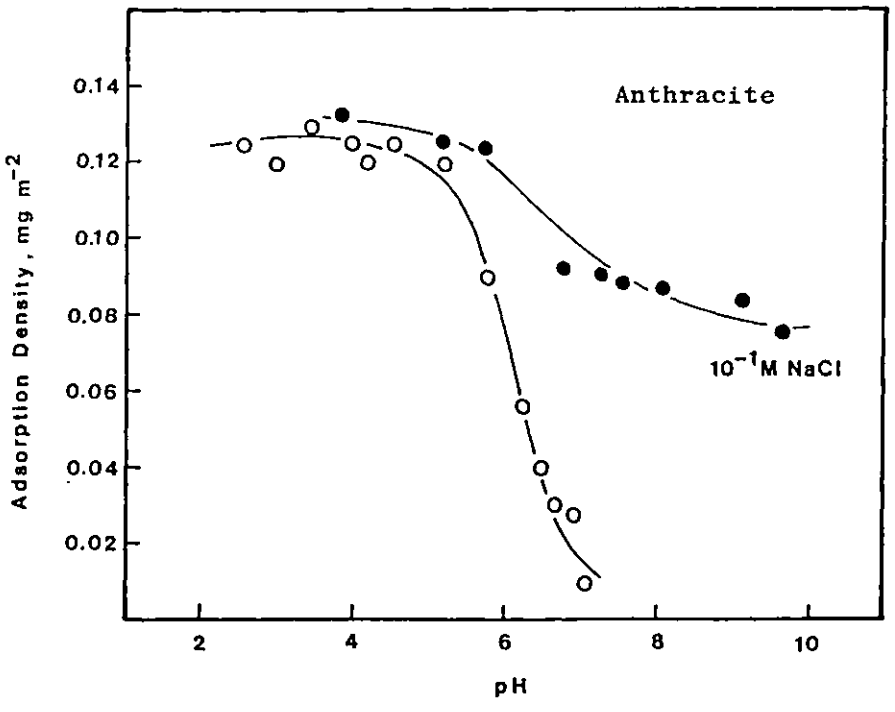

Figure 7.11 Effect of pH on adsorption of anionic PAM in the absence and presence of 10^{-1}M NaCl
(Initial anionic PAM conc. 10 p.p.m.)

cite and graphite. These adsorption isotherms show the characteristic shapes of those usually obtained for macromolecules (114). The effect of pH on the adsorption density of anionic PAM on anthracite is given in Figure 7.11. As was predicted from the flocculation tests the adsorption density was found to be dependent on pH. Adsorption of this polymer on anthracite in the presence of NaCl is also shown in Figure 7.11. Comparison of the adsorption measurements in the presence and absence of the NaCl clearly shows that ionic strength has an effect.

To determine whether or not polymer adsorption is dependent on the presence of H-bonding sites on anthracite and graphite attempts were made to remove all sites which contain "active" hydrogen by methylation. Adsorption data for polymers on methylated samples are given in Figures 7.12 and 7.13. It can be seen that either PEO or anionic PAM adsorption on methylated anthracite and graphite did not significantly change compared to that on untreated samples.

The effect of oxidation on the adsorption of polymers is shown in Figures 7.14, 7.15, 7.16, and 7.17. It can be seen that an increase in the degree of oxidation progressively reduces the amount of PEO adsorbed on anthracite. This reduction on oxidized anthracites was not due to the changes in the surfaces accessible to polymer, since negligible reductions were obtained in the surface area measurements of the samples as a result of oxidation. (Although it could be argued that the surface area available for adsorption will not be the same as that measured by BET apparatus where nitrogen gas is used as the adsorbate.) These results are consistent with previous reports on the effect of oxidation on coal properties,

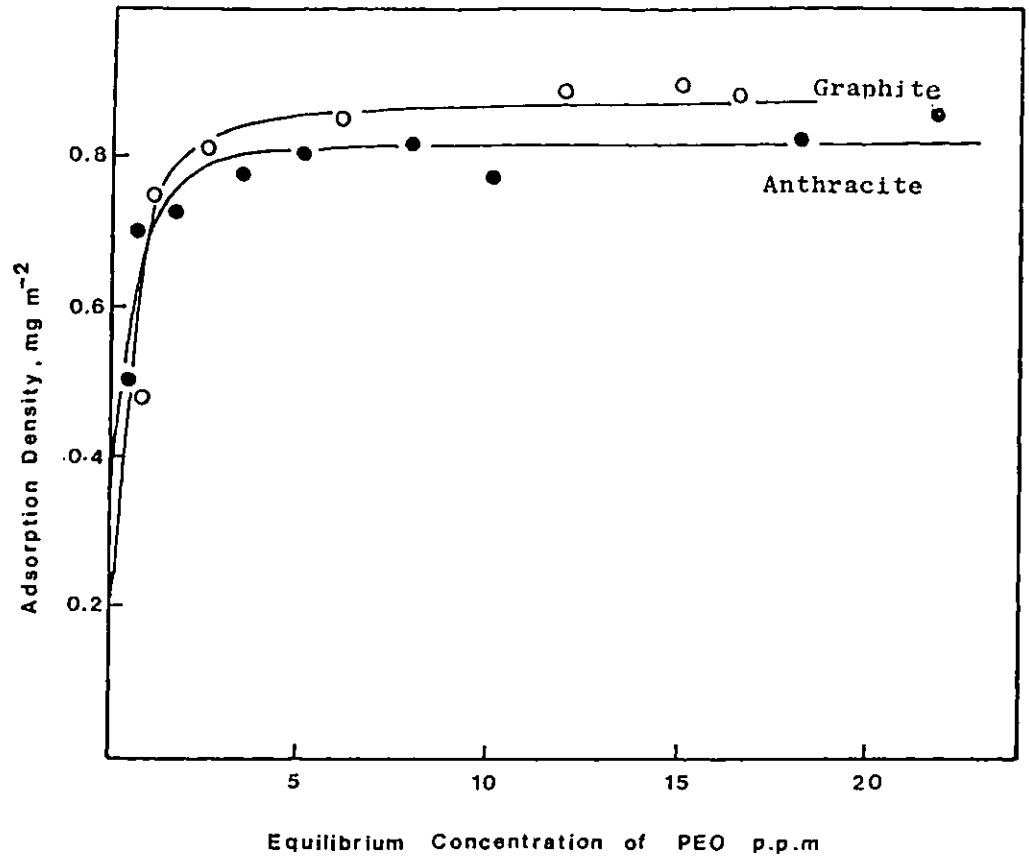

Figure 7.12 Adsorption isotherms for PEO on methylated anthracite and graphite

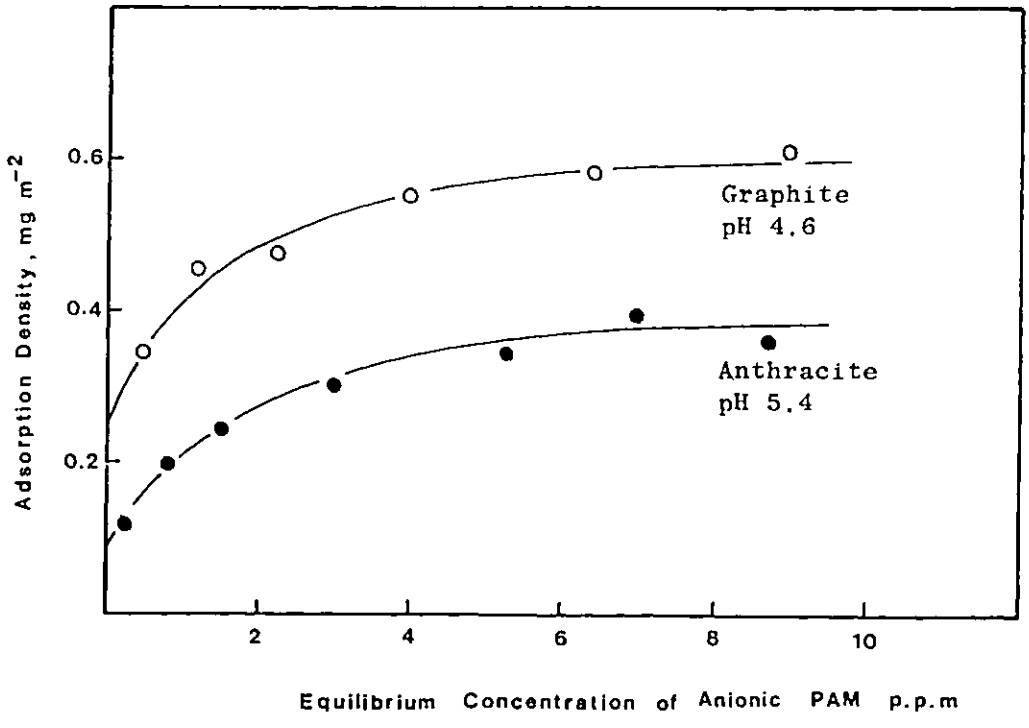

Figure 7.13 Adsorption isotherms for anionic PAM on methylated anthracite and graphite

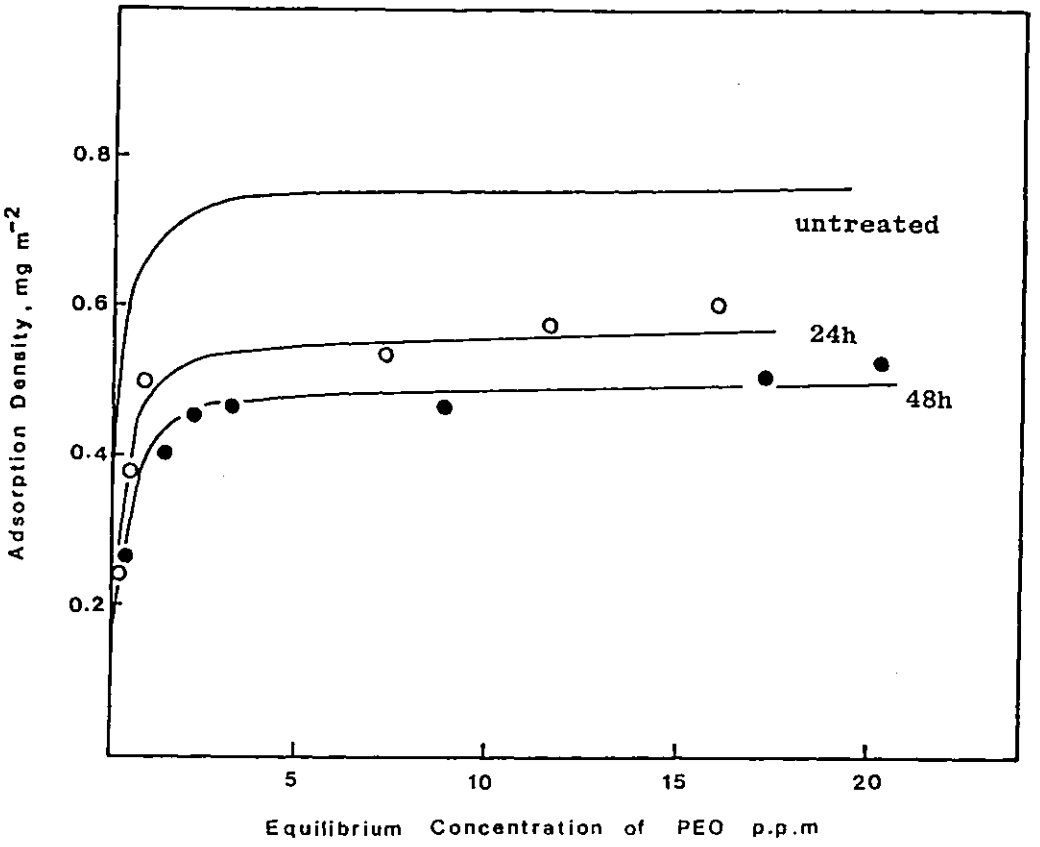

Figure 7.14 Adsorption isotherms for PEO on anthracite (oxidized with air at 100°C)

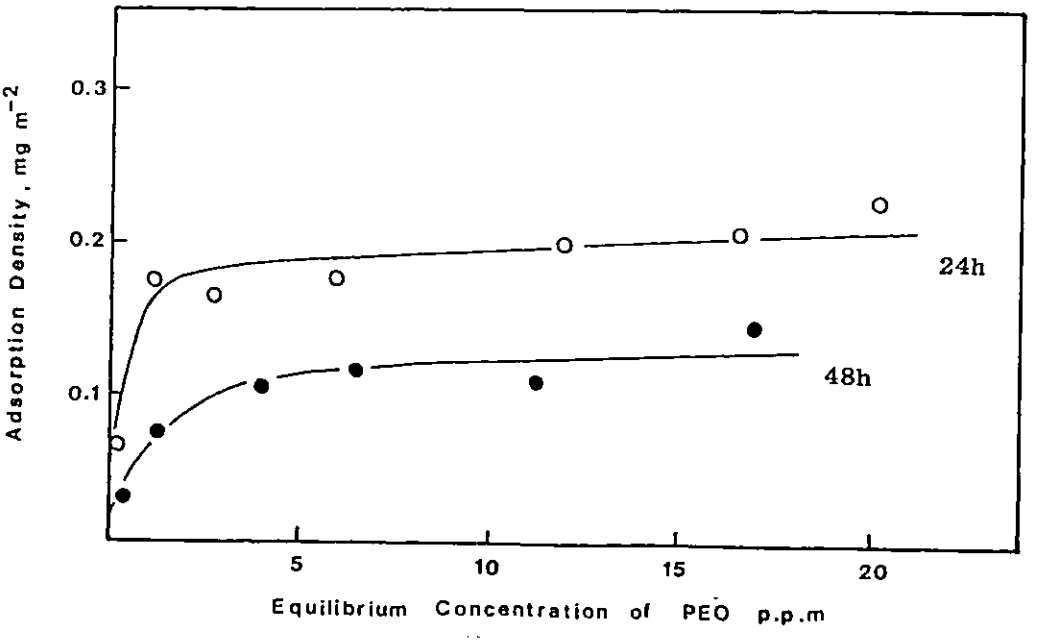

Figure 7.15 Adsorption isotherms for PEO on anthracite (oxidized with air at 200°C)

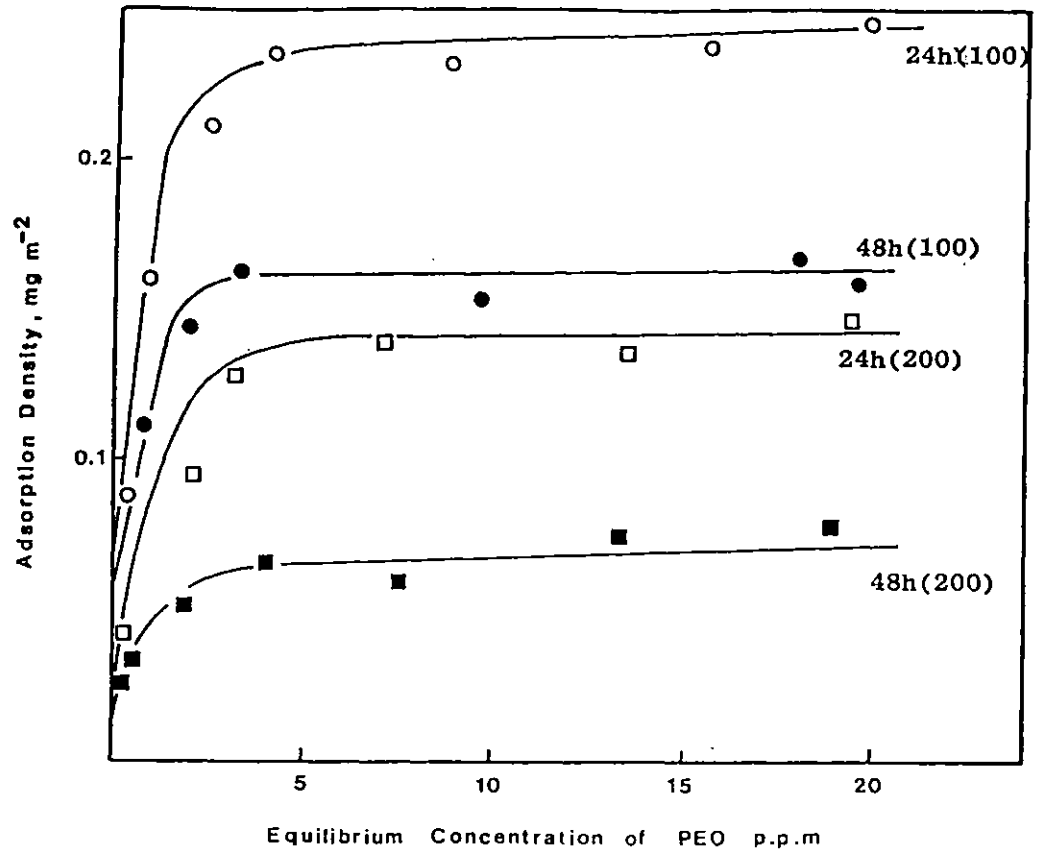

Figure 7.16 Adsorption isotherms for PEO on anthracite oxidized with oxygen at 100°C and 200°C

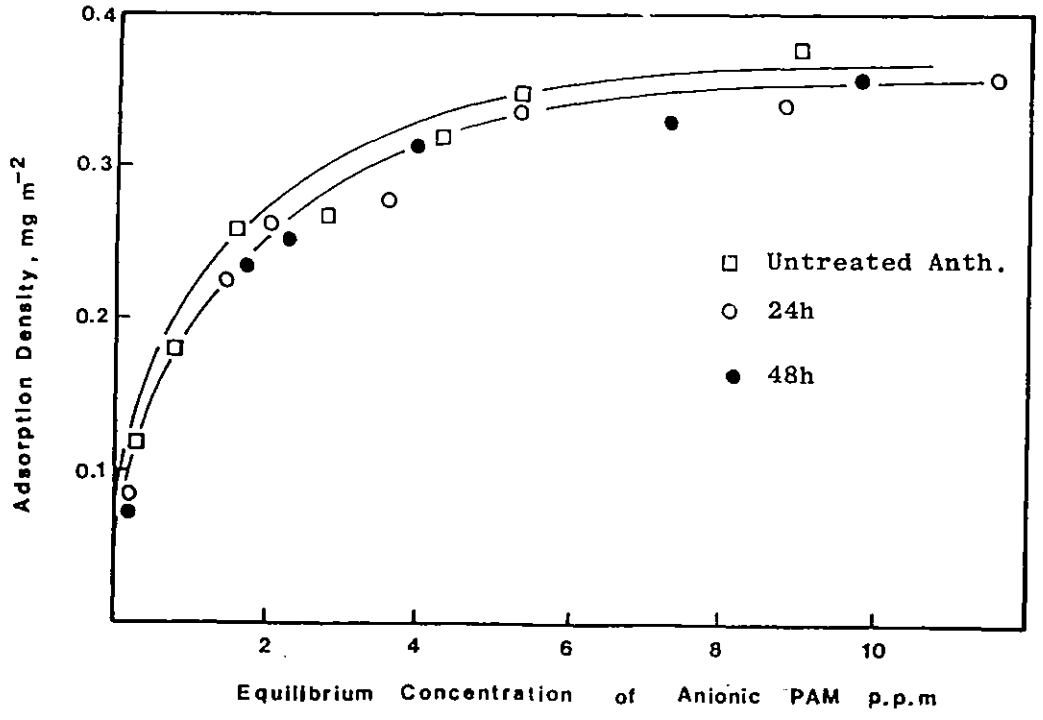

Figure 7.17 Adsorption isotherms for anionic PAM on anthracite oxidized with oxygen at 200°C

such as the loss in flotation response due to oxidation (115), and reduced adsorption of nonionics on oxidized carbons (116).

The amount of anionic polymer adsorbed on oxidized anthracite however, did not significantly change from that on unoxidized sample (Fig. 7.17).

As was previously stated, it was not possible to oxidize graphite under the same conditions used to oxidize anthracite. However, polymer adsorptions were measured on the graphite samples which were subjected to the treatment applied to anthracites. The results showed that no significant changes in the amount of PEO or anionic PAM adsorption occurred on those graphite samples, as was expected.

7.4 Mechanisms of the adsorption of polymers

PEO-Anthracite system: Attempts have already been made to understand the several contributions that lead to adsorption of a PEO molecule at various surfaces, but no quantitative analysis could be achieved. From a comparison of the reported flocculation studies of different dispersions by PEO, it appears that this polymer is a good flocculant for those solids which may be referred to as somewhat "hydrophobic".

Initially, it may be reasonable to assume that because PEO contains strong electron donor groups, namely the oxygen of the ether group, these may be held to the anthracite or graphite surface by hydrogen bonds. However, the experimental results obtained in this study generally confirm that PEO adsorbs by hydrophobic interactions at the coal surface.

The effect of pH on the adsorption of PEO shows that the adsorption does not depend on the surface charge of the anthracite. Since

dissociation of carboxyl groups, occurring at pH > 4 or 5, effectively prohibits the formation of hydrogen bonds between carboxyl groups and the polymer, it can be concluded that the adsorption of PEO from water cannot be characterised by this mechanism. Instead hydrophobic interactions could play an important role because the ethylene, CH_2-CH_2- groups of the polymer are sufficiently hydrophobic to interact with the hydrophobic sites on the coal surface. Birkner and Edzwald (117) have suggested that H-bonding occurs between the ethylene groups in the polymer chain and oxygen atoms on a kaolin surface, although -CH_2 groups are not usually considered to act as proton donors. That the adsorption is not significantly altered by changing the pH over a wide range is also consistent with the adsorption of dextrin on bituminous coal (118) and phenol adsorption on anthracite (119) where it was suggested that the predominant mechanism of adsorption of these nonionics is through hydrophobic interactions.

Removal of possible H-bonding sites from the surfaces by methylation does not significantly affect the amount of PEO adsorbed. Since replacement of "active" hydrogen in the surface groups with a methyl group should increase the hydrophobicity of anthracite or graphite, increases in the level of PEO adsorption would be expected if the interaction mechanism is mainly due to hydrophobic associations. However, it is likely that the strongly hydrophobic anthracite or graphite surface may provide sufficient sites for PEO adsorption so that a further increase in the hydrophobic character of these surfaces has essentially no effect on the amount of PEO adsorbed. It may also be possible that because of incomplete methylation, the hydrophobicity of the samples was not increased

to an extent that would effect the adsorption density of PEO. It was previously shown that although methylation was achieved to a certain degree, it was not complete.

The predominant mechanism of PEO adsorption through hydrophobic interactions is further supported by the experiments with the oxidized samples. Increases in the acidic oxygen functional groups of the anthracite by controlled oxidation markedly decreases the level of PEO adsorption. The increase in the number of polar oxygen sites, as quantified with electrokinetic and infrared data, causes a reduction in the hydrophobic character of the coal and a decrease in the extent of PEO adsorption.

However, the effect of the H-bonding competitor, hydroxyquinoline, on the amount of PEO adsorbed on anthracite suggests that the occurrence of some H-bonding with the surface cannot be ruled out completely for this polymer. Results show that PEO adsorption on anthracite did slightly decrease in the presence of hydroxyquinoline. On the other hand, it has been suggested that the H-bonding competitors may also be adsorbed by hydrophobic association on to nonpolar areas(71). If this is true, then in the presence of competitors an increased amount of adsorption or flocculation efficiency would be expected. This was not obtained.

The amount of PEO adsorbed was higher on graphite than on anthracite. Since the graphite is more hydrophobic (or rather contains less acidic hydrophilic sites than anthracite) this observation also confirms that the PEO strongly adsorbs on hydrophobic solids.

The effect of NaCl on the PEO flocculation of anthracite is rather complicated. The addition of NaCl at a given pH (9.4) in-

creases the flocculation efficiency. It is known that addition of salt increases the concentration of charged sites on the surface. If the adsorption is due to H-bonding, the increase in the surface charge should reduce H-bonding and also the flocculation, because, with increasing surface charge, the amount of undissociated groups available for H-bonding, decreases. A decrease in the flocculation efficiency would also be expected because of the screening effect of hydrated counter ions. Thus, at higher NaCl concentrations much of the surface becomes inaccessible to polymer due to the steric hindrance of the hydrated sodium counter ions in the vicinity of the negatively charged sites. However, in the presence of NaCl, a decrease in the flocculation efficiency was not obtained. Since the characteristic viscosity of PEO solutions is independent of the NaCl concentration and pH of the solution (120), it can be assumed that the conformational state of the polymer does not change as a consequence of the effect of the NaCl concentrations. Also, it was shown by the stability tests that the NaCl concentrations used in the flocculation experiments are not high enough to produce electrolytic coagulation of anthracite particles (at pH 9.4) and to render the entire suspension more amenable to flocculation. Therefore, the observed increase in the flocculation efficiency may be explained by the ionic strength effect which can be ascribed to reduction in the long-range double layer repulsion between anthracite particles; the double layer thickness may then become small enough to allow PEO molecules to bridge the gap.

The presence of ferric and aluminium salts did not change the efficiency of PEO as a flocculant. If PEO is adsorbed by hydro-

phobic interactions then the presence of hydroxide precipitates of those metals is unlikely to influence flocculation using non-ionic PEO.

Anionic PAM-Anthracite system: The adsorption measurements of anionic PAM on anthracite in the absence and presence of NaCl clearly show that this polymer only adsorbs on the anthracite in alkaline medium when the electrostatic repulsion between the anionic surface sites and the anionic polymer groups is reduced by increasing the ionic strength.

Below neutral pH values both flocculation and adsorption was obtained, in the absence of added salt, indicating that there may be some non-ionic mechanism of adsorption available. In acidic medium, above the IEP, where carboxyl groups are partly dissociated and the zeta potential of the anthracite is low, it is likely that H-bonding is operative between the undissociated carboxyl or the amide groups of the polymer and the anthracite surface.

In the absence of added salt, zero adsorption above pH 8 corresponded to a zeta potential of about -40 mV. Above this pH the carboxyl groups fully ionize. Therefore the polyanion has a maximum negative charge and since the anthracite is also negative, interaction is prevented by Coulombic repulsion.

In the anionic flocculation of anthracite, the effect of NaCl appears to be to reduce the negative zeta potential of the particles so that long range repulsion provides less opposition to adsorption.

Surprisingly, anionic PAM adsorption on methylated samples did not change from those of untreated samples. It was expected that

the removal of possible H-bonding sites by methylation would reduce the adsorption of anionic PAM. The results suggest that either another mechanism of adsorption, apart from H-bonding, is operative or the unmethylated groups provide sufficient adsorption sites for anionic PAM so that the difference cannot be observed experimentally.

The effect of oxidation of anthracite on the adsorption of anionic PAM is also complicated. No significant change in the adsorption was obtained from that on an unoxidized sample. Since oxidation generates more oxygen-containing active sites on the surface some specific chemical interaction between these sites and the anionic PAM may give the adsorption density values obtained.

Another anomalous observation was that the amount of anionic PAM adsorbed on graphite is higher than that on anthracite. It was established that the graphite contains less H-bonding sites than anthracite (as evidenced by the electrokinetic data and the OH^- ions abstraction). If anionic PAM adsorbs on these samples by H-bonding, the opposite result would be expected. One explanation for the observed result may be the existence of H-bonding sites on both graphite and anthracite with different activation energies for polymer adsorption.

Cationic polymer-anthracite system: As above pH 3.5 the anthracite particles are negatively charged, positively charged (i.e., cationic) polymers should be effective in the flocculation. In this case the adsorption process should primarily involve electrostatic interactions, the positively charged groups of the polymer being attracted by the negatively charged surface of the anthracite

particles regardless of the chemical nature of the polycation.

Although detailed study of the interaction of cationic polymers with the anthracite was not carried out, the flocculation tests show that a cationic polymer is effective for flocculating anthracite in the pH range where it was negatively charged. Moreover, the addition of H-bonding competitors to the suspensions did not make any difference to the power of this flocculant suggesting that H-bonding is not operative in the system.

7.5 Selective flocculation tests

The principles of the selective flocculation process have been known for many years and it has been found empirically by several authors that various polymeric flocculants exhibit some degree of specificity when applied to mixed dispersed systems (121). However, attention has been directed recently to its potential in the processing of finely divided minerals. Most of the work has involved only laboratory scale experiments (122), but the process has also been incorporated in two large plants (123)(124).

A review of a number of separations by selective flocculation and the feasibility of its use in binary, ternary and multi-mineral system has been presented by Read and Hollick (122). In general the concentrations ratios obtained with this process are far from meeting commercially acceptable specifications, but the method can be efficient enough to be used for the selective rejection of gangue as a preliminary step for another concentration process. Most of the work has been concerned with the treatment of clays, iron minerals, phosphates and potash (125)(126). The best concentration ratios have been obtained from laboratory trials only in optimum conditions of low

solid content, high feed grade and high specific gravity of the component to be flocculated.

7.5.1 Adsorption of PEO on silica

It has been well established that the surface charge of silica in water is created by the dissociation of the silanol groups. PEO is adsorbed on the silica surface as a result of the formation of hydrogen bonds between undissociated silanol groups and the ether groups of the polymer, as may be seen from infrared spectroscopic studies (120). It has been found that pH had a marked effect on the adsorption of PEO on silica. The decrease in the adsorption of the polymer with a rise of pH was attributed to a reduction in the number of undissociated silanol groups available for H-bonding. This hypothesis was also supported by the decrease in the PEO adsorption on silica samples subjected to heat treatment, which leads to a decrease in the concentration of the surface silanol groups. Furthermore, there is little influence of PEO on the zeta potential of quartz in the basic pH region where the concentration of undissociated silanol group decreases. It has also been found that fully hydrated silica does not adsorb PEO, although the hydrated silica surface has a lot of silanol groups. This observation was explained by a mechanism involving the hydrogen bonding of neighbouring silanol groups via water molecules. In this condition binding of ether oxygen groups is prevented, the polymer does not adsorb and no flocculation is observed. In a recent study, it was suggested that where the silica surface is hydrophobic, there appears to be hydrophobic association with the $-CH_2-CH_2-$ hydrocarbon chain of the PEO. (127).

From the foregoing, H-bonding as a mechanism of interaction of non-ionic PEO with silica has been well established. Hydrophobic interaction has also appeared to be a further contributor. However, this interaction mechanism of PEO with silica surfaces still needs further clarification.

Whatever the mechanism of PEO adsorption on silica, it is clear that it does not adsorb the PEO at high pH. In this study it was found that PEO adsorbs on the anthracite independent of pH and it produces good flocculation efficiencies with large flocs. Therefore, a basis may exist to expect a selective separation of anthracite from anthracite/quartz mixture. However, one of the disadvantages of the selective flocculation tests is to flocculate the low specific gravity material (coal) and leave the high specific gravity solid (quartz) in suspension.

7.5.2 Selective flocculation of anthracite from anthracite/quartz mixture

The selective flocculation tests were carried out on synthetic mixtures of anthracite and quartz. The same flocculation technique was applied as described in Chapter 4 except that the flocculated product was taken from the bottom of the glass cylinder by stopcock. The grade (ash) of the flocculated product was used as the measure of effectiveness of the selective flocculation. Throughout the tests the pH was kept constant at pH 11$\pm$ 0.5. In parallel with reported successful selective flocculation of other mineral combinations, an important prerequisite is to obtain a fully dispersed state initially. In this study no chemical dispersant was used

but highly dispersed system was achieved by stirring the suspensions at 1000 rpm for 15 min in baffled cylinders.

The preliminary flocculation tests showed that around pH 11 quartz particles did not adsorb PEO and no flocculation was observed.

Table 7.1 shows a preliminary result obtained with synthetic mixtures of anthracite and quartz. As can be seen from the difference in the ash contents of the feed and flocculated material, selective separation of anthracite from quartz may be possible. However, since the tests were carried out with quartz particles of -45μm some sedimentation of the larger particles occurred over a period of 2 min, due to their high specific gravity. Therefore, selectivity may have been effected by the size of the quartz particles used.

Table 7.1 Results of selective flocculation of anthracite

pH = 11.0 - 11.2, PEO Conc. = 7.5 p.p.m. Solid Conc. = 1%
Settling time = 2 min., Mixing Cond. = 1000 rpm for 3 min. after PEO addition + 100 rpm for 2 min.

		Flocculated fraction	
Initial mixture	Ash content of the Initial mixture, %	% Wt	% Ash
5% Quartz + 95% Anthracite	6.5	90.9	4.5
10% Quartz + 90% Anthracite	11.2	90.7	7.0
20% Quartz + 80% Anthracite	21.4	84.7	12.4
50% Quartz + 50% Anthracite	51.2	67.6	34.1

In further tests the quartz used was obtained by sedimentation technique in which the particles remaining in suspension after 30 min. were filtered and dried. This fraction was then mixed with 45μm

anthracite for selective flocculation tests.

The selective flocculation results are given in Table 7.2. It is clear that, for the stated conditions, ash contents of the flocculated fractions considerably decreased.

Table 7.2 Results of selective flocculation of anthracite

pH = 10.8 - 11.2, PEO Conc. = 7.5 p.p.m., Solid Conct. = 1% Settling time = 2 min. Mixing Cond. = 1000 rpm for 3 min. after PEO addition + 100 rpm for 2 min.

Initial mixture	Ash content of Initial mixture, %	Flocculated fraction	
		%Wt	% Ash
5% Q + 95% A	6.5	89.2	2.8
10% Q + 90% A	11.2	87.8	4.7
20% Q + 80% A	21.4	81.7	8.0
50% Q + 50% A	51.2	66.7	26.5

When the above flocculated fractions were redispersed in clean medium under high shear and reflocculated with trace amount of PEO, ash contents of the final fractions further improved, probably because entrapped quartz was progressively released. The result is shown in Table 7.3

Table 7.3 Results of selective flocculation of anthracite

pH = 11.0, PEO Conc. = 2 p.p.m., Solid Cont. = 1%
Settling time = 2 min., Mixing cond. = 1000 rpm
for 5 min. after PEO addition + 100 rpm for 2 min.

Initial mixture	Ash content of initial mixture, %	Flocculation fraction	
		%Wt	% Ash
5% Q + 95% A	6.5	78.6	2.6
10% Q + 90% A	11.2	77.4	4.5
20% Q + 80% A	21.4	70.3	6.8
50% Q + 50% A	51.2	60.9	17.4

In order to overcome the entrainment problem stirring at 1000 rpm after flocculant addition was suddenly stopped after 3 min., and slow agitation of the flocculated system was not carried out so that further floc growth was prevented. In this way the smaller flocs showed decreased ash contents but at the same time most of the anthracite particles were also left in the suspension (Table 7.4).

Table 7.4 Results of selective flocculation of anthracite

pH = 11.0 - 11.2, PEO conc. = 7.5 p.p.m., Solid cont. = 1%
Settling time = 2 min., Mixing cond. = 1000 rpm for
3 min.

Initial mixture	Ash content of initial mixture, %	Flocculated fraction	
		%Wt	% Ash
5% Q + 95% A	6.5	75.4	3.0
10% Q + 90% A	11.2	70.1	4.5
20% Q + 80% A	21.4	67.2	7.0
50% Q + 50% A	51.2	46.8	19.8

Some selective flocculation tests were also carried out with an addition of PEO below the optimum concentration. It was thought this would produce smaller flocs so that entrapment may be further reduced. The ash contents of the flocculated products are considerably decreased. However, unflocculated anthracite particles left in suspension produced low % Wt material in the flocculated fraction. (Table 7.5).

Table 7.5 Results of selective flocculation of anthracite

pH = 11.2, PEO conc. = 4 p.p.m., Solid cont. = 1% Settling time = 2 min., Mixing cond. = 1000 rpm for 3 min. after PEO addition + 100 rpm for 2 min.

		Flocculated fraction	
Initial mixture	Ash content of initial mixture, %	%Wt	% Ash
5% Q + 95% A	6.5	74.0	3.0
10% Q + 90% A	11.2	69.6	4.4
20% Q + 80% A	21.4	54.8	8.2
50% Q + 50% A	51.2	32.0	20.8

Only those tests that resulted in selective flocculation are reported here. These preliminary results suggest that selective flocculation of anthracite-quartz suspensions is possible. However, a considerable number of trials would be required to establish suitable conditions to obtain selective flocculation from these synthetic mixtures.

CHAPTER 8. CONCLUSIONS

CONCLUSIONS

A study has been carried out to determine the surface chemical properties of coal. The results obtained were correlated with the flocculation behaviour of coals with the objective of establishing the mechanism of polymer adsorption.

The coals in general are extremely heterogenous materials whose complexity of composition, due to the presence of organic and inorganic substances, is considerably enhanced because of variations in the levels of concentration of the constituents.

The number of samples utilized in this study by no means represents the whole spectrum of different coals. However, the general similarity between previously published results and some of those reported here give an indication of the reproducibility that can be obtained on such a diverse system.

The results obtained in this study permit the following conclusions to be made.

1. The surface chemical study of the coal/water interface which involved measurements of the electrokinetic and acid-base properties of coal indicate that a coal surface has a negative double layer potential which increases with pH. The net adsorption of hydroxyl ions increases with both pH and ionic strength. H^+ and OH^- ions appear to be potential determining ions for coal and its lithotypes. The isoelectric point of the anthracite, high volatile and medium volatile coal occur at pH's of 3.5, 4.0 and 4.4 respectively. The zero points of charge occur at a lower pH.
2. On oxidized coal, an increase in the degree of oxidation increases

the negative value of the electrophoretic mobility and decreases the isoelectric point. The potential determining effect of H^+ and OH^- ions with extensively oxidized coal is uncertain.

3. The electrophoretic mobility of methylated coal is more negative than an untreated sample although the OH^- ion abstraction is reduced. The reason for this phenomenon was unclear.
4. Monovalent salts behave as indifferent electrolytes, whereas multivalent cations of salts markedly decrease the coal's electrophoretic mobility and can reverse the sign.
5. The various acid groups on the coal surface cannot be titrated to give an indication of the proportion of groups of various strengths because of the microporous nature of the surface.
6. The polymers used, namely polyethylene oxide, anionic PAM and cationic polymer all flocculate the coal suspension into large and rapidly settling flocs. Oxidation has no effect on the flocculation of coal using the anionic PAM, however polyethylene oxide does not flocculate an oxidized coal.
7. The adsorption isotherms for all polymers exhibit typical Langmuir-type behaviour.
8. Non-ionic polyethylene oxide adsorbs by hydrophobic interactions at the coal surface. The solution pH has no effect on polyethylene oxide adsorption. Oxidation causes a reduction in the hydrophobic character of the coal and hence adsorption of polyethylene oxide decreases after oxidation.
9. Anionic polyacrylamide relies upon the presence of a simple electrolyte to reduce the coal's electrokinetic potential and allow the adsorption of the polyanion by H-bonding.

10. The mechanism of adsorption of a cationic polymer is consistent with that of Coulombic attraction.

11. The separation of coal from quartz by selective flocculation is possible using non-ionic polyethylene oxide. Selective flocculation is favoured by highly alkaline conditions (approximately pH 11).

REFERENCES

1. Meloy, T.P. The treatment of fine particles during flotation. Froth Flotation - 50th Anniversary Volume, Ed. D.W. Fuerstenau. (A.I.M.E. 1962).

2. Jones, W.I., Surface characteristics and coal preparation. Proceedings Int. I. Conf. on Coal Prep., paper D-4, 1950, 336-349.

3. Blaschke, Z., Beneficiation of coal fines by selective flocculation. 7th Int. Coal Prep. Congr., paper E-2, 1976, 1-11.

4. Hucko, R.E., Beneficiation of coal by selective flocculation. U.S. Bureau of Mines. Report of Investigations, 8234, 1977.

5. Tschamler, H., and De Ruiter, E., Physical properties of coals. Chemistry of Coal Utilization, Supplementary Vol., Ed. H.H. Lowry (John Wiley and Sons, Inc., New York - London, 1963), 37.

6. International Committee for Coal Petrology., International Handbook of Coal Petrology, 2nd. Ed., Paris, 1963.

7. Stopes, M.C., On the four visible ingredients in banded bituminous coals. Proc. Roy. Soc., Series B, 90, London, 1919, 470.

8. Thomas, C.M., Coal petrology and its application to coal preparation. Coal Preparation, 4, 1968, 50-59.

9. Spachman, W., The maceral concept and the study of modern environments as a means of understanding the nature of coal. Trans. of the New York Acad. of Sci., Ser. II, 20, 1958, 411-423.

10. Berry, W.F., Coal petrography: Remarks on terminology and methodology. The Compass., 32, 1955, 305-318.

11. Abernethy, R.F., and Walters, J.G., Solid and gaseous fuels. Anal. Chem. Annual Rev., 41, 1969, 308R.

12. Hattman, E.A., and Ortuglio, C., Solid and gaseous fuels. Anal. Chem. Analytical Rev., 43, 1971, 345R.

13. Jensen, E.J., et al., The dry oxidation of subbituminous coal. Adv. Chem. Ser., 55, 1966, 621-642.

14. Glembotskii, V.A., Klassen, V.I., and Plaksin, I.N., Flotation, Trans. by R.E. Hammond, Ed. by H.S. Rabinovich. (Primary Sources, New York, 1972).

15. Campbell, J.A.L., and Sun, S.C., Bituminous coal electrokinetics. Trans. A.I.M.E., 247, 1970, 111-114.

16. Campbell, J.A.L., and Sun, S.C., Anthracite coal electrokinetics. ibid, 120-122.

17. Prasad, N., Electrokinetics of coal. Jour. Inst. Fuel, 53, 1974, 174-177.

18. Jowett, A., El-Sinbawy, H., and Smith, H.G., Slime coating in coal flotation pulps. Fuel, 35, 1956, 303-309.

19. Burdon, R.G., and Mishra, S.K., Improving fines flotation recovery. Coal Age, 5, 1980, 220-227.

20. Kovachev, K.P., The mechanism of action of inorganic electrolytes in the flotation of non-polar minerals. Khim. i Ind. (Sofia)., 33, 1961, 4-6.

21. Laskowski, J., and Kitchener, J.A., The hydrophilic-hydrophobic transition on silica. J. Coll. Interf. Sci., 29, 1969, 670-679.

22. Wen, W.W., and Sun, S.C., An electrokinetic study on the amine flotation of oxidized coal. Trans. A.I.M.E., 262, 1977, 174-180.

23. Jessop, R.R., and Stretton, J.L., Electrokinetic measurements on coal and a criterion for its hydropphobicity. Fuel, 47, 1968, 317-320.

24. Gelik, M., and Somasundaran, P., Effects of pretreatments on flotation and electrokinetic properties of coal. Colloids and Surfaces, 1, 1980, 121-124.

25. Boehm, H.P., Chemical identification of surface groups. Adv. in Catalysis, 16, 1966, 179-225.

26. Puri, B.R., Surface complexes on carbon. Chem. and Phys. of carbon. A Series of Advances, Ed. by P.L. Walker, 6, 1970, 191-282.

27. Ruberto, R.G., and Cronauer, D.C., Oxygen and oxygen functionalities in coal and coal liquids. Organic Chemistry of Coal, ACS Symp. Series, 71, 1977, 50-70.

28. Van Krevelen, D.W., and Schuyer, J., Coal Science. (Elsevier, Amsterdam, New York, London 1957), p. 211.

29. Studebaker, M.L., Direct titration of the acidity of carbon blacks. Proc. 5th Conf. Carbon, Vol. 2, 1961, 189-197.

30. Ihnatowicz, A., Studies of oxygen groups in bituminous coals. Proc. Central Research Mining Inst., No. 125, Katowice, 1952.

31. Schafer, H.N.S., Determination of the total acidity of low rank coals. Fuel, 49, 1970, 271-278.

32. Brooks, J.D., and Maher, T.P., Acidic oxygen-containing groups in coal. Fuel, 36, 1957, 51-62.

33. Blom, L., Edelhausen, L., and Van Krevelen, D.W., Chemical structure and properties of coal. Fuel, 36, 1957, 135-153.

34. Barton, S.S. et al., The structure of acidic surface oxides on carbon and graphite. Carbon, 16, 1978, 363-365.

35. Dryden, I.G.C., Chemical constitution and reactions of coal. Chemistry of Coal Utilization, Supplementary Vol., Ed. H.H. Lowry (John Wiley and Sons, Inc., New York - London, 1863), 264.

36. Thomas, J.M., and Hughes, E.E.G., Localised oxidation rates on graphite surfaces. Carbon, 1, 1964, 209.

37. Henning, G.R., Surface oxides on graphite single crystals. Proc. 5th Conf. on Carbon, 1, 1961, 143-146.

38. Tronov, B.V., A phenol theory of coal oxidation. Chem. Abs., 35, 1941, 1966.

39. Yohe, G.R., and Blodgett, E.O., Oxidation of coal. J. Am. Chem. Soc., 69, 1947, 2644-2648.

40. Van Vucht, H.A. et al., Chemical structure and properties of coal. Fuel, 34, 1955, 50-59.

41. Adams, W.N., and Pitt, G.J., Examination of oxidized coal by infrared absorption methods. Fuel, 34, 1955, 383.

42. Gaudin, A.M., Miaw, H.L., and Spedden, H.R., Native floatability and crystal structure. Proc. 2nd Intern. congr. Surf. Activity, 3, 1957, 202.

43. Gaudin, A.M., Flotation, 2nd ed. (McGraw-Hill, New York, 1957).

44. Taggart, A.F., et al., Oil-air separation of non-sulfide and non-metal minerals. Trans. A.I.M.E., 134, 1939, 180-206.

45. Sun, S.C., Hyphothesis for different floatabilities of coals, carbons and hydrocarbon minerals. Trans. A.I.M.E., 199, 1954, 67-75.

46. Derjaguin. B.V., and Landau, L., Theory of the stability of strongly charged lyophobic sols and the adhesion of strongly charged particles in solutions of electrolyte. Acta Physiochim., 14, 1941, 633-662.

47. Verwey, J.W., and Overbeek, J. Th. G., Theory of stability of lyophobic colloids, (Elsevier, Amsterdam, 1948).

48. Schenkel, J.H., and Kitchener, J.A., A test of the Derjaguin-Verwey-Overbeek theory with a colloidal suspension. Trans. Faraday Soc., 56, 1960, 161-173.

49. Kruyt, H.R., (ed.) Colloid science, Vol. 1 (Elsevier, Amsterdam, 1952).

50. Fuerstenau, M.C., Elgillani, D.A., and Miller, J.D., Adsorption mechanisms in non-metallic activation systems. Trans. A.I.M.E., 244, 1970, 11-13.

51. James, R.O., and Healy, T.W., Adsorption of hydrolyzable metal ions at the oxide-water interface. Parts I, II and III, J. Coll. Interf. Sci., 40, 1972, 42-81.

52. Matijevic, E., et al., Stability of colloidal silica. IV. The silica-alumina system. J. Coll. Interf. Sci., 35, 1971, 560-568.

53. Jenkel, E., and Rumback, B., Flexible polymers at a solid-liquid interface. Z. Electrochem., 55, 1951, 612.

54. Ash, S.G., Polymer adsorption at the solid/liquid interface. Colloid Science, 1, 1973, 103-122.

55. Silberberg, A., Multilayer adsorption of macromolecules. J. Coll. Interf. Sci., 38, 1972, 217-226.

56. Tomi, D.T., and Bagster, D.F., The behaviour of aggregates in stirred vessels. Minerals Sci. Engng., 12, 1980, 3-19.

57. Killmann, E., and Strasser, H.J., Infraotspektrometrische untersuchungen zur haftstellenzahl absorbierter polyathylenglykole. Angew. Makromol. Chem., 31, 1973, 163-179.

58. Joppien, G.R., Determination of the structure of adsorption layers of macomolecular compounds. Makromol. Chem., 175, 1974, 1931-1954.

59. Robb, I.D., and Smith, R., The adsorption of a copolymer of vinyl pyrrolidone and allylamine at the silica-solution interface. Eur. Polym. J., 10, 1974, 1005-1010.

60. Cosgrove, T., and Vincent, B., Makromol. Chem., to be published.

61. Doroszkowski, A., and Lambourne, R., The measurement of the dependence of the strength of steric barriers on their solvent environment. J. Coll. Interf. Sci., 43, 1973, 97.

62. Ottewill, R.H., and Cairns, R.J.R., Direct studies on the interaction forces between latex particles in non-aqueous media. 168th Meeting Am. Chem. Soc., Atlantic City, 1974.

63. Killmann, E., and Eckart, R., Calorimetric studies of the adsorption of macromolecules from diluted solutions. Makromol. Chem., 144, 1971, 45-61.

64. Ottewill, R.H., and Walker, T., The influence of non-ionic surface active agents on the stability of polystyrene latex dispersions. Kolloid - Zeitschrift und Z. fur Polymere, 227, 1968, 108-116.

65. Doroszkowski, A., and Lambourne, R., A viscometric technique for determining the layer thickness of polymer adsorbed on titanium dioxide. J. Coll. Interf. Sci., 26, 1968, 214-221.

66. Barsted, S.J., Nowaakowska, L.J., Wagstaff, I., and Walbridge, D.J. Measurement of steric stablizier barrier thickness in dispersions of poly (methyl methacrylate) in aliphatic hydrocarbon. Trans. Faraday Soc., 67, 1971, 3598-3603.

67. Stromberg, R.R., Tutas, D.J., and Passaglia, E., Conformation of polystyrene adsorbed at the Θ - temperature. J. Phys. Chem., 69, 1965, 3955.

68. Killmann, E., and Wiegand, H.G., Characterization of adsorbed layers of macromolecules by means of an ellipsometer. Makromol. Chem., 132, 1970, 239-

69. Garvey, M.J., Tadros, Th. F., and Vincent, B., A comparison of the adsorbed layer thickness obtained by several techniques of various molecular weight fractions of polyvinyl alcohol on aqueous polystrene latex particles. J. Coll. Interf. Sci., 55, 1976, 440-453.

70. Koopal, L.K., and Lyklema, J., Characterization of polymers in the adsorbed state by double layer measurements. Disc. Faraday Soc., 59, 1975, 230-241.

71. Griot, O., and Kitchener, J.A., Role of surface silanol groups in the flocculation of silica suspensions by polyacrylamide. Trans. Faraday Soc., 61, 1965, 1026-1032.

72. Michaels, A.S., Aggregation of suspensions by polyelectrolytes. Industrial and Engineering Chemistry, 46, 1954, 1485-1490.

73. Kitchener, J.A., Principles of action of polymeric flocculants. Br. Polym. J., 4, 1972, 217-229.

74. Slater, R.W., and Kitchener, J.A., Characteristics of flocculation of mineral suspensions by polymers. Disc. Faraday Soc., 42, 1966, 267-275.

75. Nemethy, G., and Scherage, H., The structure of water and hydrophobic bonding in proteins. III. The thermodynamic properties of hydrophobic bonding in proteins. J. Phys. Chem., 66, 1962, 1773.

76. Parsegian, D.A., and Ninham, B.W., Toward the correct calculation of van der Waals interactions between lyophobic colloids in an aqueous medium. J. Coll. Interf. Sci., 37, 1971, 332.

77. Tanford, C.T., The hydrophobic effect: Formation of micelle and biological membranes. (John Wiley and Sons, New York, 1973), 3.

78. Mukarjee, P., The nature of the association equilibria and hydrophobic bonding in aqueous solutions of association colloids. Adv. Coll. Interf. Sci., 1, 1967, 241-275.

79. Dahlstrom, D.A., Closing coal-preparation-plant water circuits with classifiers, thickeners and continuous vacuum filters. 2nd Symp. on Coal Prep., Leeds, 1957.

80. Matoney, J.P., et al., Fine-coal recovery and economic elimination of slime in coal-preparation plants. 3rd Int. Coal Prep. Conf., Liege, 1958.

81. Matheson, G.M., and Mackenzie, J.M.W., Flocculation and thickening of coal-washery refuse pulps. Coal Age, 1962, 94-100.

82. Fuerstenau, M.C., and Palmer, B.R., Anionic flotation of oxides and silicates. Flotation A.M. Gaudin Memorial Volume, Ed. M.C. Fuerstenau (A.I.M.E. 1976), 148-196.

83. Miller, K.J., and Deurbrouck, A.W., Evaluation of synthetic organic flocculants in the treatment of coal refuse slurries. U.S. Bureau of Mines. Report of Investigations, 7102, 1968.

84. Mirville, R.J., and Hogg, R., Polymer adsorption and flocculation in the treatment of coal preparation waste water. SME preprint, No. 79-61.

85. British standard methods for the analysis and testing of coal and coke, 1016, Part 3, 1973.

86. Tschamler, H., and De Ruiter, E., Physical properties of coal. Chemistry of Coal Utilization,, Supplementary Vol., Ed. H.H. Lowry (John Wiley and Sons, Inc., New York-London, 1963), 61.

87. The Analytical Sev. Lab., Imp. Coll., Private Communication.

88. Fales, H.M., Jaouni, T.M., and Babashak, J.F., Simple device for preparing etheral diazomethane without resorting to codistillation. Anal. Chem., 45, 1973, 2302.

89. Attia, Y.A.K., and Rubio, J., Determination of very low concentrations of polyacrylamide and polyethyleneoxide flocculants by nephelometry. Br. Poly. J., 7, 1975, 135-138.

90. Crummet, W.B., and Hummel, R.A., The determination of traces of polyacrylamides in water. J. Amer. Water Works Assoc., 55, 1963, 209-219.

91. Wiersema, P.H., Loeb, A.L., and Overbeek, J.Th.G., Calculation of the electrophoretic mobility of a spherical colloid particle. J. Coll. Interf. Sci., 22, 1966, 78-99.

92. Shaw, D.J., Electrophoresis. (Academic Press, New York-London, 1969), 43.

93. Mararu, V.N., et al., Effect of pH and ionic strength of electrolyte solutions on the ξ-potential and stability of aqueous graphite dispersions. Kolloidn. Zh., 42(5), 1980, 873-879.

94. March, J., Advances organic chemistry: reactions, mechanisms, and structure. (McGraw-Hill Book Co., New York-London, 1968), p. 1098.

95. Onoda, G.Y., and de Bruyn, P.L., Proton adsorption at the ferric oxide/aqueous solution interface. Surface Science, 4, 1966, 48-63.

96. Bolt, G.H., Determination of the charge density of silica sols. J. Phys. Chem., 61, 1957, 1166-1169.

97. Li, H.C., and de Bruyn, P.L., Electrokinetic and adsorption studies on quartz. Surface Science, 5, 1966, 203-220.

98. Tadros, T.F., and Lyklema, J., Adsorption of potential-determining ions at the silica-aqueous electrolyte interface and the role of some cations. J. Electroanal Chem., 17, 1968, 267-275.

99. Breeuwsma, A., and Lyklema, J., Interfacial electrochemistry of haematite ($\alpha - Fe_2O_3$). Disc. Faraday Soc., 52, 1971, 324-333.

100. Berube, Y.G., and de Bruyn, P.L., Adsorption at the rutile-solution interface. J. Coll. Interf. Sci., 28, 1968, 92-105.

101. Arbiter, N., et al., Surface properties of hydrophobic solids. A.I.Ch.E. Symp. Ser., No. 150, 1975, 71.

102. Shergold, H.L., and Hartley, C.J., The surface chemistry of diamond. Int. J. Min. Process., 9(3), 1982, 219-223.

103. Hiemenz, P.C., Principles of colloid and surface chemistry. (Marcel Dekker Inc., New York-Basel, 1977), 476.

104. Rendell, H.M., and Smith, A.L., Surface and electrokinetic potentials of interfaces containing two types of ionizing groups. J. Chem. Soc. Farad. I., 74, 1978, 1179-1187.

105. McKenzie, J.M.W., Zeta potential of quartz in the presence of ferric ion. Trans. A.I.M.E., 235, 1966, 82-87.

106. Baes, C.F., and Mesmer, R.E., The hydrolysis of cations. (Wiley, New York, 1976), 273, 122.

107. Stol, R.J., Van Helden, A.K., and de Bruyn, P.L., Hydrolysis-precipitation studies of aluminium III solutions. 2. A. kinetic study and model. J. Coll. Interf. Sci., 57, 1976, 115-131.

108. Lengweiler, H., Buser, W, and Feitknecht, W. Die ermittlung der loslichkeit von eisen (III) - hydroziden mit Fe II. Helvetica Chimica Acta, 44, 1961, 805.

109. Read, A.D., and Manser, R.M., Surface polarizability and flotation: Study of the effect of cation type on the oleate flotation of three orthosilicates. Trans. I.M.M., C69, 1972.

110. Kitchener, J.A., Flocculation in mineral processing. The Scientific Basis of Flocculation, Ed. K.J. Ives. (Sijthoff and Noordhoff, Netherlands, 1978), 283-328.

111. Kane, J.C., La Mer, V.K., and Linford, H.B., The filtration of silica dispersions flocculated by high polymers. J. Phys. Chem., 67, 1963, 1977-1981.

112. Baskerville, R.C., and Gale, R.S., A simple automatic instrument for determining the filtrability of sewage sludges. J. Water Pollut. Control, 67, 1968, 233-241.

113. Linke, W.F., and Booth, R.B., Physical chemical aspects of flocculation by polymers. Trans. A.I.M.E., 217, 1960, 364-371.

114. Lyklema, J., Surface chemistry of colloids in connection with stability. The Scientific Basis of Flocculation, Ed. K.J. Ives (Sijtoff and Noordhoff, Netherlands, 1978), 3-36.

115. Brown, D.J., Coal flotation. Froth Flotation - 50th Anniversary Vol., Ed. D.W. Fuerstenau, (A.I.M.E. 1962), 518-528.

116. Coughlin, R.W., Exra, F.S., and Tan, R.N., Influence of chemisorbed oxygen in adsorption onto carbon from aqueous solution. J. Coll. Interf. Soc., 28, 1968, 386-396.

117. Birkner, F.B., and Edzwald, J.K., Nonionic polymer flocculation of dilute clay suspensions. J. Am. Water Works Assoc., 61, 1969, 645-651.

118. Miller, J.D., Laskowski, J.S., and Chang, S.S., Dextrin adsorption by oxidized coal. 56th Coll. and Surf. Sci. Symp., A.I.M.E., 1982.

119. Fuerstenau, D.W., and Pradip, Adsorption of frothers at coal/water interfaces. Colloids and Surfaces, 4, 1982, 229-243.

120. Eremenko, B.V., and Sergienko, Z.A., Surface charge of silica in polyoxyethylene solutions. Effect of surface charge on the adsorption of polyethylene on silica. Kolloid. Zh., 41(3), 1979, 422-427.

121. Friend, J.P., and Kitchener, J.A., The separation of minerals from mixtures by selective flocculation. Filt. and Sep., 9, 1972, 25-28.

122. Read, A.D., and Hollick, C.T., Selective flocculation techniques for recovery of fine particles. Minerals Sci. Engng., 8(3), 1976, 202-213.

123. Anon, Tilden based on processing breakthrough. Engng. Min. J., 175, 140-142.

124. Clifford, K.G., Concentration. Min. Engng., 27, 1975, 57-58.

125. Maynard, R.N., Deutches Pat. Off., 2,329,455, Acc., 1974; Mercade, V.V., U.S. Patent, 3,701,417, Acc., 1972; Bidwell, J.I., Canadian Patent, 838,573, Acc., 1970.

126. Davenport, J.E., and Watkins, S.C., Beneficiation of florida pebble phosphate slime. Ind. Engng. Chem. Process Des. Div., 8, 1969, 533; Brogoitti, W.B., and Howald, F.B., U.S. Patent, 3,805,951, Acc., 1974.

127. Rubio, J., and Kitchener, J.A., The mechanism of adsorption of poly(ethylene oxide) flocculant on silica. J. Coll. Interf. Sci., 57, 1976, 132-142.

APPENDIX I Direct titrations

Direct titrations with different bases (sodium hydroxide, sodium carbonate, sodium bicarbonate and sodium ethoxide) were conducted to determine the relative strengths of the different acidic groups on the surfaces of the anthracite and graphite. The titrations gave rather flat curves without distinct end-points. Direct titrations were also carried out using bases of various strengths (10^{-4} to 10^{-2}M) and different amounts of solid (0.2 to 2g). The curves again failed to produce clear end-points. However, titration curves for both anthracite and graphite were similar to those found on other carbon surfaces (1). It has been suggested that such curves are not representative of carboxyl groups on the graphite surface but suggest the presence of phenol groups, since they resemble those found for phenolic resins (1). Barton et al (2) suggested a correlation between base neutralization and CO evolution (if phenolic groups are present) and between base neutralization and CO_2 evolution (if carboxyl groups are present). In their study the actual correlation found between base neutralization and CO_2 evolution indicated that a carboxyl or lactone surface oxide group gives rise to the surface acidity. It may be possible that a "frozen layer" of carbon dioxide which was suggested by Puri (3) would also give a linear correlation between base neutralization and CO_2 evolution.

It is evident from the literature that there has been considerable speculation on the structure of the oxide groups on graphite or coal. From the result of this study it would appear that H^+ or OH^- ions slowly diffuse from the porous structure so that it was not possible

to obtain clear end-points which could be attributed to specific surface groups. It is also possible that the "flatness" of the titration curves is due to a low surface density of active groups. However, slightly different OH^- ion abstraction values obtained with three bases (NaOH, Na_2CO_3 and $NaHCO_3$) might indicate that different acidic groups are present on the surface of the anthracite and graphite, although the specific groups are not known.

References

1. Garten, V.A., and Weiss, D.E., Functional groups in activated carbon and carbon black with ion and electron exchange properties Proc. Third Carbon Conf., 1957, 295-313.

2. Barton, S.S. et al., Surface studies on graphite: Acidic surface oxides. Carbon, 10, 1972, 395-400.

3. Puri, B.R., Surface complexes on carbon. Chem. and Phys. of carbon. A Series of Advances, Ed. by P.L. Walker, 6, 1970, 191-282.

APPENDIX II Calculation of Metal Species Concentrations Present in Aqueous Solutions

The variation in concentration of metal species with pH was calculated for 2 x 10^{-3}M solution of calcium and 10^{-4}M solutions of copper, aluminium and iron, in order to determine when increased hydroxylated cation concentration and precipitation of metal hydroxide occurs.

Aluminium

The relevant equilibria (1,2,3) are,

$$Al(OH)_{3(s)} \rightleftharpoons Al^{3+} + 3OH^- \qquad K_s = 3.16 \times 10^{-34} \qquad (1)$$

$$Al^{3+} + H_2O \rightleftharpoons Al(OH)^{2+} + H^+ \qquad K_1 = 1.08 \times 10^{-5} \qquad (2)$$

$$Al^{3+} + 2H_2O \rightleftharpoons Al(OH)_2^+ + 2H^+ \qquad K_2 = 5.01 \times 10^{-10} \qquad (3)$$

$$Al^{3+} + 3H_2O \rightleftharpoons Al(OH)_3(aq) + 3H^+ \qquad K_3 = 1.00 \times 10^{-15} \qquad (4)$$

$$Al^{3+} + 4H_2O \rightleftharpoons Al(OH)_4^- + 4H^+ \qquad K_4 = 1.00 \times 10^{-23} \qquad (5)$$

$$8Al^{3+} + 20H_2O \rightleftharpoons Al_8(OH)_{20}^{4+} + 2H^+ \qquad K_5 = 1.99 \times 10^{-69} \qquad (6)$$

$$Al(OH)_{3\ (s)} \rightleftharpoons Al(OH)_3(aq) \qquad K = 3.16 \times 10^{-34} \qquad (7)$$

Therefore the concentration of the metal species are dependent on the pH of the solution. The pH at which precipitation of aluminium hydroxide commences can be calculated by considering a mass balance

of all aluminium species in solution. Then the solubility (S) is given by,

$$S = [Al^{3+}] + [Al(OH)^{2+}] + [Al(OH)_2^+] + [Al(OH)_3(aq)] + [Al(OH)_4^-]$$

$$S = K_s.K_w^{-3}[H^+]^3 + K_1.K_s.K_w^{-3}[H^+]^2 + K_3.K_s.K_w^{-3}[H^+] + K + K_4.K_s.K_w^{-3}[H^+]^{-1}$$

$$S = 3.162 \times 10^8[H^+]^3 + 3.384 \times 10^3[H^+]^2 + 0.158[H^+] + 3.10^{-7} + 3.162 \times 10^{-15}[H^+]^{-1} \quad (8)$$

The pH at which precipitation occurs in a 10^{-4}M solution was calculated to be 4.5 by substitution of hydrogen ion concentrations into equation (8). Below this value it was assumed that the aluminium cation is predominant and has a concentration of 10^{-4}M. The concentration of other species was calculated from equations 2,3,4,5 and 6. For example,

$$[Al(OH)^{2+}] = K_1[Al^{3+}][H^+]^{-1} = 1.08 \times 10^{-9}\ [H^+]^{-1}$$

$$[Al(OH)_2^+] = K_2\ [Al^{3+}][H^+]^{-2} = 5.01 \times 10^{-14}\ [H^+]^{-2}$$

As the pH increases towards 4.5 accurate values for $[Al^{3+}]$ and the other species may be determined by the mass balance given in equation (9) and iteration with equations (1) to (6).

$$[Al^{3+}] = 10^{-4} - [Al(OH)^{2+}] - [Al(OH)_2^+] \quad (9)$$

The hydroxide precipitate dissolves above pH 12, then between approximately pH 4.5 and 12. $Al(OH)_3(aq)$ is equal to K. Substitution of this value into equation (4) gives the concentration of Al^{3+} which

can be used to determine the concentration of all other species.

Above approximately pH 7 the concentration of the cationic species are negligible and equation (10) may be used to calculate the aluminate and hydroxide concentrations

$$10^{-4} = [Al(OH)_3(s)] + [Al(OH)_4^-] \qquad (10)$$

The distribution diagram for a 10^{-4}M solution is presented in Figure 6.10.

Calcium

The species concentration versus pH diagram for a 2×10^{-3}M calcium solution shown in Figure 6.7 was derived using the following equilibria (3).

$$Ca(OH)_2(s) \rightleftarrows Ca^{2+} + 2OH^- \qquad K = 6.456 \times 10^{-6}$$

$$Ca^{2+} + H_2O \rightleftarrows Ca(OH)^+ + H^+ \qquad K = 1.412 \times 10^{-13}$$

Copper

The solution equilibria data given below (4) to determine the concentration - pH diagram shown in Figure 6.8.

$$Cu^{2+} + H_2O \rightleftarrows Cu(OH)^+ + H^+ \qquad K_1 = 10^{-8}$$

$$Cu^{2+} + 2H_2O \rightleftarrows Cu(OH)_2(aq) + 2H^+ \qquad K_2 = 10^{-17.3}$$

$$Cu^{2+} + 3H_2O \rightleftarrows Cu(OH)_3^- + 3H^+ \qquad K_3 = 10^{-26.3}$$

$$Cu^{2+} + 4H_2O \rightleftarrows Cu(OH)_4^{-2} + 4H^+ \qquad K_4 = 10^{-39.4}$$

$$2Cu^{2+} + 2H_2O \rightleftharpoons Cu_2(OH)_2^{2+} + 2H^+ \qquad K_5 = 10^{-10.95}$$

$$CuO(s) + 2H^+ \rightleftharpoons Cu^{2+} + H_2O \qquad K_s = 10^{7.65}$$

Iron

The solution eqiulibria for the amorphous "active" $Fe(OH)_3$ - water system are given below (4), the concentration - pH diagram shown in Figure 6.9.

$$Fe^{3+} + H_2O \rightleftharpoons Fe(OH)^{2+} + H^+ \qquad K_1 = 10^{-2.19}$$

$$Fe^{3+} + 2H_2O \rightleftharpoons Fe(OH)_2^{+} + 2H^+ \qquad K_2 = 10^{-5.67}$$

$$Fe^{3+} + 3H_2O \rightleftharpoons Fe(OH)_3(aq) + 3H^+ \qquad K_3 = 10^{-12}$$

$$Fe^{3+} + 4H_2O \rightleftharpoons Fe(OH)_4^{-} + 4H^+ \qquad K_4 = 10^{-21.6}$$

$$2Fe^{3+} + 2H_2O \rightleftharpoons Fe_2(OH)_2^{4+} + 2H^+ \qquad K_5 = 10^{-2.95}$$

$$3Fe^{3+} + 4H_2O \rightleftharpoons Fe_3(OH)_4^{5+} + 4H^+ \qquad K_6 = 10^{-6.3}$$

$$FeO(OH) + 3H^+ \rightleftharpoons Fe^{3+} + 3H_2O \qquad K_s = 10^{0.5}$$

References

1. Sillen, L.G., and Martell, A.E., Stability constants of metal-ion complexes, Special publication No. 17, The Chemical Society, London, 1964; Supplement No. 1, Special publication No. 25, 1971.

2. Latimer, W.M., Oxidation potentials (Prentice-Hall, New York, 1952).

3. Rubin, A.J., Aqueous-environmental chemistry of metals (Ann Arbor, Michigan, 1974).

4. Baes, C.F., and Mesmer, R.E., The hydrolysis of cations (Wiley Interscience, New York, 1976).